Hydrology and Nutrient Biogeochemistry of Shallow Pond-Peatland Complexes, Hudson Bay Lowlands

by

Matthew Morison

A thesis
presented to the University of Waterloo
in fulfillment of the
thesis requirement for the degree of
Doctor of Philosophy
in
Geography

Waterloo, Ontario, Canada, 2018

Examining Committee Membership

The following served on the Examining Committee for this thesis. The decision of the Examining Committee is by majority vote.

External Examiner: Dr. Kathy Young, Professor, Department of Geography, York University, Canada.

Co-supervisor: Dr. Merrin Macrae, Associate Professor, Department of Geography and Environmental Management, University of Waterloo, Canada.

Co-supervisor: Dr. Richard Petrone, Professor, Department of Geography and Environmental Management, University of Waterloo, Canada.

Internal Member: Dr. Jonathan Price, Professor, Department of Geography and Environmental Management, University of Waterloo, Canada.

Internal-External Member: Dr. Brian Branfireun, Professor, Department of Biology, Western University, Canada. Adjunct status through Department of Geography and Environmental Management, University of Waterloo, Canada.

Author's Declaration

This thesis consists of material all of which I authored or co-authored: see Statement of Contributions included in the thesis.

This is a true copy of the thesis, including any required final revisions, as accepted by my examiners.

I understand that my thesis may be made electronically available to the public.

Statement of Contributions

This thesis is structured in accordance with the manuscript option and Chapters 2 through 5 either have been accepted (Chapters 3 and 4) or submitted (Chapters 2 and 5) for publication in a peer-reviewed journal; as such, the published papers may differ from the chapters presented here based on the comments from the peer review process. As well, some repetition between chapters in background and methodology may occur. Figure formatting elements may differ and abbreviations may be repeated between chapters as per the requirements of individual journals.

Matthew Morison planned and carried out the fieldwork and laboratory work, and wrote and edited the thesis. Dr. Merrin Macrae, Dr. Richard Petrone, and Dr. LeeAnn Fishback advised on methodological protocols and provided editorial comments on Chapters 2, 3, 4, and 5, and are listed as co-authors for the submitted (Chapters 2 and 5) or published (Chapters 3 and 4) editions of these manuscripts. Dr. Olena Volik, Dr. Roland Hall, and Dr. Johan Wiklund assisted with laboratory work and provided editorial comments on Chapter 5 in the thesis and are listed as co-authors for the eventual submission of the manuscript arising from that chapter to a scientific journal.

Chapter two is submitted as:

Morison, M. Q., Macrae, M. L., Petrone, R. M., & Fishback, L. A. (2017). Climate-induced changes in nutrient transformations across landscape units in thermokarst-impacted subarctic peatlands. Submitted to *Arctic, Antarctic, and Alpine Research*, Dec 22, 2017, ID# 2017-AAAR-0003.

Chapter three is published as:

Morison, M. Q., Macrae, M. L., Petrone, R. M., & Fishback, L. A. (2017). Seasonal dynamics in shallow freshwater pond-peatland hydrochemical interactions in a subarctic permafrost environment. *Hydrological Processes*. 31:462–475. doi: 10.1002/hyp.11043

Chapter four is published as:

Morison, M. Q., Macrae, M. L., Petrone, R. M., & Fishback, L. A. (2018). Capturing temporal and spatial variability in the chemistry of shallow permafrost ponds. *Biogeosciences,* 14, 5471-5485. doi: 10.5194/bg-14-5471-2017

Chapter five is submitted as:

Morison, M. Q., Volik, O., Hall, R.I., Wiklund, J. A., Macrae, M. L., & Petrone, R. M. (2018). Evaluating the hydrological and hydrochemical responses of a High Arctic catchment during an exceptionally warm summer. Submitted to *Journal of Paleolimnology*, Jun 19, 2018, ID# JOPL-D-18-00038

Abstract

Across the circumpolar north, the degradation of permafrost in tundra and peatland landscapes has resulted in significant changes to land cover, including an increase in the extent of thermokarst landforms. Climatically-driven changes to soil hydrology and temperature have the potential to impact nutrient cycling biogeochemical processes, which have implications for plant productivity, greenhouse gas fluxes, and surface water quality. Terrestrial and aquatic ecological productivity are often nutrient-limited in subarctic permafrost environments, linking the cycling of bioavailable nutrients to the capacity of the landscape to take in and store carbon. Within these permafrost peatland catchments, the fate of small (< 1 km^2) freshwater ponds and lakes has been the subject of scientific interest due to their ubiquity in the landscape, capacity to exchange carbon and energy with the atmosphere, and their potential to inform researchers about past climates through sediment records. High latitude regions are experiencing significant climatic change, including rapid warming and changing precipitation patterns, which may result in changes in nutrient dynamics within terrestrial and aquatic systems and hydrochemical transport dynamics between them. With climate warming, thermokarst lake expansion has the potential to modify the ability of these aquatic systems to maintain these functions through changes to nutrient inputs and cycling. Through seasonal hydrometric and hydrochemical monitoring, laboratory experimentation, and paleolimnological methods, a set of pristine and thermokarst-impacted peatland catchments in the Hudson Bay Lowlands served as the study site to design research questions and methodologies to address several major themes across the pond-peatland interface. Within the peatland catchment, experimental laboratory work was used to examine the climatic controls on mineralization rates across

landscape units, which represent potential nutrient contributions along runoff flow paths. Next, seasonal variability in runoff quantity and quality from catchments to pond was explored, as well as the relationship of hydrologic drivers to how temporal patterns in pond chemistry varied spatially in the landscape among ponds. Finally, the impacts of thermokarst shoreline collapse on hydroecological functioning of a pond were studied, (including all aforementioned mineralization and runoff processes) inferred through the sediment record of a recently impacted pond in the Hudson Bay Lowlands. This work has (1) improved scientific understanding of the combined controls of hydrologic inputs and ground frost on runoff and nutrient transport between peatlands and ponds, which represent up to 60% of all snow-free water input to ponds, (2) demonstrated the importance of understanding hydrologically driven chemodynamics in permafrost ponds on multiple scales (seasonal and event scale), in particular for a set of hydrologically-driven ions (Cl^-, Na^+, K^+, Mg^{2+}, dissolved organic nitrogen), (3) provided novel insight to nutrient cycling processes in northern peatland landscapes along two spatial gradients (landscape unit and depth), including the potential for rapid nitrification of thermokarst material under oxic conditions (4.6 μg NO_3-N g^{-1} dry peat d^{-1}) and (4) furthered understanding of the hydroecological response of small surface water bodies to thermokarst shoreline expansion under a changing climate, showing that nutrient fluxes increased dramatically both prior to and following shoreline slumping, with isotopic signatures indicating a shift towards increased supply of allochthonous carbon and atmospheric nitrogen. Overall, this thesis addresses multiple and cross-cutting themes of the hydrology and nutrient biogeochemistry of shallow pond-peatland complexes in the Hudson Bay Lowlands.

Acknowledgements

The biggest lesson I learned throughout this rewarding and daunting road of grad school is that there is so much to be thankful for all around us, and most important of those things are the incredible people in our lives which we forget to thank often enough. I am grateful for the chance to do that here and am remiss for so many names which I can't fit onto these pages, but as they say - you know who you are.

To my parents, Alex & Glenn, and my sister, Mo: thank you for always being there for me, getting me to both the start line of this degree, from Cape Breton to ice cream sundaes in Hazelton to Alloway and beyond, and now also to the finish line. Lovee. To my extended family who have supported in countless ways, thank you. To Shayne, Kathy, and Hilary (you will always be family to me in my mind): thank you for your love, belief, and having me as one of the Ruston-Mann clan.

To all those who helped in the field and the lab, you are too countless to name: thank you to each and every one. From amongst this long long list, I do have to single out both Vito Lam and Alex Goodman for being such good friends in addition to be amazing colleagues with whom I spent countless hours and beyond in the field and lab together. I literally couldn't have done it without you. To all of the warm and welcoming parts of the greater university communitas, including the GSA-UW, EGSA, department, faculty, ultimate teams, friends, Cathy from Tim Hortons: thank you. I also want to thank Susie Castela and Alan Anthony for patiently going above and beyond and answering approximately 500 questions of mine (literally counted the number of emails I've sent you) over the years.

To my knights of Avondale, including the much greater community around us: thank you for being the best friends and support I could ask for, for being there, for listening, for doing all you do in the world. To my bush buddies for life, my five guys with fries, thank you for being brothers to me.

To my early career mentors and peers: Ed, Danny, Caleigh, & LeeAnn – thank you for taking me as a scared undergrad under your wing and encouraging me to just go for it. I would have never signed up for this five years of chaos without your awesome stories of how brutal but amazing it would all be. I am so glad you did and I would never have had it any other way.

To Merrin and Rich, your unwavering support has been second to none. This whole grad school process has been incredibly challenging for all sorts of reasons, both academic and personal, but your ability to keep me going through this all has been an amazing constant for the past five years and counting. I am overwhelmingly lucky to have had the chance to learn so much from you both about this journey of doing science: from fieldwork to reading to grinding through the analysis and writing and presentation and editing and revisions, all while staying balanced and in (mostly) good spirits throughout the process. We have all heard horror stories of terrible advisor-student relationships, and I felt like I had the exact opposite of that. There are few people whom are such talented scientists, teachers, advisors, and mentors, but also remain compassionate and understanding and remind us that before we are scientists, we are humans who also need to go skiing, have a beer, and spend time with family and friends. Thank you for everything. Jon and Brian, every step along the way that you have been involved I have been grateful for your presence, wise words, comfort, and strong scientific advice. Thank you.

Land Acknowledgements

I acknowledge the traditional territory of Ontario’s Aboriginal peoples, upon which we live and carry out our studies at the University of Waterloo. Specific to southwestern Ontario, I acknowledge the Anishinabek and Haudenosaunee people. Further, given the field-based nature of this thesis, I acknowledge the territory in which this field research was conducted, in Churchill, Manitoba, contemporary territory of the Thule and Dene through forced relocations on Treaty 5 land.

Dedication

This thesis is dedicated to Emily Ruston Mann, whose endless love, thoughtfulness, and compassion has inspired me throughout this thesis, and will continue to inspire me through the rest of my life.

“If ever there is tomorrow when we're not together... there is something you must always remember. You are braver than you believe, stronger than you seem, and smarter than you think. But the most important thing is, even if we're apart... I'll always be with you.”

― A.A. Milne

Table of Contents

Examining Committee Membership ii

Author's Declaration iii

Statement of Contributions iv

Abstract vi

Acknowledgements viii

Land Acknowledgements x

Dedication xi

Table of Contents xii

List of Figures xvi

List of Tables xx

Chapter 1: Introduction 1

- 1.1 Objectives and Approach 8
- 1.2 Outline of Thesis 8

Chapter 2 : Climate-Induced Changes in Nutrient Transformations across Landscape Units in a Thermokarst Subarctic Peatland 11

- 2.1 Introduction 11
- 2.2 Materials and Methods 15
  - 2.2.1 Experimental Design Overview 15
  - 2.2.2 Study Site and Soil Sampling 15
  - 2.2.3 Extraction and Incubation Procedures 18
  - 2.2.4 Peat Core Properties 20
  - 2.2.5 Statistical Techniques 21
- 2.3 Results 22
  - 2.3.1 Peat Core Properties 22
  - 2.3.2 Extractible Nutrient Pools 24
  - 2.3.3 Ammonium Mineralization 25
  - 2.3.4 Nitrate Mineralization 27
  - 2.3.5 Phosphate Mineralization 28

2.3.6 Relationships Between Peat Properties and Mineralization Rates 30
2.4 Discussion 30
2.5 Conclusions 35
2.6 Acknowledgments 36
Chapter 3 : Seasonal Dynamics in Shallow Freshwater Pond-Peatland Hydrochemical Interactions in a Subarctic Permafrost Environment 37
3.1 Introduction 37
3.2 Methods 40
3.2.1 Study Site 40
3.2.2 Research Design 42
3.2.3 Monitoring of Hydrometeorological Variables 43
3.2.4 Water Chemistry 45
3.2.5 Determination of Peat Hydrophysical Properties 46
3.2.6 Statistical Techniques 46
3.3 Results 47
3.3.1 Hydrophysical Properties 47
3.3.2 Seasonal Frost Table and Water Table Evolution 48
3.3.3 Runoff Generation 51
3.3.4 Groundwater Chemistry 55
3.3.5 Pond Hydrology and Chemical Trajectories 58
3.4 Discussion 61
3.4.1 Hydrology 61
3.4.2 Hydrochemistry 65
3.5 Conclusions 68
3.6 Acknowledgements 69
Chapter 4 : Capturing Temporal and Spatial Variability in the Chemistry of Shallow Permafrost Ponds 71
4.1 Introduction 71
4.2 Methods 75

4.2.1 Study Site and Sampling Design 75
4.2.2 Water Chemistry Sampling and Analysis 79
4.2.3 Statistical Techniques 80
4.3 Results 82
4.3.1 Spatial and Temporal Variability of Pond Chemistry 82
4.3.2 Seasonal Patterns in Pond Water Chemistry 85
4.3.3 Pond Hydrology and Linkages with Water Chemistry 87
4.3.4 Principal Component Analysis 90
4.3.5 Event-Scale Variation in Pond Chemistry 92
4.4 Discussion 94
4.4.1 Seasonal and Spatial Variability in Pond Chemistry 94
4.4.2 Event-Scale Variation in Pond Chemistry 96
4.4.3 Inferring Hydrological and Biogeochemical Process from Patterns in Pond Chemistry 97
4.4.4 Implications for Sampling Design in Future Studies 99
4.5 Conclusions 101
4.6 Acknowledgments 104
Chapter 5 : Effects of Contemporary Thermokarst Shoreline Expansion on Nutrient Dynamics and Diatom Ecology in a Subarctic Tundra Pond 105
5.1 Introduction 105
5.2 Materials and Methods 108
5.2.1 Study Site 108
5.2.2 Sediment Core Collection 109
5.2.3 Core Chronology 110
5.2.4 Sediment Core Nutrient Analysis 111
5.2.5 Diatom Analysis 112
5.3 Results 113
5.3.1 Hydroclimatic Conditions Preceding the Thermokarst Event 113
5.3.2 Sediment Composition and Nutrients 114

        5.3.3 Diatom Assemblages 115
    5.4 Discussion 117
    5.5 Conclusions 123
    5.6 Acknowledgments 124
Chapter 6 : Conclusions 125
Bibliography 128
Appendix A: 161
Appendix B: 162

List of Figures

Figure 1.1 Organization of this thesis with regards to spatial components of the pond-peatland complex system of the Hudson Bay Lowlands 9

Figure 2.1 Pictures showing four major landscape units in this study: (a) peat plateau, (b) sedge lawn, (c) channel fen, and (d) thermokarst collapse scar. 17

Figure 2.2 Peat properties through depth in each of the four landscape units: loss-on-ignition as a proxy for organic content, percent carbon by mass, percent nitrogen by mass, and percent phosphorus by mass in sample. Error bars for loss-on-ignition data are the standard deviation of three replicate samples... 23

Figure 2.3 Extractable nutrient pools of soluble reactive phosphorus, ammonium, and nitrate for each landscape unit through depth. Error bars represent the standard deviation of triplicate extractions. 25

Figure 2.4 Ammonium mineralisation rates at each landscape unit (panels) and depth (y-axis), showing the effects of both temperature (shape) and moisture (colour) treatments, with each point and bars showing the mean and standard deviation of four experimental replicates. ... 27

Figure 2.5. Nitrate mineralisation rates at each landscape unit (panels) and depth (y-axis), showing the effects of both temperature (shape) and moisture (colour) treatments, with each point and bars showing the mean and standard deviation of four experimental replicates. ... 28

Figure 2.6 Phosphate mineralisation rates at each landscape unit (panels) and depth (y-axis), showing the effects of both temperature (shape) and moisture (colour) treatments, with each point and bars showing the mean and standard deviation of four experimental replicates. ... 29

Figure 3.1 Map of the study site with different hydrological response units highlighted, located within the Hudson Bay Lowlands region, Manitoba, Canada. 43

Figure 3.2 Distribution of peat hydrophysical properties from all HRUs with depth: (a) Bulk Density; (b) Porosity; (c) Specific Yield; and (d) Saturated Hydraulic Conductivity. Saturated hydraulic conductivities were determined both in the horizontal (black symbols) and vertical (white symbols) directions. 48

Figure 3.3 Daily precipitation, hourly water level and bi-weekly frost table development relative to the peat surface in three HRUs from May to October 2014. Error bars represent the standard error of all measurements taken at different wells within an HRU, relative to the peat surface. 50

Figure 3.4 Pond response in Strange and Sandwich Ponds as a function of storm*-maximum water level for all snow-free seasons from August 2012 to October 2015. *A storm event was chosen as a period of less than 48 hours with at least 8 mm of precipitation. Any event producing less than 8 mm of precipitation over 48 hours did not generate runoff. 53

Figure 3.5 Relationship between storm event* size and runoff generation August 2012 – October 2015 grouped by number of hydrological response units demonstrating storage threshold exceedance. *A storm event was chosen as a period of less than 48 hours with at least 8 mm of precipitation. Any event producing less than 8 mm of precipitation over 48 hours did not generate runoff. 54

Figure 3.6 Water level exceedance curves for each HRU relative to the peat surface for May – October 2014, with periods during which the frost table was within 20 cm of the surface highlighted (solid black line) in comparison to the remainder of the year when the frost table was deeper than 20 cm beneath the surface (dotted line). 55

Figure 3.7 Groundwater chemistry in each HRU. Shallow groundwater was sampled from piezometers screened at 10 cm intervals between 5 and 25 cm below the peat surface and deep groundwater was from piezometers screened at 10 cm intervals between 35 and55 cm below the peat surface. Depth-integrated groundwater was sampled from wells screened through the entire depth. 57

Figure 3.8 Seasonal trajectory of pond stage in Strange Pond and Sandwich Pond with daily precipitation from May to October 2014. 59

Figure 3.9 Seasonal trajectory of pond chemistry in (a) Strange Pond and (b) Sandwich Pond from May to October 2014. 60

Figure 4.1 Site map of the general near-coastal tundra region with the catchment areas containing Frisbee, Larch, Strange, Sandwich, Left, and Erin Ponds. Inset map highlights the entire Hudson Bay Lowlands (dark-coloured region to the south of Hudson Bay) and the Churchill study region (indicated with an arrow). Map data: Google, Digital Globe, 2017. . 78

Figure 4.2 Boxplots of spatial and temporal proportional deviations for each chemical species. Significant differences between medians ($p < 0.01$) are present for all species on the left side of the panel (Cl^-, SO_4^{2-}, Na^+, K^+, Ca^{2+}), and no significant difference is present for species on the right (DON, Mg^{2+}, NH_4^+, NO_3^-).. 83

Figure 4.3 Pond normalized concentrations of all measured chemical species in each pond and precipitation for the 2015 snow-free season. In chemical species on left side of the panel (Cl^-, SO_4^{2-}, Na^+, K^+, Ca^{2+}) temporal variation exceeds spatial variation, and no significant difference is present for species on the right (DON, Mg^{2+}, NH_4^+, NO_3^-). 86

Figure 4.4 Precipitation (vertical bars, top panel), as well as depth of water column (continuous line) and runoff depths (vertical bars) in each of the instrumented study ponds over the 2015 ice-free season... 88

Figure 4.5 Comparison of the stage-concentration relationship in a (a) hydrologically driven chemical species (Cl^-, in Frisbee Pond), and (b) a non-hydrologically driven species (NH_4^+, in Larch Pond)... 89

Figure 4.6 Principal components analysis of chemical concentrations in all ponds throughout the 2015 snow-free season. The sampling date corresponds to the colour ramp with earlier dates in blue and later dates in red. PC1 primarily corresponds with the hydrologically driven chemical species while PC2 corresponds to inorganic nitrogen species (NO_3^-, NH_4^+). The hollow symbols are highlighted with solid points. 92

Figure 4.7 Short term variation in DON, Cl^-, SO_4^{2-}, and NO_3^- concentrations in (a) Frisbee pond and (b) Strange Pond during a rain event on July 3rd to 6th, 2015 (DOY 185-188, highlighted with red bars). 93

Figure 4.8 Graphical summation of major findings from this study: (a) factors driving hydrological control of particular chemical species in ponds, (b) hypothesized factors driving temporal coherence in chemical species in ponds, and (c) short-term variation in hydrochemistry can exceed seasonal-scale variation despite the large difference in timescales. 103

Figure 5.1 Frisbee pond basin; the undisturbed pond perimeter prior to the thermokarst event is highlighted in a thick black outline while the extent of the thermokarst shoreline slump is evident in the photo Imagery was obtained from DigitalGlobe, and was collected on July 29, 2014. Inset map highlights the entire Hudson Bay Lowlands (dark coloured region to the south of Hudson Bay) and the location of Frisbee pond (indicated with an arrow). 109

Figure 5.2 ^{137}Cs activity and ^{210}Pb activity through depth, interpolated CRS age-depth model, and sedimentation rate through time for the Frisbee Pond core. The timing of the thermokarst event is highlighted with a red outline. 112

Figure 5.3 Summer (June, July and August; JJA) air temperature and annual precipitation in the Churchill region, 1947 - 2015. Total annual precipitation is shown as bars, while the cumulative departure from the long-term (1947 – 2015) precipitation mean (167.0 mm) is shown as a solid line. Mean annual air temperatures 1946 – 1990 are shown as black dots, while temperatures 1990 – 2016 are shown as open circles. The thermokarst event is highlighted with a red outline. 114

Figure 5.4 Carbon, nitrogen, phosphorus, and diatom accumulation rates in the sediment core from Frisbee pond (~1940 to 2015), with isotopic composition of carbon and nitrogen. The thermokarst event of 2006-2008 is highlighted with a red outline. 115

Figure 5.5 Relative diatom abundance through the sediment core, with the thermokarst event highlighted as the gray dotted line at the 2 cm depth. Only species with relative abundance of >1% are shown. 117

List of Tables

Table 2.1 Targeted and measured values of moisture and temperature conditions, reported as mean (standard deviation)... 20

Table 2.2 Stoichiometry of major nutrients in different landscape units and depths 23

Table 3.1 Precipitation and runoff amounts for 4 study years in Strange and Sandwich Ponds. *Indicates total during study period, not for entire calendar year. **A storm event was arbitrarily chosen as a period of less than 48 hours with at least 8 mm of precipitation........ 52

Table 4.1 Physical characteristics and locations of study ponds near Churchill, Manitoba. *Shoreline development, D_L, is the ratio of measured shoreline perimeter, P, of a given pond to the shoreline perimeter of a perfectly circular pond of equal area, A, such that $DL = P2\pi A$ (Aronow, 1982).. 78

Table 4.2 Correlation coefficients among ponds for all chemical species. Values are bolded when the correlation is significant at the $p < 0.01$ level. 83

Table 4.3 Correlation coefficients among chemical species for all ponds. Values are bolded when the correlation is significant at the $p < 0.01$ level. 85

Table 4.4 Values of β_2 and root mean square error (S) from the curve $[\boldsymbol{x}] = [\boldsymbol{x_{st}}][\boldsymbol{x_s}] = \boldsymbol{\beta_1}(\boldsymbol{stage})^{\beta_2}$ for each set of normalized concentration data, $[\boldsymbol{x}]$. Chemical species were manually classified as hydrologically driven if they shared a common (approximate) β_2 value within a pond with a low S relative to other species in the same pond. Notable exceptions to the general classification in the table heading are bolded... 89

Chapter 1: Introduction

Permafrost, the state of a soil remaining less than 0 °C for two consecutive years, occurs in up to 25% of the terrestrial northern hemisphere (Anisimov & Nelson, 1997) and almost half of the Canadian land extent (Canadian Cryospheric Information Network, 2017). The spatial distribution of permafrost is driven by elevation, continentality, and latitude, with increasing coverage of permafrost poleward, in continental North America and Eurasia, and alpine environments. Climatic changes over previous millennia have resulted in changing global permafrost extent (Vandenberghe et al., 2014), while current anthropogenic-driven climatic warming continues to result in permafrost loss, including the projected elimination of all current sporadic and discontinuous permafrost in central Canada by 2100 (Camill, 2005). The thawing of permafrost has several globally important ecological implications, including changes to carbon emissions (Schuur et al., 2013) and surface water quality (Petrone et al., 2006; Frey & McClelland, 2009).

Wetlands are common features in permafrost environments due to permafrost impeded drainage and low evapotranspiration rates (Woo, 2012), dependent on both water supply and a relatively shallow frost table to inhibit deep infiltration (Woo & Young, 1998). Given the prerequisite conditions for formation, wetland hydrologic storage and transport processes in permafrost regions are frequently governed by "fill-and-spill" dynamics, described by Spence and Woo (2002, 2003) for a site in subarctic Canada near Yellowknife, Northwest Territories (62°N). Fill-and-spill systems are characterized by a series of storage units divided by topographic features, each serving a storage function until its storage capacity is exceeded and excess water spills into the next storage unit in the elevational sequence. Quinton et al. (2003) studied five basins in the Mackenzie basin and determined the runoff from each basin was controlled by fill and spill dynamics, where basins covered with flat bogs produced the least runoff. Flat bogs have great storage capacity, which is rarely exceeded (a prerequisite to the spill component of fill-and-spill), where storage in channel fens is easily exceeded, illustrating how runoff generation source area changes over time as a function of surficial and subsurficial topography reaching storage capacity (Quinton et al., 2003).

The presence of permafrost in cold regions strongly influences the hydrology of these catchments, as groundwater flows, plant root water access, and evapotranspiration are typically restricted to water seasonally held in the small active layer zone (Woo &Winter 1993). In seasonally frozen landscapes, interactions with deeper groundwater are facilitated by the annual downward migration of the frost table to a state of complete thaw. These conditions can govern the existence of longevity of wetlands in permafrost environments compared to seasonally frozen ground (Woo & Young, 2003). Interactions between the active layer and subpermafrost water are rare, and the lack thereof is among the central distinguishing features of the hydrology of permafrost systems (Woo, 2012). This segregation of zones occurs from the blocking of pores in saturated media by ice, which lowers the effective hydraulic conductivity of the media by several orders of magnitudes (McCauley et al., 2002).

Peat-accumulating wetlands are common in permafrost systems due to the slow decomposition rates related to both poor drainage (leading to oxygen-poor, saturated conditions) and low average soil temperatures (Woo, 2012). Woo and Young (1998) showed that the porous peat layer associated with wetlands lowers the thermal conductivity in the summer, insulating the ground from summer heating, resulting in a decreased active layer thickness in the wetland than in the adjacent mineral soil areas, a product of the insulating material and also the necessary conditions for wetland formation. Given the favorable environment of permafrost regions for peat accumulation, peat stratigraphy and community succession have been used to demonstrate that permafrost terrain is sensitive to climatic changes and subject to natural cycles of variability through thermal and moisture regimes (Zoltai, 1993).

In organic-covered permafrost environments, ecological productivity (and thus rates of peat aggradation and long-term carbon storage) is typically nutrient-limited (Cargill & Jefferies, 1984; Shaver & Chapin, 1980). There appears to be spatial and temporal heterogeneity in the relative importance of N and P as limiting, or co-limiting, factors for ecological productivity. Factorial addition studies have shown N and P to be co-limiting (Baddeley et al., 1994; Haag, 1974), particularly in the long-term (Zamin & Grogan, 2012). However, other studies report N (independent of P) as the key terrestrial growth limiting nutrient tundra systems (Mack et al., 2004; Weintraub & Schimel, 2005). Given this apparent uncertainty regarding the relative importance of N and P in limiting growth in different environments, currently understanding dynamics of both nutrients is important to predict ecological consequences of changing nutrient availability.

The supply of bioavailable nutrients in northern peatlands is largely governed by the rates of mineralization of nutrients from bound organic to available mineral forms, as this flux frequently represents the most substantial portion of the annual bioavailable nutrient budgets (Malmer and Nihlgård, 1980; Stark, 2007). Many factors control mineralization rates including hydrology, oxygen availability, and biochemistry of particular microbes (Robinson, 2002; Schuur et al., 2007). Soil and air temperatures may be the most important limiting factor of microbial decomposition rate of soil organic matter (Wallenstein et al., 2009; Jones et al., 2009). Annual enhanced microbial activity from both increased temperatures (increased rate) as well as a longer snow-free season (increased active timeframe) will generally result in increased liberation of N and P in bioavailable forms (Weintraub & Schimel, 2005). However, the role of moisture conditions throughout the peat column in these wetlands also exerts a strong control on biogeochemical cycling and the turnover of nutrients in peatlands (Reddy & DeLaune, 2008). Increased fluctuations in water table position and moisture storage likely result in an increases in mineralization (Lipson et al. 2012) and nitrification-denitrification (Fisher and Acreman, 2004), as well as enhance phosphatase activity and could result substantial release of phosphate (Song et al., 2007; Venterink et al., 2002). Given the combined effects climatic change is likely to have on soil moisture and temperature regimes, additional research focusing on the joint effects of warming and wetting/drying on nutrient mineralization is required to project future nutrient turnover and availability.

Hydrological transport is the primary pathway for redistribution of dissolved and suspended species of nutrients on many spatial scales (Schlesinger & Bernhardt, 2012). In permafrost systems, antecedent moisture and ground frost conditions play a large role in determining the degree and intensity of runoff generation. Dugan et al. (2009) observed that two summer storms in a high Arctic basin at Cape Bounty, Nunavut (74°N) produced a runoff ratio of 0.74, but runoff was contingent on soil storage satisfied by either ground ice melt or abundant precipitation. Vegetation cover is capable of also being a factor in mitigating runoff generation; Kane et al. (2004) observed a runoff ratio of 0.41 in the Low Arctic at Imnavait, Alaska (67°N). In this environment, a complete tundra vegetative cover, thicker active layer allowing deep storage, and greater summer evaporative capacity work in concert to deplete basin moisture and attenuate runoff in comparison to high Arctic basins. This hydroecological linkage further underscores the importance of feedbacks between hydrology, nutrient supply, and vegetation productivity. Future work is needed to understand the role of runoff hydrology in redistributing nutrients and the role of seasonal frost and permafrost controls the timing and access of flow pathways both in terms of runoff quality and quantity.

Flat topography and flow restrictions in permafrost peatlands frequently result in small terminal ponds in patterned ground, ribbed fens, headwater lakes, and other lentic surface water bodies in either closed basin or flow-through systems (Boike et al., 2008; Laurion et al., 2010; Duguay & Pietroniro, 2005). The majority of surface water features in permafrost landscapes are typically shallow and small (< 1 ha; Muster et al., 2013). These small water bodies have less total storage capacity than larger temperate systems and thus are sensitive to climatically-driven changes in pond hydrology and nutrient cycling. These small ponds have disproportionately large (relative to their size) rates of carbon cycling (Abnizova et al., 2012), and storage (Macrae et al., 2004), as well as act as indicators of past, present, and future climate change (Liljedahl et al., 2016; Smol et al., 2005). Given the frequent limitation of primary production by availability of nutrients in aquatic permafrost systems (Levine & Whalen, 2001; Burpee et al., 2016), there have been recent calls for further understanding of the controls on nutrient dynamics in these ponds (Koch et al., 2018) on multiple timescales to project future feedbacks between climatic change and pond carbon exchange. Typically, inorganic nutrient species in permafrost ponds are depleted throughout the snow-free period as they are consumed and stored in autotrophic tissues and passed up through trophic levels (Hinzman et al., 1998). Generally, additional nutrient inputs to ponds incite phytoplankton growth, leading to a darkening of the water column and decreased light availability for phytobenthos from both organism growth and dissolved/suspended nutrient loadings (Rautio et al., 2011). These organisms typically dominate pond ecology and significantly contribute to nutrient uptake in ponds during pulse input events (Eichel et al., 2014; Symons et al., 2012). Given the potential for sensitive temporal changes to pond chemistry in these highly chemodynamic systems, research into the relative temporal and spatial variability of hydrologic controls on pond chemical concentrations is required. This research gap further relates to earlier research gaps on the ability of the catchment to contribute nutrients through supply (mineralization) and transport (runoff) processes.

The presence of permafrost in peatlands is a driver of landscape geomorphology (Woo, 2012), resulting in formations such as palsas (e.g., Kershaw & Gill, 1979), pingos (e.g., Burr et al., 2009), and regular patterned peat plateaus (Kessler & Werner, 2003). All of these cryomorphic features are subject to catastrophic disturbance if the underlying or neighbouring permafrost is lost due to climate warming (Riordan et al., 2006). Yoshikawa and Hinzman (2003) examined recently formed thermokarst ponds as a result of permafrost decay and their interactions with taliks in discontinuous permafrost near Council, Alaska (64°N). As thermokarst ponds grew and increased in storage capacity, this coincided with the formation of taliks contiguous to the ponds providing an internal drainage mechanism and causing the ponds to shrink throughout the snow-free season. The thermokarst-driven perturbation of natural pond hydroecology, including the sum of changes to nutrient cycling and transport processes, requires urgent understanding under the future of a warming subarctic climate projected to rapidly increase thermokarst occurrence.

The Hudson Bay Lowlands are North America's largest contiguous wetland complex and are distributed across areas of continuous, discontinuous, and sporadic permafrost. In this ecoregion, 25-40% of the land surface is covered by shallow water bodies (Duguay and Lafleur, 2003). These ponds range from 400 m^2 to 0.04 km^2 in surface area and from 0.1 to 1 m in depth (Macrae et al., 2004). These ponds play important roles in surficial energy balance (Petrone et al., 2008), water budget (Boudreau and Rouse, 1995), supporting diverse benthic communities (Bonilla et al., 2005) and carbon cycling and storage (Macrae et al., 2004). The small and shallow nature of ponds in the Hudson Bay Lowlands renders them vulnerable to hydroclimatic stresses. Macrae et al. (2014) review the implications of a changing climate to pond sustainability in the HBL through instrumental records collected 1943-2009, modeling of two periods (1953-2009; 1961-2100), and remote sensing/imagery analyses of available data from 1947-2008, concluding that ponds in this region are not vulnerable to drying and may instead be at risk for great expansion due to a lack of evaporation increase coincident with increases in precipitation. In addition to stressors of direct climate forcing, Payette et al. (2004) found a dramatic increase of features indicative of permafrost decay in a subarctic peatland in the Hudson Bay Lowlands from 1957 to 2003, including thermokarst ponds and plateau collapse scars.

1.1 Objectives and Approach

To understand the future trajectory of permafrost peatlands and their role in global climate, a combination of field observations and modelling studies of the influence of climate-induced hydrologic change on supply, transport, and fate of nutrients is required. The objective of this thesis is to understand the hydrology and biogeochemistry of shallow pond-peatland complexes in the Western Hudson Bay Lowlands under the context of a changing climate. The specific objectives are to:

1. experientially investigate the impact of changing temperature and moisture regimes on nutrient mineralization in different peatland landforms;
2. determine how moisture storage and annual frost table development control runoff generation processes both in terms of quality and quantity;
3. examine temporal and spatial variability in ponds and determine the extent to which hydrology drives these variations; and
4. elucidate the effects of recent thermokarst shoreline expansion on nutrient deposition and diatom production in a shallow pond.

1.2 Outline of Thesis

This thesis is organized into components, by chapter, corresponding to several distinct scientific studies which comprise the entire body of work. The introduction, Chapter 1, provides a broad overview of the themes throughout the thesis: specifically, hydrology and biogeochemistry of permafrost peatland systems and recent climatic and environmental changes across these regions. Chapters 2-5 are the results and exploration of direct field and laboratory based research focused on the hydrology and nutrient biogeochemistry of several patterned pond-peatland catchments in the Hudson Bay Lowlands, integrating different spatial components of the pond-peatland complex system (Figure 1.1).

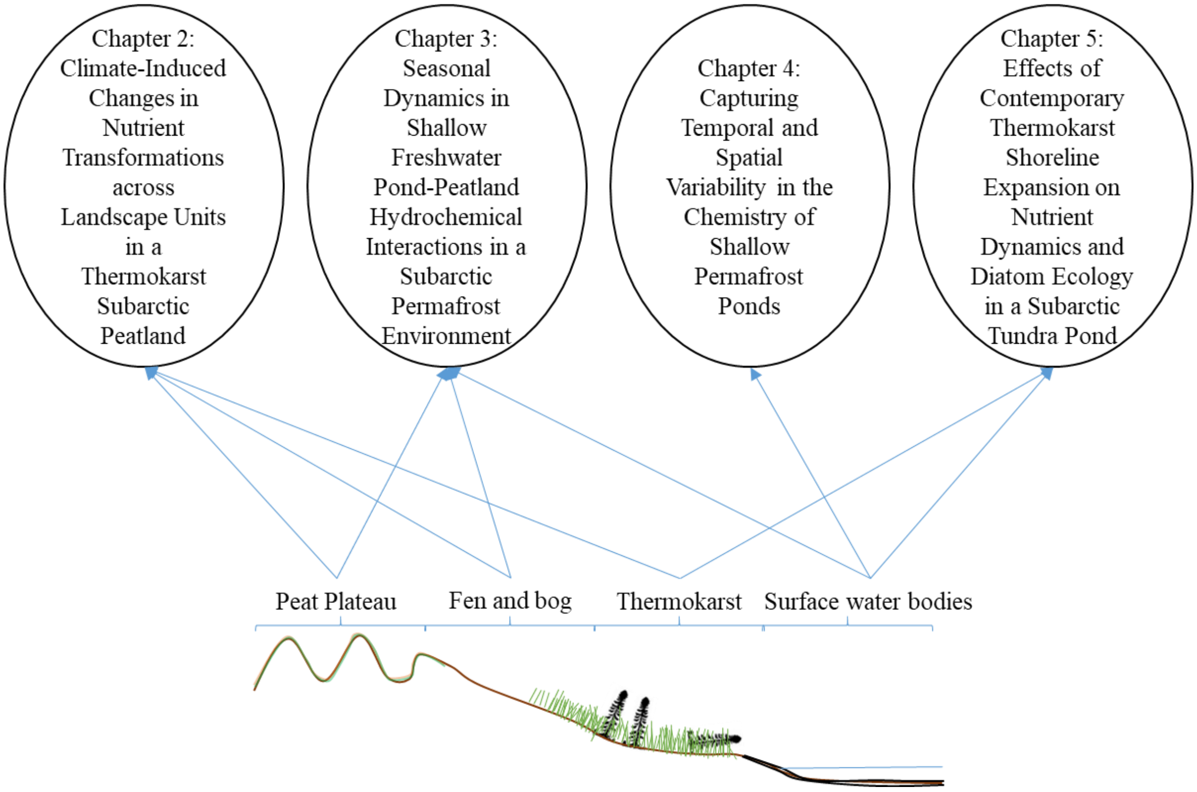

Figure 1.1 Organization of this thesis with regards to spatial components of the pond-peatland complex system of the Hudson Bay Lowlands

A laboratory-based experiment to investigate the combined effects of temperature and moisture on nitrogen and phosphorus transformations across landscape units is presented in Chapter 2, addressing objective 1. The catchment-scale runoff hydrology and seasonal hydrochemical linkages between catchments and ponds is presented in Chapter 3, addressing objective 2. The role of hydrology in driving seasonal pond chemical concentration trajectory and spatial synchronicity is presented in Chapter 4, addressing objective 3. A paleolimnological investigation of nutrient and carbon sedimentation as well as shifts in diatom ecology in a recently-disturbed thermokarst pond is presented in Chapter 5, addressing objective 4. Chapter 6 summarizes and concludes the central work of this thesis, incorporating both the results from the individual chapters as well as a brief synthesis of the greater themes and major findings of the whole body of research.

Chapter 2: Climate-Induced Changes in Nutrient Transformations across Landscape Units in a Thermokarst Subarctic Peatland

2.1 Introduction

Many northern cold-region landscapes are favourable environments for the accumulation of peat (Kuhry & Turunen, 2006) where the decomposition rate of organic matter is retarded by low mean annual soil temperatures and prolonged anoxia due to a perched water table overlying relatively impermeable permafrost (Woo, 2012). The insulating properties of peat are favourable for the development and preservation of underlying ground frost (Vitt et al. 1994; Woo & Young, 2003). Climatic changes, and in particular warming global temperatures, are projected to be amplified at northern latitudes where permafrost peatland coverage is currently widespread (Callaghan et al. 2010; Cohen et al. 2014; Kaufman et al. 2009). Long-term observational evidence has shown that permafrost has thawed extensively in the past century (Payette et al. 2004; Jorgenson et al. 2006) and is projected to continue to do so (Schaefer et al. 2011; Schuur et al. 2013; Lawrence et al. 2012). Recent permafrost degradation has been shown to change both hydrologic pathways (Walvoord & Kurylyk, 2016, Connon et al. 2014) as well as carbon (C) cycling regimes (Schuur et al. 2008). However, the potential for changes to nutrient cycling from climatic changes and permafrost thaw are less constrained (Vonk *et al*., 2015), and have important implications for further modifying the ecological and C storage functions of northern ecosystems.

In northern peatlands, the internal cycling of nutrients stored in organic matter often represents a much larger fraction of an annual nutrient budget than external inputs and total export (Malmer & Nihlgård, 1980). The supply of nutrients plays a large role in C cycling and peat accumulation rates, as peat-forming terrestrial biomass and aquatic productivity are typically chiefly limited by nitrogen (N) and phosphorus (P) (Symons et al. 2012, Shaver & Chapin, 1980; Cargill & Jefferies, 1984). However, the low annual average soil temperatures in northern peatlands limit the rates at which biogeochemical processes occur (Stark, 2007). Generally, microbial decomposition remains the rate limiting factor in nutrient cycling (Andersen et al. 2013). Thus, soil and air temperatures are often the limiting factors dictating the rate of microbial decomposition of soil organic matter in cold regions (Wallenstein et al. 2009; Jones et al. 2009; Uhlirova et al. 2007). It is predicted that enhanced soil microbial activity from both increased temperatures (increased rate) as well as a longer snow-free season (increased active period) will result in the increased liberation of N and P in bioavailable forms from organic matter (Weintraub & Schimel, 2005; Brown & Braaten, 1998). Experimental warming of boreal and arctic soils has increased soil inorganic N and P pools (Schimel et al. 2004; Natali et al. 2011) through increased ammonification, nitrification, and P mineralisation (Rustad et al. 2001). Temperature projections for northern regions show increases in temperature between 1°C and 10 °C, varying across space and seasonally; however, changes to precipitation regimes are less certain and more variable across space (Bintanja & Andry, 2017). As such, some regions may become drier and others may become wetter. Moreover, with permafrost thaw resulting in geomorphic disturbance, previously dry upland areas may become ephemerally or permanently saturated (Payette et al. 2004). Although the individual effects of changes in moisture or temperature on nutrient transformations have been examined, less is known about the combined effects of simultaneous moisture and temperature manipulations on net mineralisation rates.

Typically, the unsaturated zone maintains oxic conditions dominated by efficient aerobic processes resulting in high decomposition rates (Golovchenko et al. 2007). With a drawdown in water table, increase in unsaturated zone depth (Roulet et al. 1992; Macrae et al. 2013) and associated additional oxygen supply in drier soils, there will be an increase in available plant nutrients resulting from products of oxidation of organic matter. Loss of soil structure through permafrost and ground ice thaw may lead to the development of thermokarst collapse scars, which can facilitate the transport of nutrients and solutes from areas that would otherwise be hydrologically inaccessible (Jorgenson & Osterkamp, 2005; Lafrenière & Lamoureux, 2013). These geomorphic disturbances have the potential to expose deeper portions of the soil profile (typically inundated and suboxic/anoxic) to oxic conditions when exposed to the surface. As peat is generally a poor thermal conductor, surface peat is most responsive to air temperatures while deeper peat is less sensitive. However, with thermokarst activity, deeper portions of the soil profile may warm and dry rapidly when exposed to the surface climate through structural disturbance. These hydrologic changes may alter nutrient transformations in a manner which depends on the consistency and duration of new moisture regimes. For example, repeated drying-wetting cycles enhance phosphatase activity and may therefore result in the release of phosphate (Song et al. 2007). Alternatively, sustained drying followed by rewetting can decrease phosphorus supply as a result of increased metal complexing (Richardson et al. 1985). In the case of nitrogen, sustained drying as well as re-wetting cycles can result in large increases to ammonification and denitrification rates, respectively (Venterink et al. 2002). Sustained wetting, can also lead to elevated N and P mineralisation by increasing heat transfer through increased thermal conductivity and elevated temperatures (Lipson et al. 2012). Thus, while the effects of changing moisture conditions on nutrient cycling are complex, it is necessary to consider the effects of temperature and moisture regime changes in tandem rather than in isolation from one another due to their natural linkages.

The rate and climatic controls of nutrient mineralisation through organic matter decomposition are strongly related to the quality of the litter parent material and recalcitrance, and consequently are not uniform through heterogeneous patterned landscapes (Van Breemen & Finzi, 1998; Eppinga *et al*., 2010). The partitioning of peatland ecosystems into landscape units is a common practice to understand how biogeochemical dynamics vary with topography and hydrological responses (Allan *et al*., 1993; Quinton *et al*., 2003) and can be used to study how different elements on the landscape, and their differing litter parent material, contribute to whole-system nutrient cycling. Thus, it important to determine how peat biogeochemical properties vary between depths and landscape unit position, and further, to determine which properties are the key drivers in nutrient mineralisation responses to temperature and moisture conditions. To address these needs, the objectives of this study were to: (1) assess the variability in nutrient pools (total and extractable) between different landscape units and through depth in a thermokarst-impacted permafrost bog; (2) experimentally determine the individual and combined effects of temperature and moisture on net mineralisation rates of N and P; and (3) determine if and how these controls differ as a function of litter quality.

2.2 Materials and Methods

2.2.1 Experimental Design Overview

Four replicate peat cores were collected and sectioned into three depths (0 – 10 cm, 10 – 20 cm, >20 cm) at each of four landscape units (collapse scar, channel fen, sedge lawn, peat plateau) in a subarctic peatland catchment. Using a factorial design, peat subsamples were subjected to three temperature (4, 12, and 20 °C) and three moisture (air dry, field moist, saturated) treatments and incubated for three weeks in a controlled laboratory setting to determine net mineralisation rates of NO_3^-, NH_4^+, and PO_4^{3-} under the different conditions.

2.2.2 Study Site and Soil Sampling

The study site is a peat plateau bog near Churchill, Manitoba (58°48' N, 94°09' W) in the catchment of a lake in a recent thermokarst shoreline collapse expansion state. The climate of the region is strongly influenced by its proximity to Hudson Bay (Rouse, 1991) and is underlain by near-continuous permafrost with an active layer depth ranging from 40 cm to 1 m (Dyke & Sladen, 2010). Four landscape units were selected in the catchment that were representative of the variability in topographic, vegetative, and moisture conditions in the region, following a classification scheme and approach of Quinton *et al* (2003) (Figure 2.1). Fen channels (FC) are characterized by near-surface saturation and may develop in frost wedge polygon cracks or as diffuse pathways over land (Woo & Young, 2006). Fen channels are dominated by *Carex aquatilis* and *Plagiomnium spp*. Sedge lawns (SL) are intermediary zones between upland frost-driven landforms and low-lying FCs. Given the transitional nature of SL, a wide variety of vascular plants (e.g. *Vaccinium, Rubus,*), sedges (*Carex mitis*), mosses (primarily *Dichranum* with some *Sphagnum*), and lichens (*Cladina, Cetraria spp.*) may be present, in addition to the presence of sparse tree islands (*Picea mariana, Picea glauca, Larix laricina*; Mamet & Kershaw, 2013). Peat plateaus (PP) are dry upland areas developed via frost action between peat and underlying substrates (Sannel & Kuhry, 2009). In contrast with the dominance of *Carex* spp. in FC and SL landforms, *Carex* are absent in PP and vegetation communities are instead lichen-heath communities (*e.g. Empetrum, Rubus, Dichranum, Cladina, Cetraria, Vaccinium, Ledum,* with some *Salix*). The collapse scar (CS) is a thermokarst feature examined in this work is a collapsed upland area encompassing the shoreline of the small lake resulting from inundation and enhanced heat conduction leading to the failure of soil structure through permafrost thaw. In this region, thermokarst features often develop adjacent to existing pond edges and are either bare of any living vegetation or colonized by *Carex* spp, and characterized by the presence of dying trees (Payette & Delwaide, 2000). In this landscape, catchment pore water is generally higher in dissolved nutrient concentrations than surface water, with most dissolved inorganic N occurring as NH_4^+ (<0.01 to 0.57 mg NO_3^--N L^{-1}, <0.01 to 4.17 mg NH_4^+-N L^{-1}, <0.01 to 1.12 mg soluble reactive P L^{-1} in groundwater, <0.01 to 0.50 mg NO_3^--N L^{-1}, <0.01 to 1.12 mg NH_4^+-N L^{-1}, <0.01 to 0.02 mg soluble reactive P L^{-1} in surface water; Morison et al., 2017).

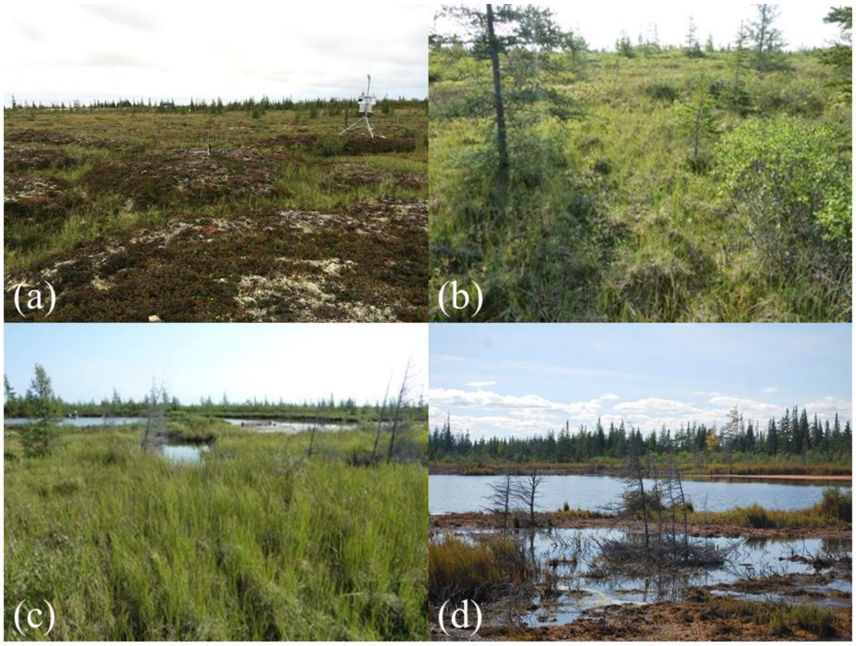

Figure 2.1 Pictures showing four major landscape units in this study: (a) peat plateau, (b) sedge lawn, (c) channel fen, and (d) thermokarst collapse scar.

Soil samples were collected from September 19-21, 2015, to capture a period when the seasonal ground frost had fully thawed and to facilitate the collection of the entire active layer. A 10.16 cm interior diameter PVC core was inserted from the surface until frozen ground was encountered at four sampling sites within each landscape unit (16 cores in total, four sites for each of four landscape units). Cores were packed on ice and stored at -4 °C to simulate winter freezing conditions until being gradually thawed over seven days at 4 °C, following Kelley et al. (2012). In the laboratory, each core was then sectioned into three depths: (1) 0 – 10 cm, (2) 10 – 20 cm, and (3) greater than 20 cm depth, with the total depth varying between cores, the shallowest core being 45 cm and the deepest being 75 cm. The four spatial samples for each landscape unit at each depth were composited (three depths at four landscape units) following Chambers *et al* (2004) and DeBusk & Reddy (1998) to maintain representatives from multiple sites within each landscape unit, while providing an estimation of central tendency of the population (Boone et al., 1999; Osborne & DeLaune, 2013). All visible roots were manually removed from samples, and all samples were manually blended in sealed plastic bags until visibly homogenous. This compositing technique, although a form of pseudoreplication (Davies & Gray, 2015), has been employed previously in laboratory incubation studies measuring nutrient mineralisation (Austin & Vitousek, 1998; Whalen et al., 2001; Long et al., 2017) to explore differences in treatments, rather than within-site differences. While within-landscape unit heterogeneity in nutrient mineralisation rates requires further investigation to fully understand ecosystem nutrient cycling, this was not the primary aim of this study.

2.2.3 Extraction and Incubation Procedures

In the laboratory, 5 g (field moist mass) of each peat sample was extracted in 50 ml of either 2 M KCl (for NO_3^- and NH_4^+) or deionized water (for water extractable phosphorus) by shaking at 350 rpm for one hour on an orbital shaker table and then gravity filtered through 2.5 μm filter paper (Whatman No.4). Analytical triplicates of each of the 12 soil groups were immediately extracted to determine nutrient pools prior to incubation.

Four analytical replicates of 5 g from each soil group were then incubated aerobically in darkness in a sterile plastic cup in one of nine different treatment groups (3 temperatures x 3 moisture conditions) for a 21-day period (n = 4 analytical replicates x 12 soil groups x 3 temperatures x 3 moisture treatments = 432 samples incubated). Temperature levels were set at 4, 12, and 20 °C in separate growth chambers with HOBO temperature loggers deployed to monitor deviations from the target temperature. Three moisture conditions were attained in each soil group by (1) air-drying the soil for 24 hours in a ventilated area with paired sealed control samples exposed to the same room temperature for pre-incubation extraction comparisons, (2) maintaining field moisture conditions, and (3) wetting to saturation with deionized water. Temperature and moisture contents remained within the targeted values throughout the incubation period (Table 2.1) and fell within the range of values recorded through one season (May to September, 2014) of *in situ* weekly monitoring of surface (0 – 5 cm) temperature and moisture values at the study site where the cores were collected. Gravimetric moisture content of each soil group at each of the three moisture conditions was determined by oven-drying at 95 °C for 24 hours. During the 21-day incubation period, samples were weighed every 48 hours and re-wetted with deionized water to their initial weight to replace moisture lost to evaporation, with total wet sample mass change never exceeding 10% over a 48-hours period. Following incubation, samples were extracted in the same manner as the paired samples prior to incubation.

At the University of Waterloo Biogeochemistry Laboratory, extracted samples were analyzed for nitrate, ammonium, and orthophosphate concentrations using colorimetric methods (Bran-Luebbe AutoAnalyzer III, Seal Analytical: Methods G-102-93, (NH_4^+-N); G-103-93 (SRP-P), G-109-94 (NO_3^--N)). Results for NH_4^+, NO_3^-, and soluble reactive P have a detection limit of 0.001 mg N L^{-1} or 0.001 mg P L^{-1}. No samples were below the detection limit during analysis of ammonium and orthophosphate. During nitrate analysis, when a sample was determined to have a concentration below the detection limit (0.001 mg N-NO_3^- L^{-1}, which occurred in 14% of samples) the concentration was assumed to be half of the detection limit (0.0005 mg N-NO_3^- L^{-1}) for the purposes of determining net nitrification rates which did not represent a substantial error in the calculation. The mineralisation rate was calculated as the difference between the concentration of incubated sample extract, normalized per gram of dry soil, and the concentration of initial extract, normalized per gram of dry soil. Extractable pools of N and P in soil are expressed as mass of N or P per mass of dry soil, while net mineralisation rates are expressed as mass of N or P per mass of dry soil per incubation day.

Table 2.1 Targeted and measured values of moisture and temperature conditions, reported as mean (standard deviation)

Target Moisture	Actual Moisture (% wet mass)	Target Temperature (°C)	Actual Temperature (°C)
Air Dry	71.7 (5.2)	4	4.2 (0.2)
Field Moist	83.4 (4.4)	12	12.2 (0.1)
Saturated	89.2 (1.7)	20	21 (1.1)

2.2.4 Peat Core Properties

Subsamples from each soil group were analyzed for organic content using loss on ignition (LOI), where homogenized samples were heated to 550 °C for 4 hours following a drying stage of heating to 95 °C for 24 hours, following Heiri et al. (2001). Additional subsamples were freeze-dried, ball-milled, and analyzed for bulk composition of total C and N at the University of Waterloo Environmental Isotope Laboratory through a 4010 Elemental Analyzer (Costech Instruments) and for total P through the digestion method of Parkinson & Allen (1975) and subsequent analysis of digested P as phosphate through standard colorimetric methods at the University of Waterloo Biogeochemistry Laboratory (Bran-Luebbe AutoAnalyzer III, Seal

Analytical: Method G-103-93). Using 5% duplicate analytical replicates throughout all steps of the method, data for total C and N both show analytical precision of <1% (average of 0.2% and 0.3%, respectively), while total P data showed an average analytical precision of 1.8%.

2.2.5 Statistical Techniques

To address the first objective of this study, I ran a one way analysis of variance (ANOVA; F-statistic) of all phosphate, nitrate, and ammonium mineralisation rate data using landscape unit as the fixed factor. To address the second objective, I ran a two-way ANOVA of all net mineralisation rate data using temperature (4, 12, and 20 °C) and moisture (air dry, field moist, saturated) treatments as fixed factors. In each case, data were tested for normality (with a Shapiro-Wilk test) and homoscedasticity. If these assumptions were not met, a nonparametric two-way ANOVA on ranks (Scheirer-Ray-Hare test; H-statistic) was used instead. Following each ANOVA, provided there was a significant effect of an individual factor without a significant interaction term between factors, post-hoc comparisons were assessed with a t-test (if data were normally distributed) or Mann-Whitney U test (if data were not normal), with a Bonferroni adjustment for the number of comparisons. To address the third objective of this study and determine the control of initial extractable nutrient pools and total nutrient stoichiometry (totals and ratios of N, P, C) on mineralisation rates, Pearson product moment correlations were performed between mineralisation rates and these soil properties.

Due to a contamination error in one subsample in the experimental design (peat plateau, 0 – 10 cm depth subsample for analysis of water-extractable phosphorus assigned to air dry and 20° C treatments), this sample was removed from all analyses. All statistical analyses were conducted with R software (version 3.3.2, R Development Core Team, 2016).

2.3 Results

2.3.1 Peat Core Properties

Organic content (as $\mathrm{LOI}_{550°C}$) generally decreased with depth (from 0 cm to >20 cm) in all landscape units from ~90% in surface peat to 78% in material deeper than 20 cm (Figure 2.2). Organic content was greatest in PP, least in CS, and intermediate in SL and CF at all depths. Total C generally decreased with depth (from 0 cm to >20 cm) in all landscape units, and was least in SL and greatest in PP. Total N varied most with depth in PP (from 1.1% to 3.5%) but was more consistent through depth in SL (mean of 1.9 ± standard deviation of 0.2 %), CF (1.9 ± 0.1), and CS (2.3± 0.3). In shallower material (0 – 10 cm and 10 – 20 cm), SL and CF had greater total P than PP and CS but all landscape units had similar total P in deep material. C:N ratios fluctuated most with depth in PP (ranging from 12 to 44), and were less variable across other landscape units (all other values ranging from 17 to 26). C:N ratios were greatest in the surface peat (0 – 10 cm) in all other landscape units except PP (Table 2.2). N:P ratios tended to be greatest in CS in surface samples (0 – 20 cm), driven by low P content, while neither N:P or C:P ratios appear to have a consistent pattern through depth across landscape units.

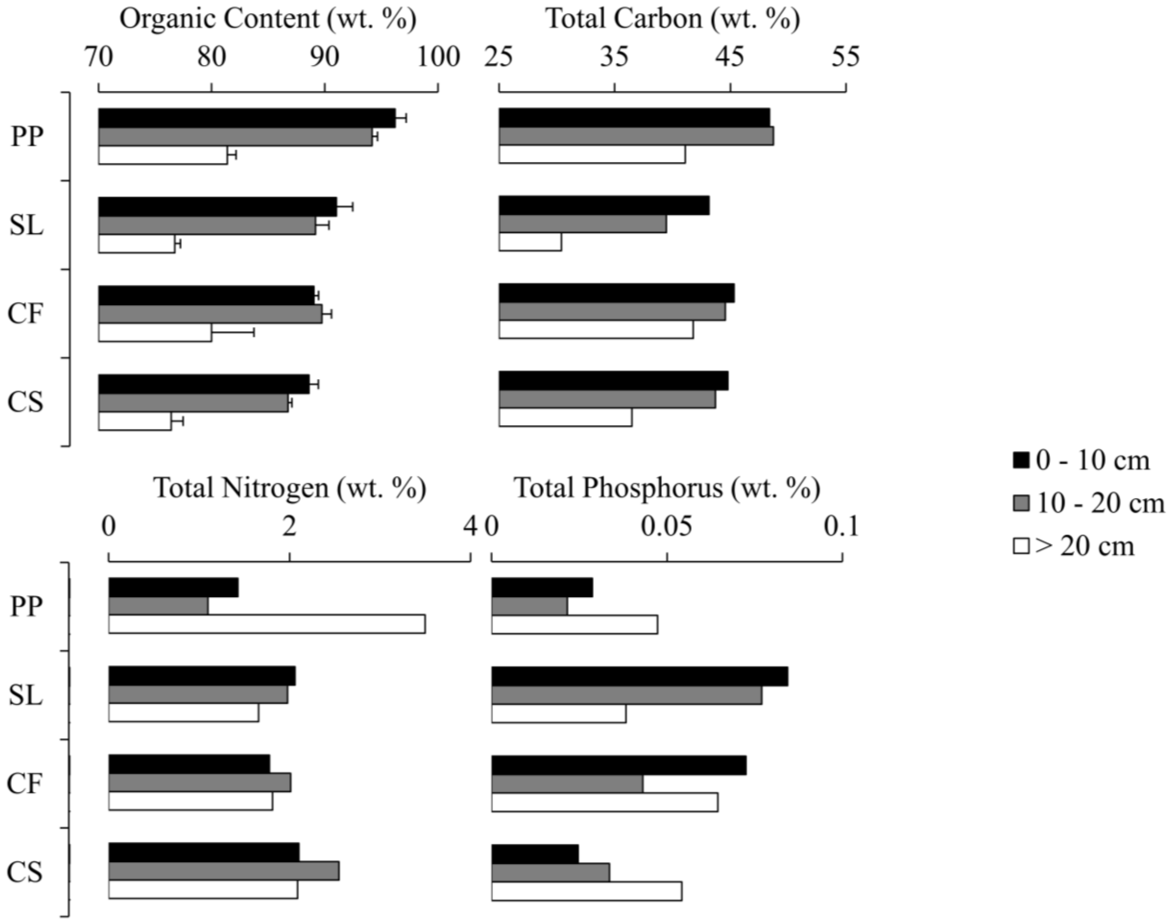

Figure 2.2 Peat properties through depth in each of the four landscape units: loss-on-ignition as a proxy for organic content, percent carbon by mass, percent nitrogen by mass, and percent phosphorus by mass in sample. Error bars for loss-on-ignition data are the standard deviation of three replicate samples.

Table 2.2 Stoichiometry of major nutrients in different landscape units and depths

Landscape Unit	Depth	C:N (g g^{-1})	N:P (g g^{-1})	C:P (g g^{-1})
Peat Plateau	0 – 10 cm	34	50	1686
	10 – 20 cm	44	51	2255
	> 20 cm	12	74	869
Sedge Lawn	0 – 10 cm	21	24	511
	10 – 20 cm	20	26	513
	> 20 cm	18	43	794
Channel Fen	0 – 10 cm	26	25	625

	10 – 20 cm	22	47	1034
	> 20 cm	23	28	648
Thermokarst	0 – 10 cm	21	85	1813
	10 – 20 cm	17	76	1301
	> 20 cm	17	39	673

2.3.2 Extractible Nutrient Pools

In the pre-incubated extracted samples, the inorganic N pool was dominated by NH_4^+ (Figure 2.3). Across all soil groups an average of 95% of total inorganic N (TIN; NH_4^+ + NO_3^-) was NH_4^+ with two major exceptions, surface peat (0 – 10 cm) in CF and deep material (> 20 cm) in PP, which had appreciable nitrate concentrations. Other samples had little detectable NO_3^- (< 0.1 μg N – NO_3^- g^{-1} dry soil). Extractable NH_4^+ pools tended to decrease with depth and increase along a moisture gradient in landscape units (lowest in PP, greatest in CS). Extractable P pools were greatest in surface peat (0 – 10 cm) driven by high concentrations in CF (16.4 ± 8.2 μg P – PO_4^{3-} g^{-1} dry soil) and PP (4.4 ± 1.1 μg P – PO_4^{3-} g^{-1} dry soil).

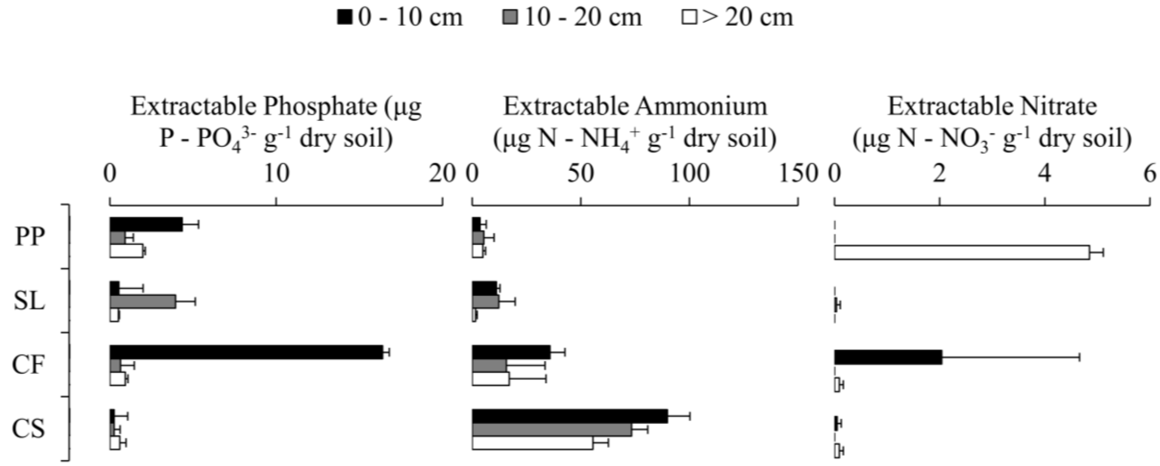

Figure 2.3 Extractable nutrient pools of soluble reactive phosphorus, ammonium, and nitrate for each landscape unit through depth. Error bars represent the standard deviation of triplicate extractions.

2.3.3 Ammonium Mineralization

Net ammonification varied by landscape position and depth where CF and CS had much more variable responses to treatments than the drier areas (PP and SL; Figure 2.4). With the exception of the surface layer in the CS, the median net ammonification rates across all treatments were zero or slightly below zero. In most but not all cases across the treatments, saturation favoured negative rates whereas dry conditions favoured positive rates; however, this was most apparent in the wetter areas (CS, CF) and very subtle in the dry (PP, SL) areas. A notable exception to this was the surface layer in the CF, which showed the reverse pattern (i.e. net ammonification under saturated conditions). Temperature did not change these overall relationships, but instead appeared to amplify them in these two landscape units, although the responses to temperature were variable within the moisture treatments. For example, in the wet areas (CF, CS), negative ammonification observed under saturated conditions was greatest in warm peat and dampened in cold peat. In contrast, the positive net ammonification observed under the dry treatment was greatest for cold peat and dampened in warm peat. These differences with temperature were not observed for the drier (PP, SL) areas. In general, CS material displayed the widest response (both negative and positive net ammonification) through depth and across treatments compared to non-disturbed peat. CS displayed the greatest range of response to temperature and moisture treatments within each depth category. There was a significant effect of moisture ($H_{2,96} = 7.664$, $p < 0.001$) with air drying treatments resulting in significantly greater net ammonification than saturated ($p < 0.01$) or field moist ($p < 0.001$) samples, with no significant effect of temperature or interaction between temperature and moisture effects. There was also a significant effect of landscape unit ($H_{3,96} = 6.445$, $p < 0.001$) with a significantly lesser (negative rate) median in CF than all other landscape units ($p < 0.05$ in each case), and no significant differences among PP, SL and CS ammonification rates.

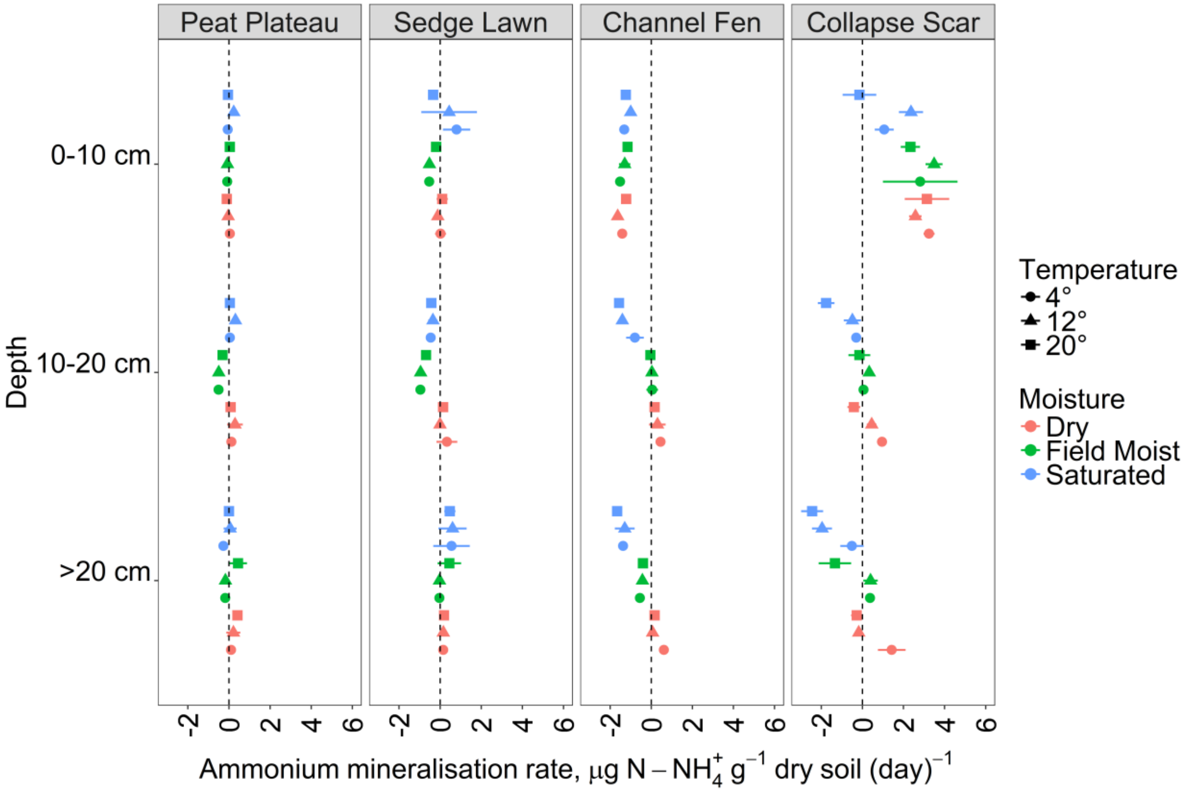

Figure 2.4 Ammonium mineralisation rates at each landscape unit (panels) and depth (y-axis), showing the effects of both temperature (shape) and moisture (colour) treatments, with each point and bars showing the mean and standard deviation of four experimental replicates.

2.3.4 Nitrate Mineralization

Across all treatments, landscape units, and depths, net nitrification was generally low (typically close to zero; Figure 2.5). No appreciable negative nitrification was observed (study-wide minimum value of -0.005 mg N g dry soil^{-1} over the entire 21-day incubation period). There was very low net nitrification (< 10 µg N g^{-1}) in PP and SL, and minimal (primarily < 2 µg N g^{-1} d^{-1}) responses to treatments in CF material. Net nitrification in the CS material generally increased at all three depths, although muted at 10-20 cm depth, and only for the 20 °C treatment in the field moist and saturated samples. There were no significant individual effects or interactions of temperature and moisture treatments. Marginal changes were observed for dry samples or cooler temperatures across most landscape units and depth. There was a significant effect of landscape unit ($H_{3,96} = 17.051$, $p < 0.001$), with significantly higher nitrification occurring in both CF and CS than PP and SL ($p < 0.01$ in each case).

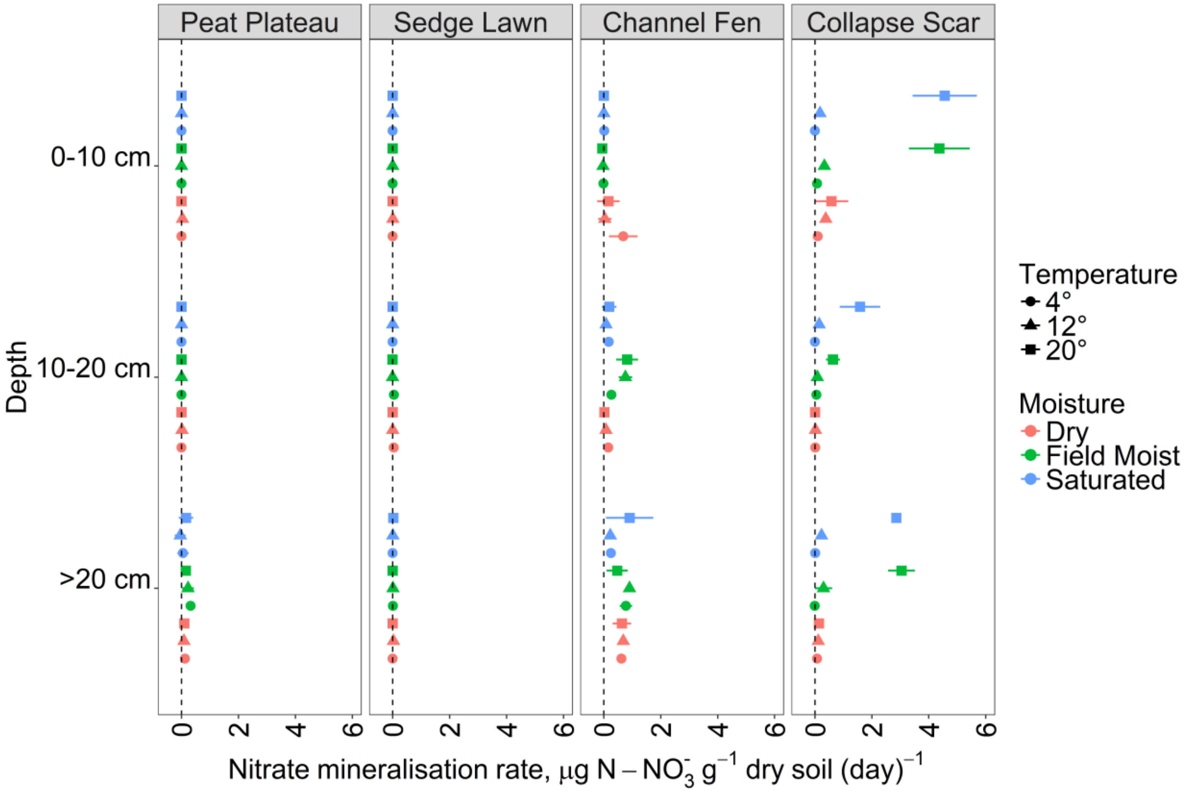

Figure 2.5. Nitrate mineralisation rates at each landscape unit (panels) and depth (y-axis), showing the effects of both temperature (shape) and moisture (colour) treatments, with each point and bars showing the mean and standard deviation of four experimental replicates.

2.3.5 Phosphate Mineralization

Overall, net P mineralisation was very low, typically close to zero, with the exceptions of surficial material (0 – 10 cm) in PP and CF landscape units, and in SL material at 10 – 20 cm (Figure 2.6). Similar to net ammonification, there was a mixed response to treatments with both negative and positive net P mineralisation rates, with a significant effect of landscape unit ($H_{3,96} = 11.950$, $p < 0.001$). There was significantly more negative P mineralisation in PP, SL and CF than CS ($p < 0.001$ in each case), but no significant differences among PP, SL and CF net P mineralisation rates. Both PP and CF had different phosphate transformations under dry conditions than were observed in field moist or saturated treatments; however, the changes observed differed in direction between the two units. In the surface (0 – 10 cm) PP, drying marginally increased net phosphate mineralisation, whereas in surface CF, drying led to marginally more negative rates (Figure 2.6) although moisture and temperature did not have significant main effects or interaction.

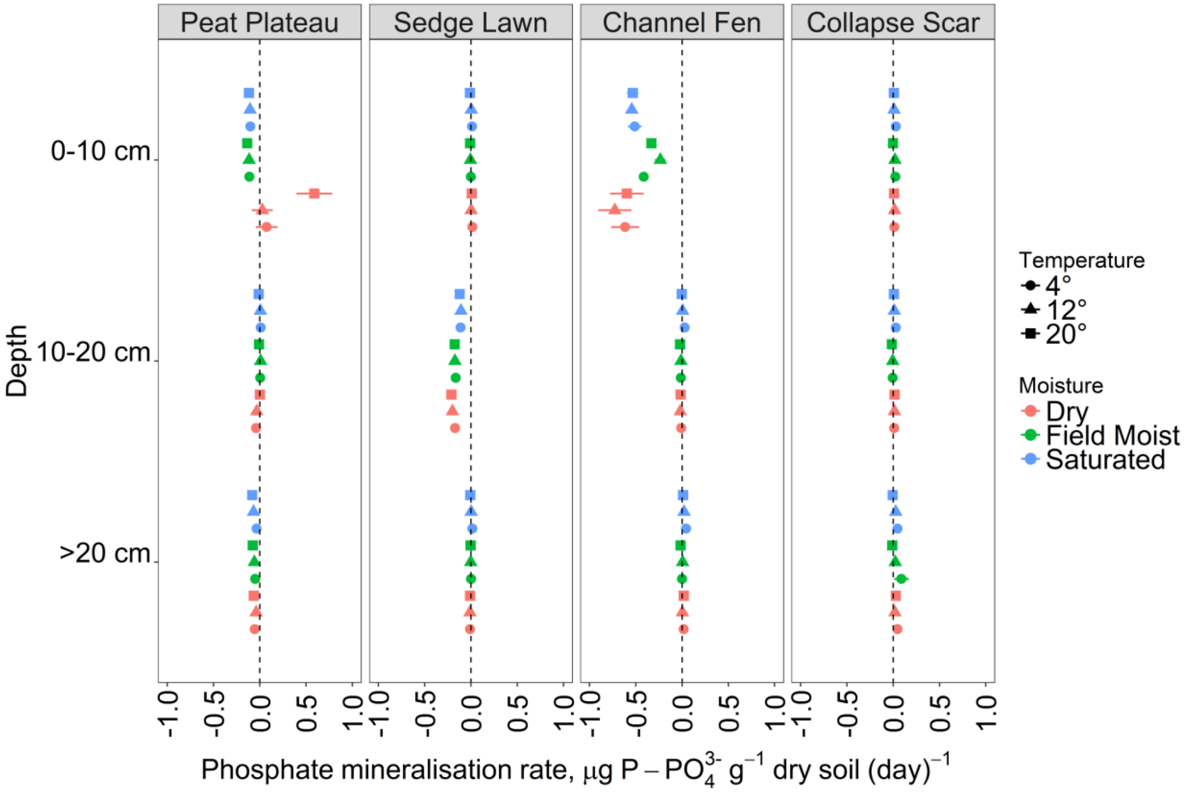

Figure 2.6 Phosphate mineralisation rates at each landscape unit (panels) and depth (y-axis), showing the effects of both temperature (shape) and moisture (colour) treatments, with each point and bars showing the mean and standard deviation of four experimental replicates.

2.3.6 Relationships Between Peat Properties and Mineralization Rates

There was a significant positive relationship between the initial ammonium pool and the net nitrification rate (*r* = 0.77, *p* < 0.010), indicating the potential for nitrification of ammonium under oxic conditions. There were no other significant relationships between either net nitrification or ammonification with either initial extractable ammonium or nitrate pool size or total N. The presence of an appreciable initial water extractable phosphorus pool was significantly negatively related to P mineralisation rates (*r* = -0.96, *p* < 0.010), but did not significantly correlate with total P content.

2.4 Discussion

Extractable nutrient pools varied between landscape units and depth in this study, with the majority of TIN as NH_4^+, which tended to decrease with depth and increase downslope across landscape units. Extractable P pools were greatest in surface peat and diminished with depth. Temperature did not have a significant effect on any net mineralisation rates in this study, while moisture had a significant effect on net ammonification. In each of net ammonification, nitrification, and P mineralisation, there was a significant effect of landscape unit on cycling rates. There were two strong relationships between extractable pools and mineralisation rates: a strong positive relationship between the initial ammonium pool and the net nitrification rate, and a strong negative relationship between the initial extractable phosphate pool and net P mineralization rate.

The significant correlation between the initial extractable pool of NH_4^+ and the net nitrification rate suggests that available ammonium may be readily nitrified under oxic conditions. This result, primarily as changes to extractable ammonium as opposed to nitrate, is consistent with results reported in field based studies conducted by Rosswall & Granhall (1980), Williams & Wheatley (1988) and Bayley et al. (2005). Similarly, in a lab-based study under oxic conditions, Venterink et al. (2002) found that an increase in extractable nitrate in dried soils was attributed to increased ammonification and nitrification, not decreased denitrification, in which soil drying stimulated net total N mineralisation (3 times higher) and reduced denitrification (5 times lower) compared to continuously wet soils, and that re-wetting may significantly increase P availability. In contrast, Macrae et al. (2013) found that drying conditions decreased net nitrification rates across the landscape, but did not affect net PO_4^{3-} mineralisation rates. In this study, the greatest negative rates of P mineralisation corresponded to the biggest initial pools of PO_4^{3-} (Figure 2.6), and changes to net P mineralisation with moisture or temperature were not observed in landscape units with low initial PO_4^{3-} pools.

Both net ammonification and net nitrification rates in our study are comparable with results from a wide range of both field-based and laboratory-based investigations of N and P mineralisation in northern peatland and subarctic tundra soils, when normalized to a gravimetric and per day basis (Appendix A, Table A.1). In our study, CF and PP show both negative and positive net mineralisation of phosphate in surface peat which is within the upper range/orders of magnitude of other peatlands, comparable to a set of natural and harvested fen and bog sites in the Netherlands (Verhoeven et al., 1990), Canadian western boreal plains (Wood *et al*., 2016), and tundra/heath systems in Alaska (Nadelhoffer *et al*., 1991). As well, in collapse scar material in this study, which is absent in previous mineralisation studies, the potential for extreme nitrification rates under different temperature and moisture treatments indicate distinct N dynamics in thermally disturbed material from undisturbed landscape units in this study and studies from across other Boreal and Northern environments. The difference in magnitude of rates between our study and others may also be related to length of incubation period and initial decomposition status. Decomposition and net mineralisation rates have been shown to be dynamic over time and thus average rates (normalised to a per day basis) will differ depending on the incubation length (Arunachalam et al. 1996). Thormann & Bayley (1997) show decreasing rates of decomposition over the course of a long-term incubation experiment (456 days) in a boreal peatland. This could potentially indicate that this relatively short-term study (and other studies of similar length) would capture, higher rates than long-term studies when rates are normalized to a per day basis, but this comparison is complicated by the fact that long-term in-situ incubations would be carried out across multiple seasons with changing temperature and moisture regimes. Our incubation period of 21 days is comparable with the shorter end of the range of incubation lengths of several other *in-situ* and laboratory studies (Table 2.3), which spans from a minimum of three weeks to multi-year incubations.

Given the strong relationships between initial extractable ammonium pools and nitrification rates as well as between phosphate pools and net P mineralisation, it is also important to contextualize extractable pool sizes within other comparable study regions. Values of extractable TIN pools that are reported in this study for our non-thermally-disturbed landscape units (PP, SL and CF) are comparable with ranges from several peatland and tundra sites (Table 2.3). The partitioning of TIN into NH_4^+ and NO_3^- in our study is similar to other Boreal peatland regions as well with the majority of TIN occurring as NH_4^+, as Wood et al. (2016), Andersen et al. (2013), and Macrae et al. (2013) all report NH_4^+ as >70% of TIN. The stratification of NH_4^+ with depth in our results in consistent with the findings of Williams &

Wheatley (1988) in a Scottish bog, attributed to similar stratification of decreasing concentrations of ammonifying bacteria with depth. In comparison with tundra communities, our extractable TIN pools are generally greater than results reported by Haag (1974) for a tundra birch-willow-heath system in Alaska of 0.5 to 1.0 µg N-TIN g^{-1}, although following fertilization experiments of up to 200 kg N ha^{-1}, their extractable nitrogen pools are comparable with our results. The collapse scar material in our study contained extractable NH_4^+ which were much greater than both the non-thermally-disturbed landscape units in this study (PP, SL and CF) as well as reported values from many comparable studies (Table 2.3). The water extractable P pool in this study is also similar to comparable environment with the exception of CF and PP surface peat (corresponding as well to anomalously high P mineralisation rates). All other extractable phosphate pools in our study are in the range of other permafrost environments, similar to our results in tundra heath (1 – 11 P-PO_4^{3-} g^{-1}) and sedge meadow (3 – 6 P-PO_4^{3-} g^{-1}) sites as reported by Haag (1974), as well as tussock/sedge tundra and heath systems (0 – 5 µg P-PO_4^{3-} g^{-1}) in Alaska as reported by Nadelhoffer et al. (1991).

The significant effect of landscape unit on net mineralisation of all nutrient species in this study indicates the varying response to similar environmental controls between different portions of ecosystems, which has been observed at the field scale (Bridgham et al. 1998; Mettrop et al. 2014). Further, there appeared to be an effect of depth within landscape units on nutrient cycling, such as the increased net nitrification experienced at surface (0 – 10 cm) and deep (> 20 cm) material in collapse scar material under warm and saturated conditions, but this effect was muted in the 10 – 20 cm material. There were differences in litter quality (total C:N:P ratios) in different landscape units and depths, but there were no significant relationships between total C, N and P and any of ammonification, nitrification, and P mineralisation rates. This suggests that there may be more complex factors, such as microbial community composition and the availability of C:N:P in more labile forms (as opposed to bulk totals) may be the key factors for determining mineralisation response to hydroclimatic drivers across landscape units and depth. Nutrient stoichiometric ratios of C:N:P in this study generally fell within the expected range for peatlands and tundra sites (Table 2.3). Wang et al. (2015) also report C:N values from 50:1 to 20:1 generally decreasing with depth for bog peat across a gradient of 400 peat profiles and peatland types in Ontario, where our study found an average C:N of 23:1. Our C:N values are generally slightly higher than most subarctic tundra environments (Kelley et al., 2012; Nadelhoffer et al., 1991) driven by larger organic carbon content due to peat accumulation in the Hudson Bay Lowlands. Our N:P and C:P ratios are also slightly greater than those reported in literature at peatland sites due to low total P concentrations in our samples (Table 2.3; Figure 2.2). The relationship of C:P is close to the critical quotient for net P loss of 800-1200 demonstrated by Moore et al. (2008) and the C:N ratios in this study are primarily below the critical quotient of 33-68 for net N loss.

This work did not address the relative magnitude of all individual components in net ammonification, nitrification, and P mineralisation, including microbial immobilization (Schmidt et al. 1999), denitrification (Aerts & Ludwig, 1997), and ammonia volatilization (Bouwman et al. 1997) although not all of these processes are expected to contribute fluxes of any considerable magnitude depending on the pH and oxic status (Skrzypek et al. 2015; Rosswall & Granhall, 1980). Through root removal and the absence of living vegetation, this study constrains some potential pathways for nutrient transformation such as plant uptake and biological atmospheric fixation, which are inherently present in field studies, and of non-negligible magnitude in northern environments (Stark, 2007). Further, other environmental processes, which are naturally incorporated in field-based studies are absent here on multiple timescales. On an annual scale, atmospheric deposition of nutrients (both wet and dry) and hydrologic transport pathways both play a central role in nutrient supply and redistribution in the environment (Eppinga et al. 2010; Rosswall & Granhall, 1980). On shorter time scales, diurnal temperature fluctuations and hydraulic redistribution can influence nutrient transport and cycling processes on short timescales, in contrast to the constant conditions maintained throughout the study period in this work.

2.5 Conclusions

This work has implications for future projections of nutrient dynamics in thawing permafrost ecosystems under a changing climate. Climatic changes will affect different components of the landscape distinctly, and thermokarst collapse scar material particularly has the potential for unprecedented nitrogen turnover under warm conditions, specifically, net ammonification in surface material and net nitrification under moist conditions. As existing and newly thawed collapse scars becomes exposed to oxic conditions, pulses of plant-available nitrogen in the form of ammonium may be mineralised at a rate higher than undisturbed sites in warmer and either dryer or wetter conditions. There appears to be a temperature and moisture-driven nitrification threshold in collapse scar material, which was activated only in the twenty-degree treatment and in the two moist treatments. When collapse scars become exposed to oxic conditions through soil structure disturbance or through a drawdown of the water table, increased net nitrification under warm and moist conditions may result in up to a 100x increase in extractable nitrate concentrations from initial extractable pools over a matter of weeks. These results show potential for substantial plant-available nitrogen release to a nutrient limited-environment, impacting both local basin and downstream systems depending on the hydrological transport potential. Phosphate concentrations were low across landscape units and depths, and was generally showed a negative mineralisation response under all temperature and moisture conditions and in all parts of the landscape, indicating the potential for microbial demand for the loosely-bound (water extractable) P pool. This suggests that phosphates liberated from decaying organic matter in permafrost peatlands may be rapidly immobilized into less labile pools, although process-based microbial ecology studies are required to understand the magnitude of this pathway. The significant effect of landscape unit controlling all mineralisation rates in this study has important implications for understanding the complex controls on N and P mineralisation potential, which likely are highly dependent on peat origin (landscape unit, depth) and chemical properties.

2.6 Acknowledgments

The funding for this research came from Natural Sciences and Engineering Research Council Discovery Grants (Macrae, Petrone), Natural Sciences and Engineering Research Council Northern Supplement (Petrone) and the Northern Scientific Training Program. I thank D. Gibson for field assistance and J. Williamson, H. Rogers, K. Lutes, V. Lam, W. Mark, J. Harbin, J. Plach and J. Cober for lab assistance.

Chapter 3: Seasonal Dynamics in Shallow Freshwater Pond-Peatland Hydrochemical Interactions in a Subarctic Permafrost Environment

3.1 Introduction

Northern peatlands contain vast stores of organic matter (Gorham, 1991) in the form of organic carbon (C), nitrogen (N) and phosphorus (P). Much attention has focused on the importance of organic C stored in peat and its potential to be cycled to the atmosphere as methane and carbon dioxide (McGuire et al., 2009; Roulet, 2000). However, less is known about the storage, transport, and cycling of N and P in these landscapes, despite the potential of N cycling to the atmosphere as nitrous oxide (Elberling et al., 2010; Repo et al., 2009; Marushchak et al., 2011). Further, both terrestrial and aquatic productivity are typically nutrient-limited in tundra ecosystems (Shaver & Chapin III, 1980; Verhoeven et al., 1996; Cargill & Jefferies, 1984), linking N and P cycles and transport with C cycling. Given that northern environments are particularly vulnerable to climatic change (Serreze et al., 2008; Hinzman et al., 2005), increased supplies of N via warming-induced peat mineralization (Lipson et al., 2012) and permafrost thaw (Keuper et al., 2012) are expected in terrestrial ecosystems under a warming climate. Little is known about the potential for P transfer under a warmer climate.

Biogeochemical processes and an increased supply of nutrients may be coupled with more efficient N and P transport in runoff due to hydroclimatic change (Harms & Jones, 2012; Frey & McClelland, 2009). At present, high latitude regions (e.g., Quinton & Pomeroy, 2006) have a nival climate in which snowmelt is the largest annual event for hydrochemical transport. With increased permafrost thaw and changes in regional precipitation patterns (Macrae et al., 2014; Hinzman et al., 2005; Shook & Pomeroy 2012), the contribution of runoff to surface water bodies may occur at times other than snowmelt throughout the snow-free season (Dyke & Sladen, 2010; Frey & McClelland, 2009), with runoff pathways moving deeper through the previously-frozen soil profile. It is unclear if changes in hydrologic connectivity and pathways among landscape units throughout the ice-free season will also result in enhanced nutrient mobilization in the landscape, and/or if changes in seasonal dynamics will modify the speciation of nutrients.

Environments at higher latitudes are comprised of patterned ground that influences and is influenced by hydrology. Work done in catchments with varying degrees of permafrost decay and associated geomorphic disturbance has identified long-term and short-term changes in chemical export regimes (Mack et al., 2004; Walvoord & Striegl 2007; Lewis et al., 2012; Abbott et al., 2015; Lamoureux & Lafreniere, 2014). However, the sources of mobilized constituents have not been clearly identified at subwatershed scales. In addition to terrestrial landscapes, shallow freshwater bodies have been the subject of interest due to their ubiquity in the landscape (Dyke & Sladen, 2010; Macrae et al., 2004), their control on the landscape energy balance (Eaton et al., 2010), their role as habitat for diverse ecological communities (Vonk et al., 2015), and, their capacity to store and exchange C (Macrae et al., 2004; Abnizova et al., 2012; MacDonald et al., 2014), N and P (Eichel et al., 2014; Wolfe et al., 2011; MacDonald et al., 2014). This C storage function (via primary productivity), as with terrestrial production, has been shown to be nutrient-limited in subarctic and arctic freshwater bodies (Levine & Whalen, 2001; Bergström et al., 2005; Bergström, 2010; Bonilla et al., 2005; Symons et al., 2012) although the conditions of N and P limitation are spatially variable (Hogan et al., 2014). Open water bodies in permafrost are sensitive to climatic changes that impact ponds both directly, through changing precipitation and evaporation, and indirectly, through changing catchment hydromorphology and runoff inputs (Walvoord & Kurylyk, 2016). Studies from across the circumpolar north have identified unprecedented rates of desiccation that may threaten the sustainability of these important ecosystem services provided by shallow ponds and lakes (Yoshikawa & Hinzman, 2003; Bouchard et al., 2013). In particular, in the Hudson Bay Lowlands, thermokarst expansions act as a mechanism for lateral seepage and loss (Payette et al., 2004) leading to increased connectivity among landscape units, also impacting seasonal chemical trajectories (White et al., 2014). Previous studies of the water balances of ponds in the Hudson Bay Lowlands have focused on atmospheric fluxes of water between ponds and the atmosphere (Boudreau & Rouse, 1995; Macrae et al., 2014), with less known on the capacity for baseflow and runoff generation (Macrae et al., 2004). Pond and wetland storage and transport processes in subarctic permafrost regions are known to be governed by "fill-and-spill" dynamics, described by Spence and Woo (2003), with a threshold moisture exceedance prerequisite for runoff generation (Ali et al., 2015). This non-linear runoff generation mechanism has been observed in a wide variety of both permafrost and non-permafrost environments with varying soil and bedrock conditions (Oswald et al., 2011; Phillips et al., 2011; Spence et al., 2010; Woo & Mielko, 2007; Wright et al., 2009).

A subwatershed approach has yet to be used to investigate linkages between hydrological mobilization and nutrient export. In this chapter, I characterize interactions between ground frost, runoff, and biogeochemical transport throughout the snow-free period in a subarctic permafrost pond-peatland system to address the following questions: (1) How is runoff generation into ponds across a range of peatland landscape units influenced by antecedent moisture storage and frost conditions? (2) Do groundwater N and P chemistry evolve seasonally within and across peatland landscape units, and is this reflected in seasonal pond chemical trajectories?

3.2 Methods

3.2.1 Study Site

The study site is located 24 km east of the town of Churchill, Manitoba (58° 72’ N, 93° 84’ W) in the Churchill Wildlife Management Area (CWMA), approximately 5 km inland from the coast of Hudson Bay. The regional climate is influenced by the close proximity to Hudson Bay (Rouse, 1991). Average air temperatures in the region (1980-2010 normals; Environment Canada, 2016) are -6.5°C (annually) with the snow-free season between June and October, average July temperatures of 12.7 °C, and average January temperatures of -26.0 °C. Annual average precipitation is 452.2 mm, with 44% of this precipitation (201.2 mm) occurring as snowfall between September and June. The region has experienced, and is expected to continue to experience, rapid warming coupled with an increase in liquid phase precipitation over the snow-free season (Macrae et al., 2014; Sauchyn & Kulshreshtha, 2008; Kaufman et al., 2009).

Churchill is approximately 100 km north of the southern boundary of continuous permafrost, with an average active layer depth ranging from 40 cm in dry upland peat plateaus to 1 m in saturated vegetated fen channels (Dyke & Sladen, 2010). The area has a very low regional topographic gradient of 1-1.5 m km^{-1} (Boudreau & Rouse, 1995), although local features such as polygonal peat plateaus are characterized by relief up to 1-2 m over surrounding fen (Dyke & Sladen, 2010). The Hudson Bay Lowlands are underlain by fine silts and clays of glaciomarine origin, deposited at the base of the Tyrrell Sea, with overlying moderately fibrous peat accumulation of 30-40 cm in the coastal region near Churchill with increasing peat thickness inland (Dredge, 1979; Dyke & Sladen, 2010). Regional geology has been influenced by glaciations, and is undergoing rapid isostatic rebound at a rate of 9.7 mm/yr (Wolf et al., 2006). Shallow ponds occupy up to 50% the landscape in the region, are typically less than 1 m in depth, ranging from 30 m to 1 km in diameter, and freeze completely to the bottom during winter (Macrae et al., 2014). Ponds are isothermal and aerobic because they are well-mixed by wind action (Bello & Smith, 1990). Some ponds are hydrologically disconnected from surrounding peats throughout much of the open water season (e.g., Macrae et al., 2004; Wolfe et al., 2011), whereas others appear to receive hydrologic inputs from adjacent landscape units (White et al., 2014; Wolfe et al., 2011). In general, many shallow ponds and their catchments are hydrologically isolated year-round from the larger regional watershed due to the low topographic gradient and shallow active layer restricting plateau-wetland-pond complexes from contributing to streamflow (Dyke & Sladen, 2010) or interacting with deeper groundwater (Macrae et al., 2004). Delineation of total contributing area for each pond is subject to uncertainty due to the complex microtopographic depressions, low landscape topographic gradient, and variable frost table topography.

Hydrological response units (HRUs) are a land-cover classification scheme based on topographic position and moisture regime. An HRU approach has been employed in northern wetlands to understand controls on water balance (Boudreau & Rouse, 1995), runoff (Pietroniro et al., 1996) and C cycling (Chasmer et al., 2012). In this study, an HRU approach is used to monitor frost table development, water table position, and groundwater chemistry within and between landscape positions. In the Hudson Bay Lowlands, three terrestrial HRUs representative of landscape variability in topographic position, water table response, and frost table development were selected, following terminology of Quinton et al. (2003). There is some small variation in these properties within each HRU, although the differences between each unit exceeded the variation within each unit. Fen channels (FC) are characterized by near-surface saturation and may develop in frost wedge polygon cracks or as diffuse pathways over land (Woo & Young, 2006). Fen channels are dominated by *Carex aquatilis* and *Plagiomnium* spp. Sedge lawns (SL) are intermediary zones between upland frost-driven landforms and low-lying channels FCs. Given the transitional nature of SL, a wide variety of vascular plants (e.g., *Vaccinium, Rubus,*), sedges (*Carex mitis*), mosses (primarily *Dichranum* with some *Sphagnum*), and lichens (*Cladina, Cetraria* spp.) may be present. The third HRU, peat plateaus (PP), are dry upland areas developed via frost action between peat and underlying substrates. Contrasted with the dominance of *Carex* spp. in FC and SL landforms, *Carex* are absent in PP and vegetation communities are lichen-heath communities (e.g., *Empetrum, Rubus, Dichranum, Cladina, Cetraria, Vaccinium, Ledum,* and some *Salix*).

3.2.2 Research Design

Two adjacent closed-basin catchments containing shallow ponds in the CWMA were selected for monitoring (Figure 3.1): Strange Pond (perimeter 424 m, area 6307 m^2) and Sandwich Pond (perimeter 548 m, area 17146 m^2). Ponds were selected as they have been the subject of previous studies and are representative of other ponds in the region (Macrae et al., 2004; White et al., 2014). Continuous water levels in peatlands and ponds were measured from 2012 to

2015. Manual frost table measurements and discrete measurements of water quality (nutrient concentrations) were measured in groundwater and ponds throughout 2014.

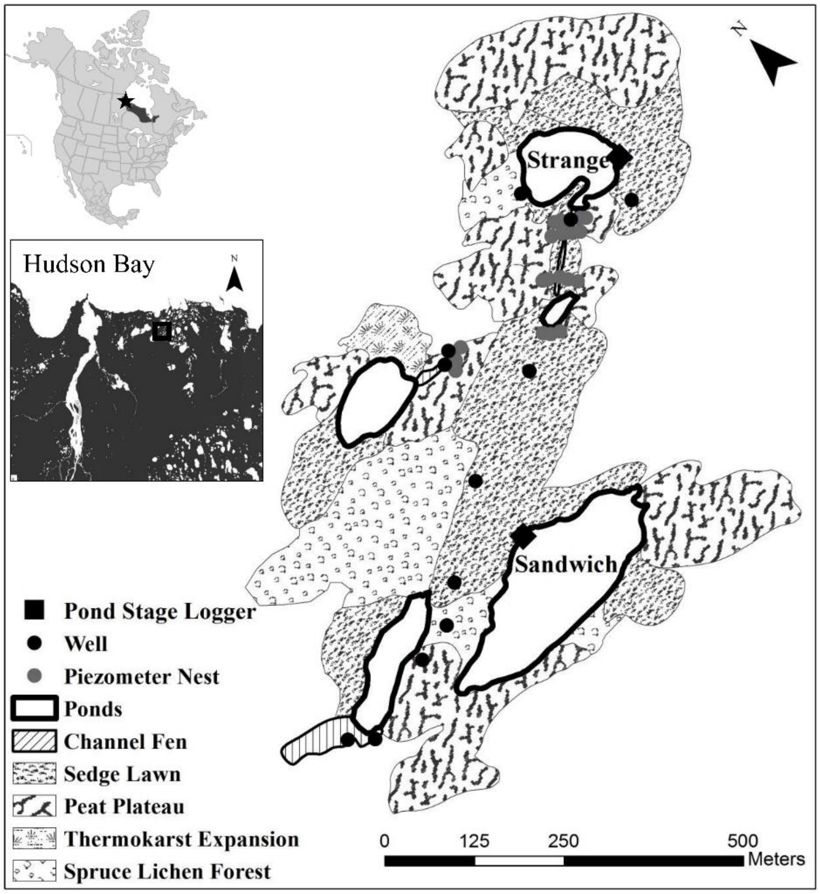

Figure 3.1 Map of the study site with different hydrological response units highlighted, located within the Hudson Bay Lowlands region, Manitoba, Canada.

3.2.3 Monitoring of Hydrometeorological Variables

Wells and piezometers were constructed using 2” interior diameter polyvinyl chloride pipes, with each nest consisting of a well (screened throughout total length) and up to five piezometers with a 10 cm screen (midpoints at 5, 15, 25, 35, and 45 cm) wrapped in a non-reactive fibreglass filter mesh. Piezometers were progressively installed throughout the 2014 snow-free season as the frost table deepened to allow insertion until further installations were prevented by an impenetrable substrate. A Juno SB handheld GPS (Trimble, USA; differentially corrected global accuracy of ± 5 m) was used to survey pond perimeters, and well and piezometer nest locations. Continuous hourly water level measurements were made between August 2012 and October 2012 and between May and October from 2013 to 2015 in Strange and Sandwich Ponds as well as in terrestrial wells spanning three HRUs, using pressure transducers (HOBO U20-001-01 Water Level Logger; Hoskin Scientific, Canada). A barometric logger was used to correct the submerged loggers and was housed in an identical well pipe directly beside Strange Pond to minimize differences in thermal regime between the barometric logger and water level loggers (McLaughlin & Cohen, 2011). Manual frost table measurements were taken in triplicate at each nest and well location biweekly throughout May to September 2014 with a steel rod until underlying substrate (glacial tills) prevented further use of the method.

Precipitation was measured from June 2013 to September 2014 with a tipping bucket rain gauge with a 0.2 mm tipping interval (Hobo Onset; Hoskin Scientific, Canada). For periods when the rain gauge was not installed, precipitation data from the Environment Canada Churchill station (20 km West of the study site) was used. A comparison between the Churchill airport daily rain data and the tipping bucket showed a reasonable agreement ($R^2 = 0.831$; adjusted $R^2 = 0.830$). Pond runoff response, R, was assumed to be the difference between the maximum change in pond storage, ΔS (from the hour previous to a rain event until up to 36 hours following the conclusion of a rain event), and the total precipitation for the storm, P, that is, $R = \Delta S - P$ during the storm event, assuming negligible evaporation during and immediately following rain events. This sign convention indicates a positive value as the quantity of water entering the pond, as opposed to the conventional $R = P - \Delta S$. Runoff, storage, and precipitation are reported as a depth over the pond surface and were determined for all precipitation events greater than 8 mm over a 48 hour period. An 8 mm threshold was chosen, since no event over the study period during which less than 8 mm of precipitation fell produced any measured runoff.

3.2.4 Water Chemistry

Samples of shallow groundwater and pond water were collected and placed in sterile, triple-primed 50 ml polyethylene containers. Pond water samples were collected approximately bi-weekly throughout the melt and snow-free season of 2014 (May to October). Piezometers were purged and allowed to recharge 48 hours prior to sampling to ensure representative groundwater chemistry. Polyethylene rain collectors were cleaned with deionized water and left open to collect rainwater samples over the course of rain events; they were closed while no wet deposition was occurring. Samples were preserved on ice in the field and passed through a 0.45 μm cellulose acetate filter within two hours of collection. A subsample was acidified to a final concentration of 0.2% H_2SO_4 (sulfuric acid), and subsequently digested (Kjeldahl method, Seal Analytical Hot Block Digestion System BD50) for the determination of total dissolved P (TDP) and total dissolved Kjeldahl N (TDKN). At the University of Waterloo Biogeochemistry Laboratory, samples were analyzed for N and P species using colorimetric methods (Bran-Luebbe AutoAnalyzer III, Seal Analytical: Method G-102-93, NH_4-N; G-188-097, TDP; G-189-097, TDN) and for chloride using ion chromatography (DIONEX ICS 3000, IonPac AS18 analytical column). Reported results for NH_4, TDN and TDP have a detection limit of 0.001 mg N L^{-1} or 0.001 mg P L^{-1}. Dissolved organic N (DON) was calculated as the difference between measured TDN-N and NH_4-N in a sample.

3.2.5 Determination of Peat Hydrophysical Properties

Peat cores were collected using 4” interior diameter polyvinyl chloride pipes in September 2014, at the near-maximum extent of active layer depth at six locations (coincident with transects of piezometer nests) at each HRU (six samples in each of FC, SL and PP). Minimal (<5mm) core compaction was observed. Cores were frozen and separated into increments of 10 cm depth. Cores were returned to the laboratory and thawed, and subsequently tested for a suite of hydrophysical properties (saturated hydraulic conductivity, bulk density, porosity, and specific yield) using standard laboratory techniques. Saturated hydraulic conductivity was determined for each 10 cm section in either vertical or horizontal orientation in the laboratory with a Ksat System (UMS GmbH, Munich, Germany) using the falling-head method (DIN ISO 18130-1). Saturated hydraulic conductivity values were normalized to 25°C. Bulk density was determined by dry weight over volume after samples were dried for 24 h at 95°C with no visible charring of the peat observed (O’Kelly & Sivakumar, 2014). Porosity (%) was determined gravimetrically by subtracting the dry weight of the peat from the saturated weight and dividing by core volume. Specific yield was determined by weight following 24 h undisturbed gravity drainage of saturated samples.

3.2.6 Statistical Techniques

Differences in hydrophysical properties across HRUs were tested using a series of one-way ANOVA tests (non-parametric for bulk density and specific yield, which were not normally distributed, and parametric for porosity and natural-log-transformed saturated hydraulic conductivity, which met the assumption of normality). Differences in hydraulic conductivity with orientation (horizontal, vertical) were tested using a Mann-Whitney U test. Relationships between each hydrophysical property and depth were tested using a Pearson product-moment correlation coefficient (when normally distributed) or Spearman rank correlation coefficient (when non-normally distributed).

Dissolved organic N and ammonium groundwater concentrations were logarithmically transformed (resulting in normal distributions) whereas total dissolved phosphorus concentrations could not be transformed to meet the assumption of normality. Groundwater data were grouped by depth into categories of shallow (5-25 cm) and deep (> 25 cm) by piezometer depth and water table position in wells. Differences in DON and NH_4^+ across HRUs and depth were tested using an ANOVA (with HRU and Depth as factors) with a post-hoc Bonferroni correction between HRUs. Differences in TDP across HRUs and depth were tested with a non-parametric 2-way ANOVA (Sheirer-Ray-Hare test). In all tests, differences were accepted as significant at the $p < 0.05$ level.

3.3 Results

3.3.1 Hydrophysical Properties

No significant differences were observed between HRUs for bulk density, specific yield, or porosity ($p > 0.05$). Thus, those peat hydrophysical properties were aggregated by HRU and stratified with depth (Figure 3.2). Bulk density was lowest at the surface and increased with depth ($p < 0.001$). Porosity and specific yield did not change significantly with depth ($p > 0.05$ in both cases). Saturated hydraulic conductivity decreased significantly with depth logarithmically (p = 0.006), decreasing by several orders of magnitude within 25 cm of the surface.

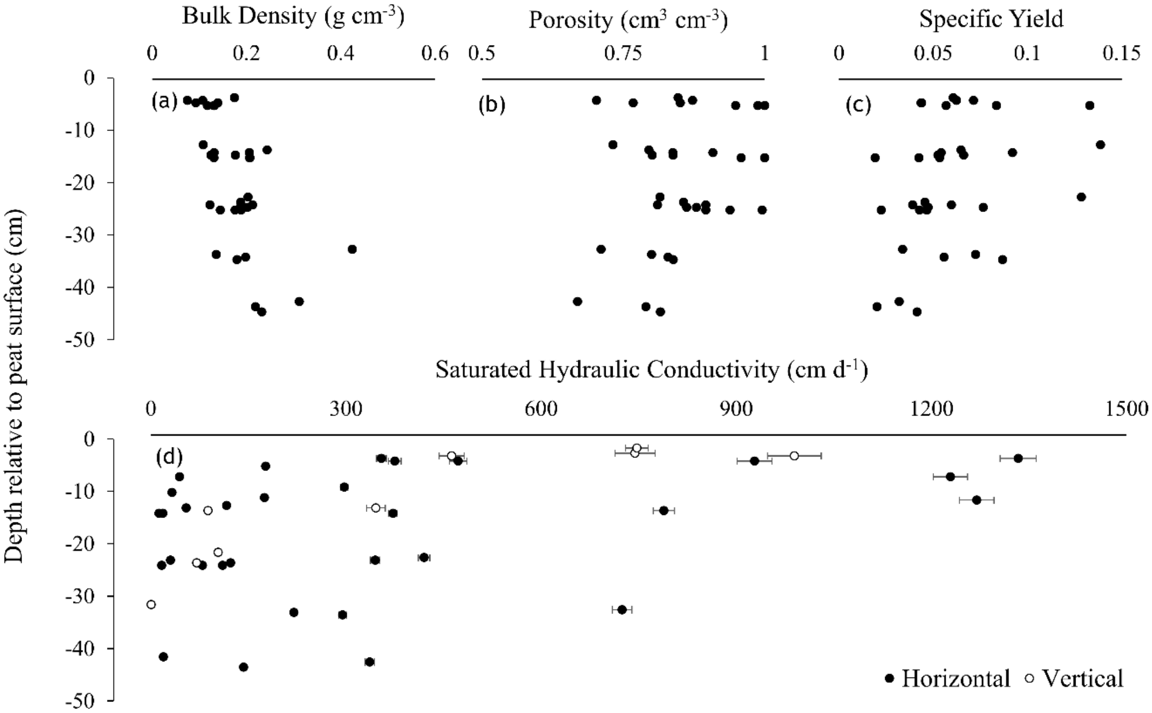

Figure 3.2 Distribution of peat hydrophysical properties from all HRUs with depth: (a) Bulk Density; (b) Porosity; (c) Specific Yield; and (d) Saturated Hydraulic Conductivity. Saturated hydraulic conductivities were determined both in the horizontal (black symbols) and vertical (white symbols) directions.

3.3.2 Seasonal Frost Table and Water Table Evolution

Despite differences in elevation at different well positions within the catchment, the standard error of water table and frost table positions relative to the peat surface was small (Figure 3.3). Thus, one representative well from each HRU within the catchment was employed to monitor changes to catchment moisture storage. During the year when frost table measurements were taken (2014), the frost table developed most rapidly at the beginning of the season from melt to early-mid June, at which point all HRUs had thawed to 20 cm depth (Figure 2.3; May-June mean thaw rates of 0.5 cm/d in PP; 0.7 cm/d in FC; 1.0 cm/d in SL). By late June, frost table development rates diverged further between HRUs, when wetter conditions facilitated deepest frost table development in FCs (50 cm) compared to SL and PP (both 30 cm) by the end of June. Water table depths below the surface were highest post-melt (coinciding with a shallow frost table in all HRUs) followed by a lowering of the water table during precipitation-free periods over the open-water period from June to August (Figure 2.3). This led to a lack of detectable water level for much of the mid-season in PP (persistently dry, no water table on top of permafrost) and SL (ephemeral wetting and drying with precipitation events), whereas the FC had a persistent water table, and often standing water, over the entire season. The annual average water table position was 10 cm higher in FC (-1.8 cm subsurface) than in SL (-11.7 cm). All HRUs returned to post-melt water levels following a series of precipitation events during the autumnal wet-up (September-October).

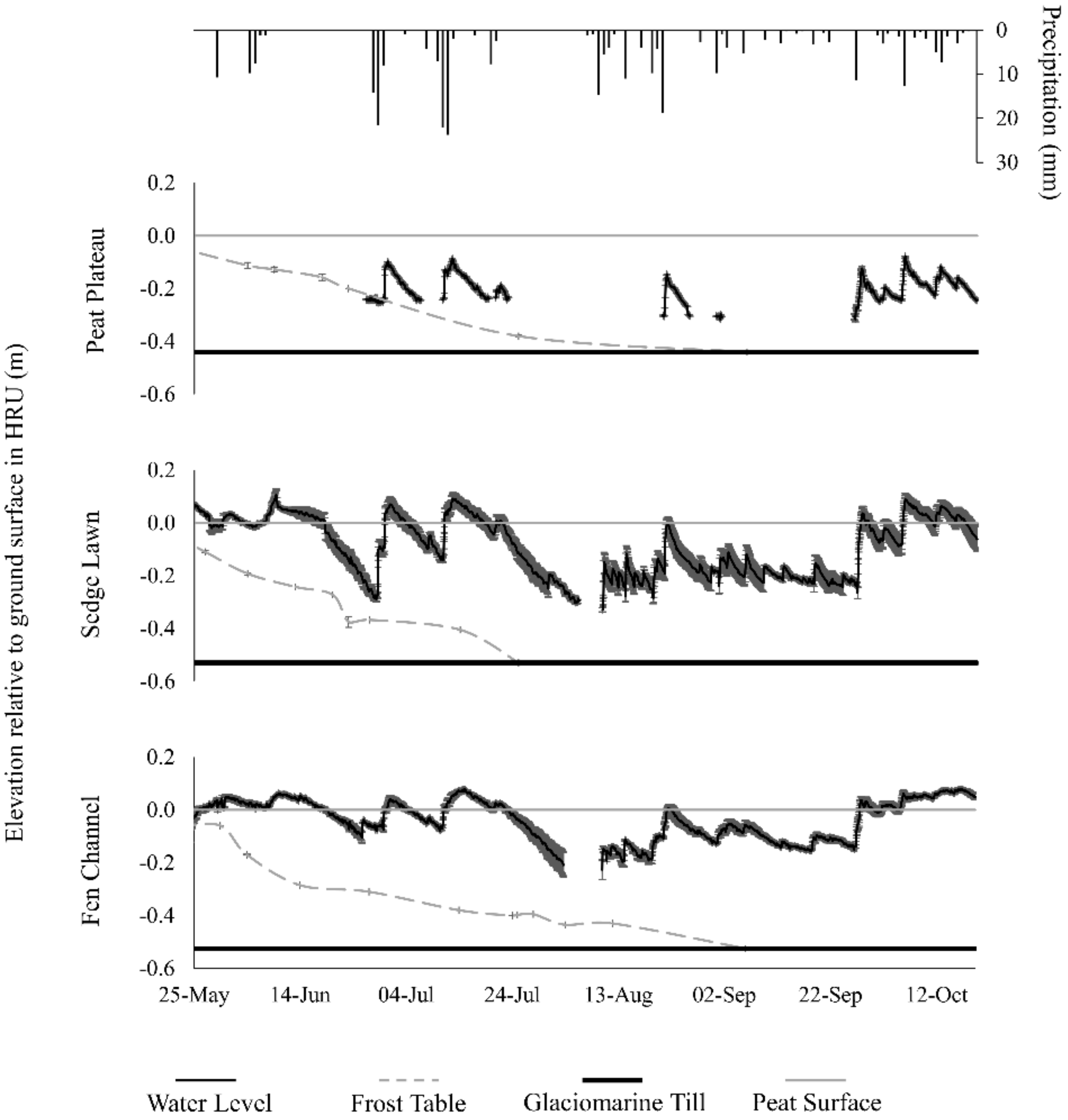

Figure 3.3 Daily precipitation, hourly water level and bi-weekly frost table development relative to the peat surface in three HRUs from May to October 2014. Error bars represent the standard error of all measurements taken at different wells within an HRU, relative to the peat surface.

3.3.3 Runoff Generation

For each study year (2012-2015), annual runoff volumes into Strange and Sandwich Ponds were related to the total precipitation and number of storm events (defined as 8 mm over a 48 hour period; no event with < 8 mm of precipitation produced any runoff response; Table 3.1). Moreover, runoff depths (expressed over pond surface area) received by Strange Pond were consistently 2.7 times greater than what was observed in Sandwich Pond, reflecting differences in the pond surface area (Strange 6307 m^2; Sandwich 17146 m^2). Twenty-five storms were selected for analyses (meeting the condition of >8mm precipitation over a 48-hour period) during the study period (August 2012-October 2015) where storage in different HRUs was compared to changes in pond stage. During precipitation events, changes in pond water levels corresponded, at minimum, to the amount of precipitation received (i.e. 1:1 relationship). However, some precipitation events resulted in changes to pond stage that exceeded rainfall received and thus reflected some form of runoff from peatlands to ponds. This was only observed when an apparent storage threshold was exceeded in each HRU, and, storage thresholds for runoff generation varied considerably among HRUs (Figure 3.4). One representative well from each HRU within the catchment was employed to monitor changes to catchment moisture storage. At the representative wells for each HRU, shallow subsurface flow dominated the PP and SL, with runoff thresholds of 18 and 2 cm below ground surface, respectively. Surface ponding exceeding 4 cm above the ground surface was required for overland flow to be produced from the representative FC well.

Table 3.1 Precipitation and runoff amounts for 4 study years in Strange and Sandwich Ponds. *Indicates total during study period, not for entire calendar year. **A storm event was arbitrarily chosen as a period of less than 48 hours with at least 8 mm of precipitation.

Year	Study period	Precipitation* (mm)	Number of storm events**	Total precipitation during events** (mm)	Total Strange runoff (mm)	Total Sandwich runoff (mm)
2012	August 28 - Oct 12	87.7	1	52.2	40.4	17.7
2013	May 27 - Oct 15	298.6	9	164.5	241.8	89.3
2014	May 24 - Oct 19	308.1	9	222.9	224.0	82.7
2015	May 25 - Oct 21	242.7	7	168.3	168.0	79.4

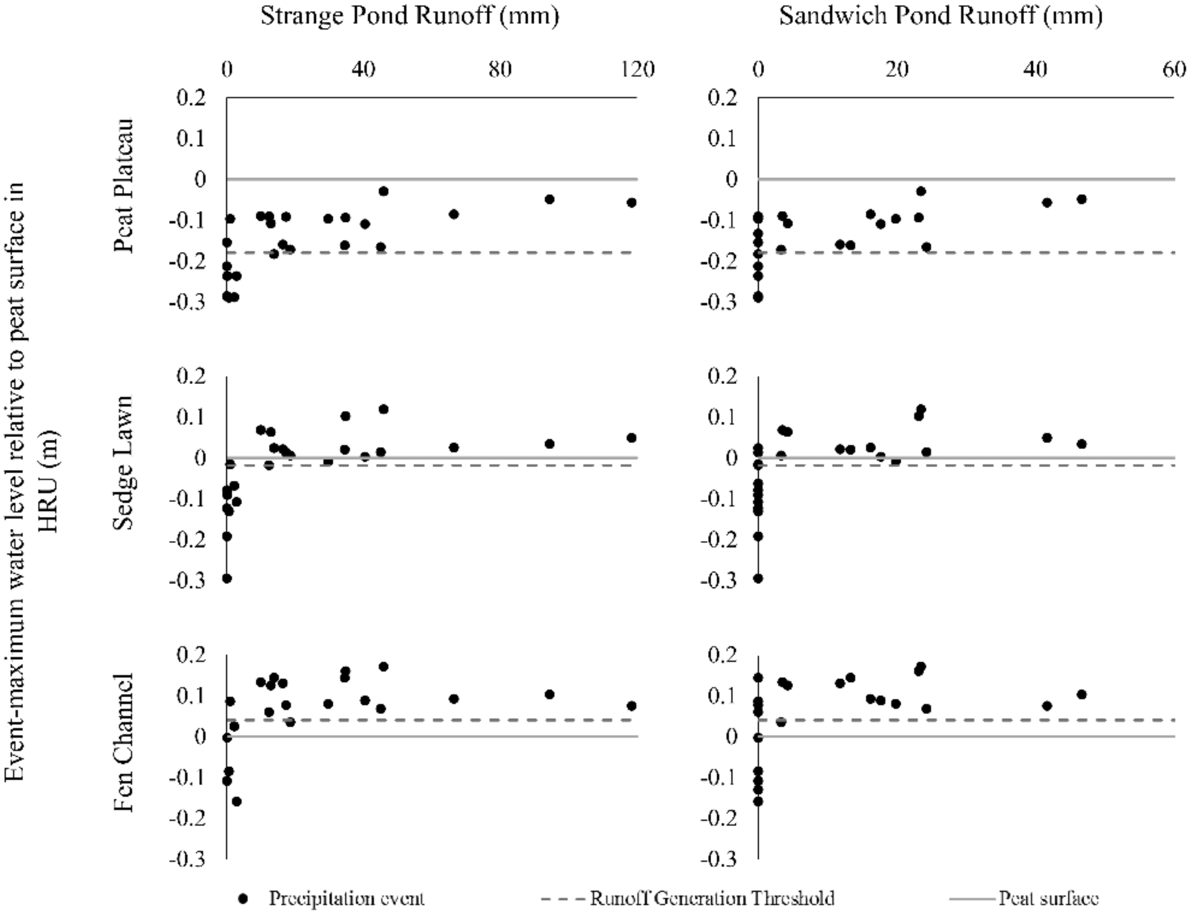

Figure 3.4 Pond response in Strange and Sandwich Ponds as a function of storm*-maximum water level for all snow-free seasons from August 2012 to October 2015. *A storm event was chosen as a period of less than 48 hours with at least 8 mm of precipitation. Any event producing less than 8 mm of precipitation over 48 hours did not generate runoff.

Storage was a greater control than precipitation in determining runoff generation (Figure 3.5), where the amount of runoff did not strongly depend on the amount of precipitation, and the amount of rain did not determine if runoff occurred. Rather, storage threshold exceedance in all HRUs determined whether or not runoff occurred. Of 25 storms analyzed, 15 storms resulted in storage threshold exceedance in all three HRUs, three exceeded storage in some but not all (1-2) HRUs and seven storms resulted in no threshold exceedance in any HRU (Figure 3.5). Of the 15 storms resulting in storage threshold exceedance in all three HRUs, 14 resulted in runoff (at least 10 mm) to Strange Pond and 12 resulted in runoff (at least 3 mm) to Sandwich Pond. In contrast, of the seven storms that did not result in storage exceedance in any HRU, Sandwich received no runoff and Strange received less than 3 mm of runoff in each case, independent of the precipitation amount.

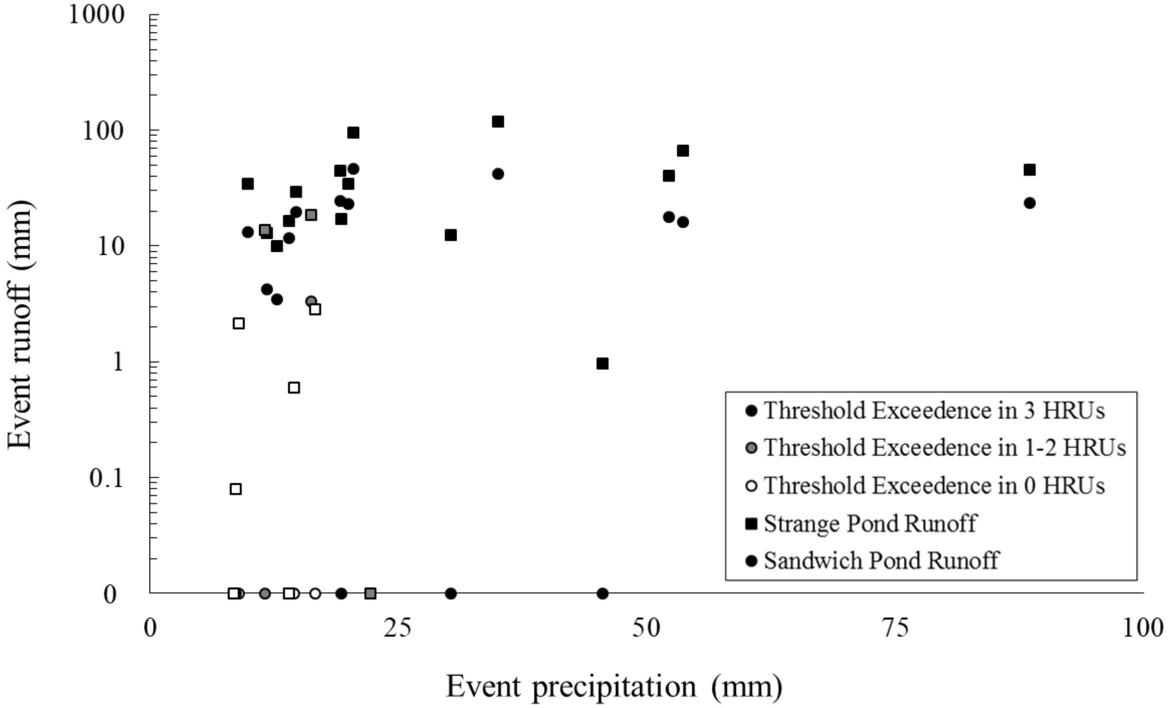

Figure 3.5 Relationship between storm event* size and runoff generation August 2012 – October 2015 grouped by number of hydrological response units demonstrating storage threshold exceedance. *A storm event was chosen as a period of less than 48 hours with at least 8 mm of precipitation. Any event producing less than 8 mm of precipitation over 48 hours did not generate runoff.

During the periods of the year with a shallow frost table (< 20 cm depth), the water table remained perched in the shallow subsurface, at or near threshold runoff-generation storage (Figure 3.6). The perched nature of the water table on the frost table allows for a much greater likelihood of precipitation events occurring early in the snow-free season to produce runoff than later in the season when the frost table has receded into the underlying glaciolacustrine till.

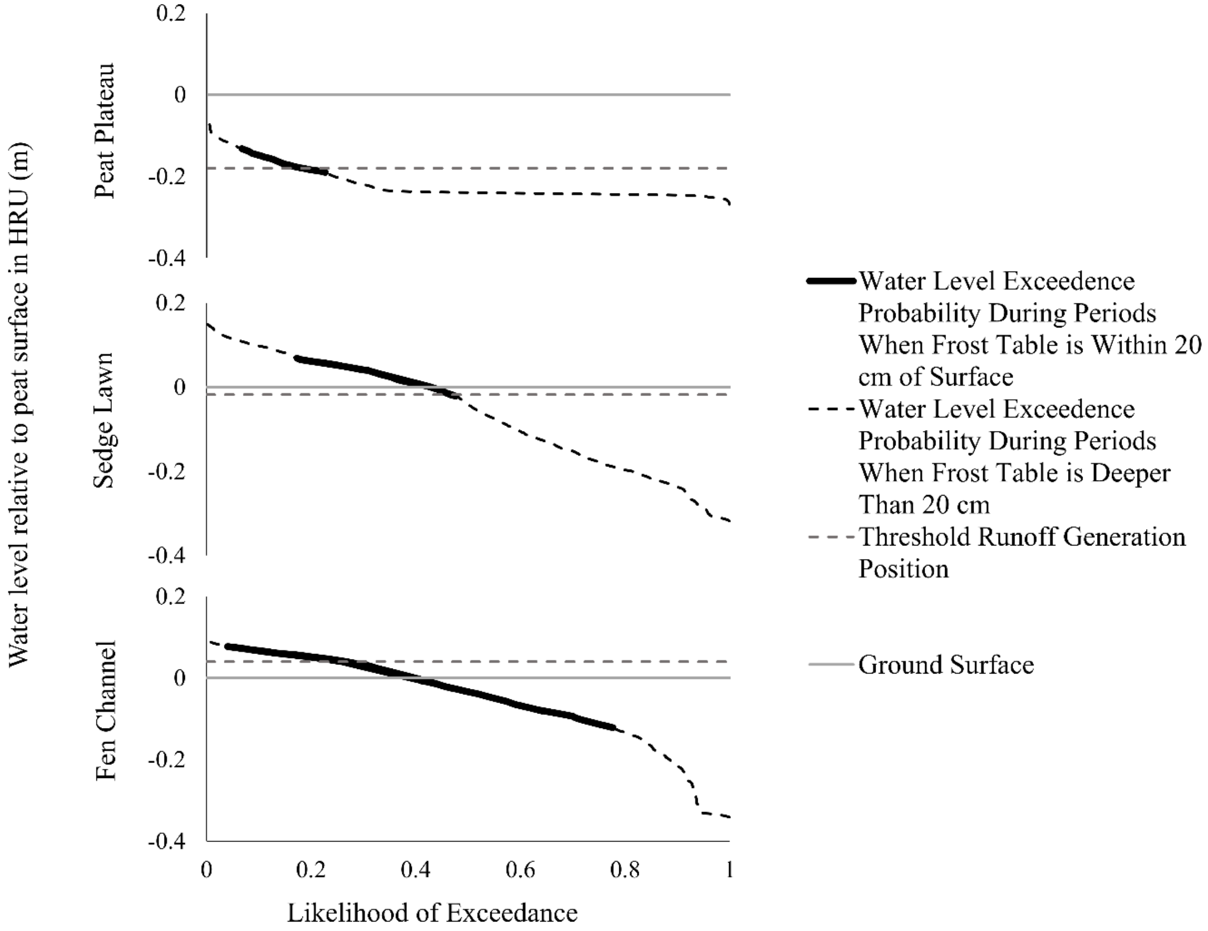

Figure 3.6 Water level exceedance curves for each HRU relative to the peat surface for May – October 2014, with periods during which the frost table was within 20 cm of the surface highlighted (solid black line) in comparison to the remainder of the year when the frost table was deeper than 20 cm beneath the surface (dotted line).

3.3.4 Groundwater Chemistry

Generally, groundwater chemistry differed temporally (Figure 3.7), but this was driven by differences in portions of the peat depth profile accessed at different times of the season. During the groundwater sampling campaign (May to September 2014), NH_4 concentrations did not vary significantly with HRU ($F_{2,2} = 1.891$, $p > 0.05$) or depth ($F_{1,2} = 0.072$, $p > 0.05$), with no significant interaction between HRU and depth ($F_{2,2} = 6.151$, $p > 0.05$). DON concentrations were significantly higher in shallow groundwater than deep groundwater ($F_{1,2} = 5.245$, $p = 0.011$), however the differences with depth were only significant in PP ($p < 0.001$), not in SL or CF ($p > 0.05$). Between HRUs, DON was greater in SL than CF and PP ($p = 0.001$ and $p < 0.001$, respectively). Deeper groundwater accessed later in the season was low in DON, primarily ranging 0.2 to 1 mg N L^{-1}. TDP concentrations followed a similar temporal trajectory to DON concentrations although the differences between HRUs were more pronounced (greatest in PP and SL, ranging from 0.05 mg P L^{-1} to 1 mg P L^{-1}, and significantly lower in FC than PP and SL [$p = 0.004$ and $p = 0.001$, respectively], generally < 0.1 mg P L^{-1}). Overall depth was not a significant factor for TDP concentrations ($H_{1,2} = 9.841$, $p > 0.05$).

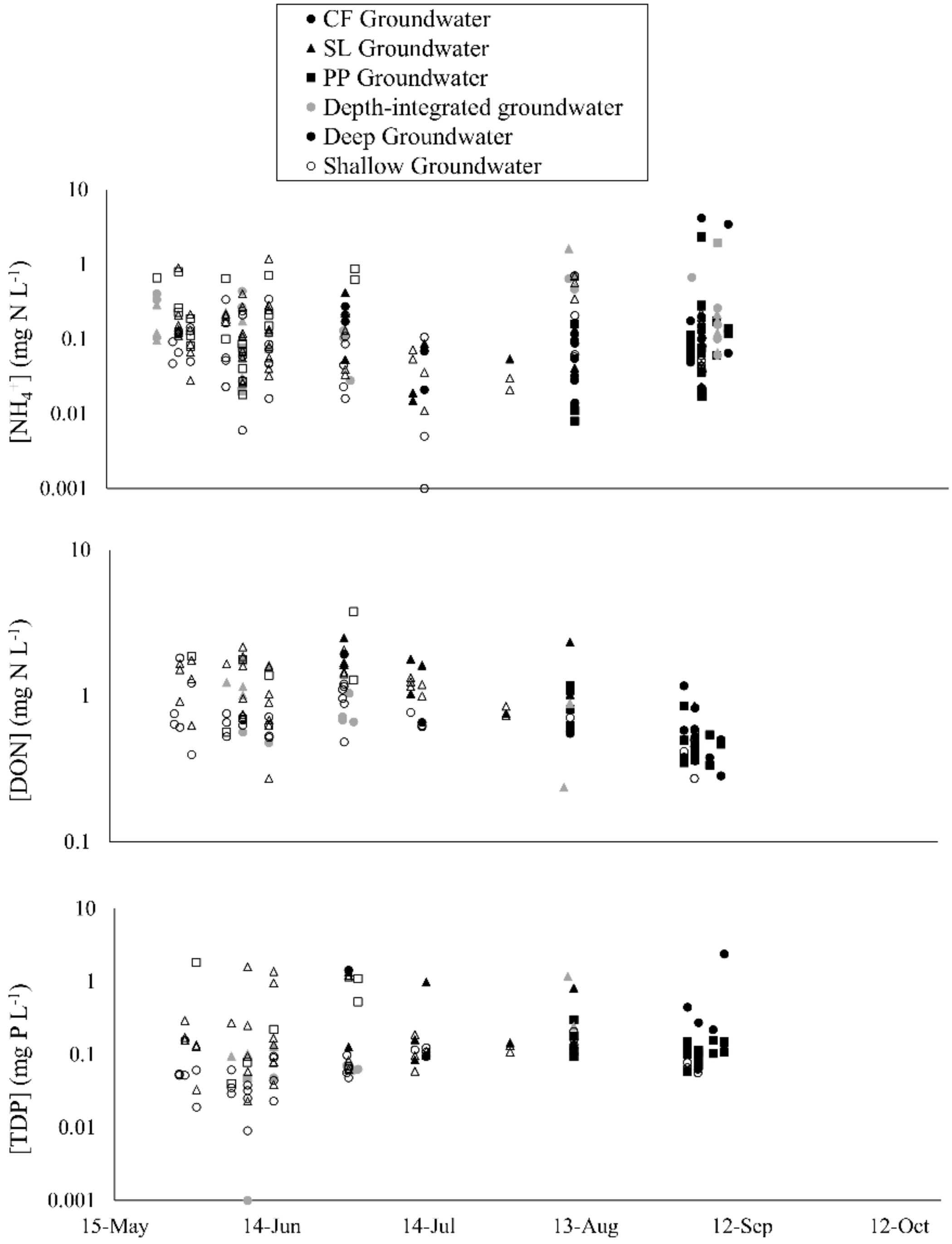

Figure 3.7 Groundwater chemistry in each HRU. Shallow groundwater was sampled from piezometers screened at 10 cm intervals between 5 and 25 cm below the peat surface and deep groundwater was from piezometers screened at 10 cm intervals between 35 and55 cm below the peat surface. Depth-integrated groundwater was sampled from wells screened through the entire depth.

3.3.5 Pond Hydrology and Chemical Trajectories

During the pond chemistry sampling campaign (May to October 2014), pond stage (Figure 3.8) and terrestrial water levels (Figure 2.3) were highest in the early season post-melt, falling during precipitation-free periods and rebounding during and immediately following precipitation events. Generally, there was a wet period post-melt, drying with occasional wetting during summer, and a re-wetting into autumn. Periods of hydrologic connection (early- and mid-summer) in which threshold runoff-generating conditions were met resulted in three major runoff events, coinciding with periods of DON and TDP increase to a seasonal maxima and NH_4 decrease to a seasonal minima in both ponds (Figure 3.9). Intensive sampling during rainfall and runoff events showed that increases in DON and TDP concentrations during this time occurred particularly during the runoff period following three storms. NH_4 concentrations were most variable during and throughout rain/runoff events, although generally returned to approximate pre-storm conditions by the following sampling date. Extended mid-summer drying resulting in hydrologic disconnection between pond and catchment. This resulted in a lack of runoff events contributing to the pond, and coincided with a period of DON and TDP stationarity and decrease while NH_4 began to increase to early season post-melt concentrations.

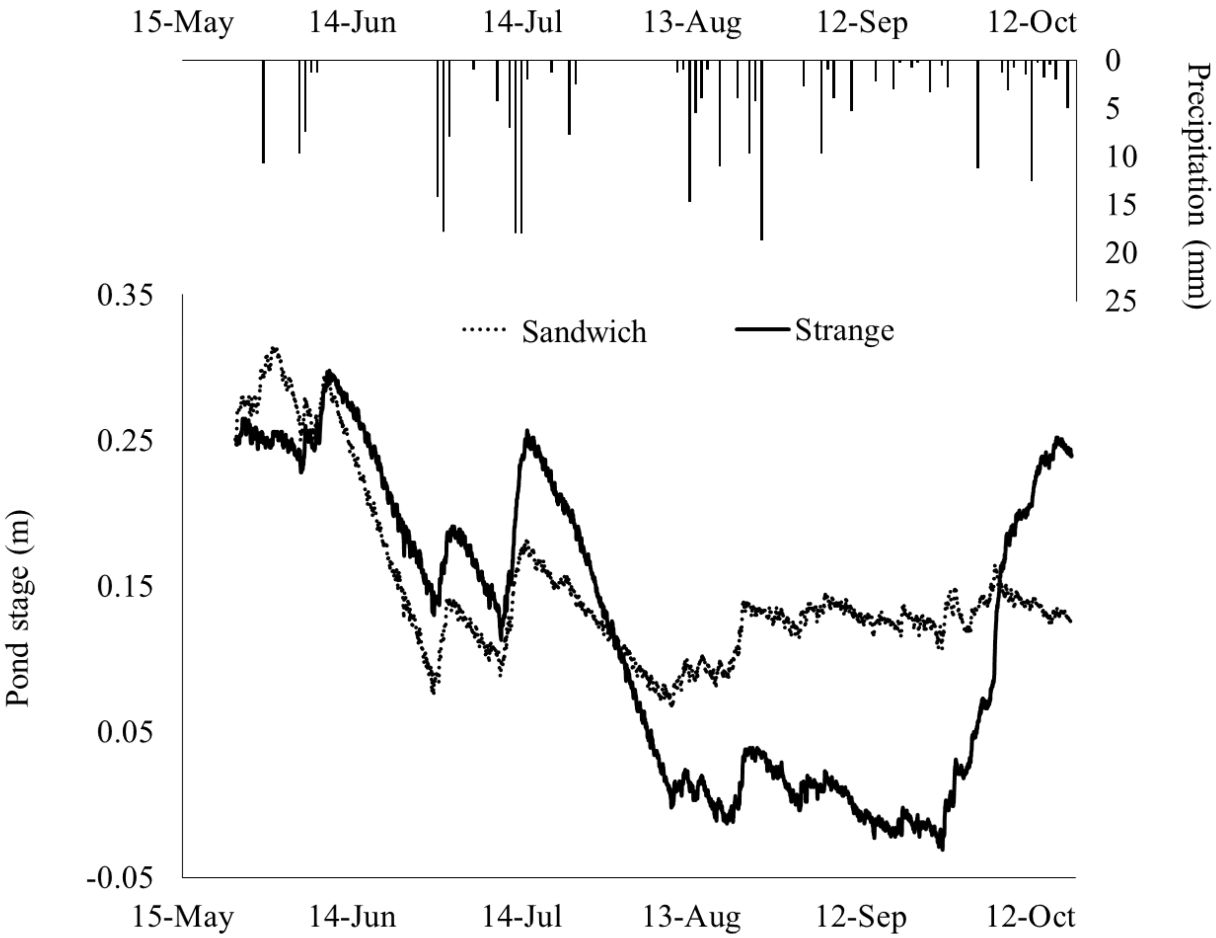

Figure 3.8 Seasonal trajectory of pond stage in Strange Pond and Sandwich Pond with daily precipitation from May to October 2014.

(a) Strange Pond

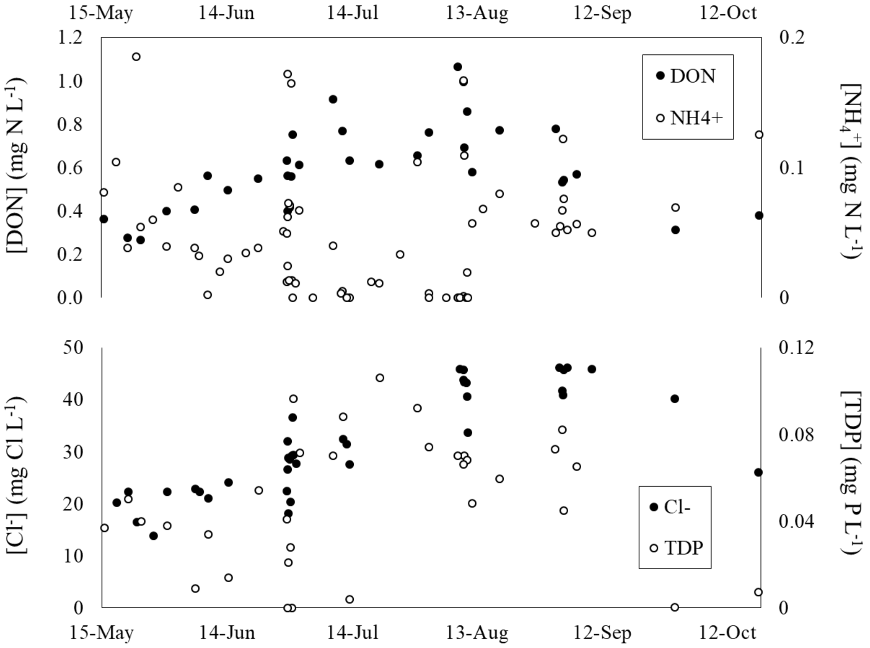

(b) Sandwich Pond

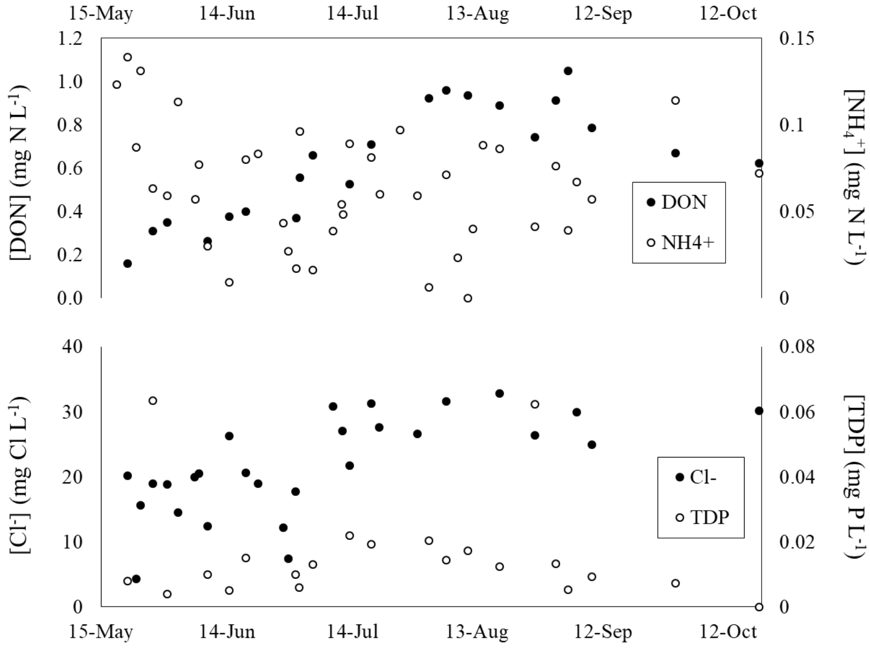

Figure 3.9 Seasonal trajectory of pond chemistry in (a) Strange Pond and (b) Sandwich Pond from May to October 2014.

Throughout 2014, Strange and Sandwich Ponds displayed similar ranges and temporal trajectories of values for both N species (NH_4 and DON, although the DON trend was more temporally coherent than the NH_4 trend). However, TDP concentrations were frequently an order of magnitude greater in Strange (ranging from detection limit to 0.10 mg P L^{-1}) than in Sandwich (ranging from detection limit to 0.022 mg P L^{-1}). In addition, the seasonal maxima of TDP concentrations occurred earlier in Sandwich (mid-July) pond than Strange Pond (early September) and was decoupled from the DON seasonal trajectory, whereas the temporal trends of DON and TDP were linked in Strange Pond. To investigate the role of evapoconcentration in pond nutrient concentrations, the relationship between pond stage (total pond storage) and chloride concentrations, as a conservative marker of evapoconcentration, was investigated. Both ponds experienced an increase in chloride concentrations coincident with an associated drawdown in stage throughout the mid-summer and a decrease in chloride concentrations coincident with the rebound of pond stage during the autumnal wet-up, however the chloride concentration maximum was temporally decoupled from nutrient concentration maxima.

3.4 Discussion

3.4.1 Hydrology

Given the storage-exceedance threshold mechanism of runoff generation, the timing and amount of precipitation is important, with rainfall during moist antecedent conditions contributing to pond volume and chemistry, while rainfall occurring during extended dry periods contributed only to the catchment, and not to runoff generation. Individual event precipitation amount did not have a clear relationship with event runoff, while other event characteristics such as rainfall intensity and duration may have determined the relative contributing area for each event, in addition to the partitioning of event water as runoff or catchment storage (Reaney et al., 2007). Hourly data was not available for all storms in this study, however, variations in rainfall intensity and duration may be a driving force for either the capacity for a storm that does not exceed storage thresholds to generate runoff, or for a storm which did exceed storage threshold yet produce no runoff (Figure 3.4). In addition, the residence and transit time of water along the catchment may be an important factor for runoff generation in a permafrost peatland (Quinton et al., 2003). In this study, hourly pressure transducer measurements showed that all HRUs tended to exceed storage thresholds simultaneously. This was observed at both the event-scale (15 storms showed simultaneously exceedance in all three HRUs out of 18 storms, which led to storage exceedance in at least one HRU) and the seasonal scale (Figures 3.3 and 3.4).

During the autumnal wet-up of 2014, catchment storage returned to threshold-runoff generating conditions in all HRUs and catchments began to interact hydrologically with ponds again. Threshold runoff generation coincided with highly-conductive soil layers (Figure 3.2) in the case of PP (18 cm below peat surface) and SL (2 cm below peat surface), and overland flow in FC, although some microtopographic variations with each HRU could have impacted the exact depth of these runoff generation threshold positions. As hydrophysical properties did not vary significantly between HRUs, the storage and lateral movement of water did not vary at the HRU scale and instead is primarily driven by topographic and moisture gradients at the landscape and between-HRU scale. The threshold storage for FC of overland flow indicates that surface connection appears to be a required condition for delivering runoff to ponds, similar to findings reported by Quinton et al. (2003) and Connon et al. (2014) in a discontinuous permafrost peatland terrain in the Northwest Territories, Canada.

Although only the upper 50 cm of peat was selected for determination of hydrophysical properties in this study, results from a permafrost catchment with a comparable organic layer depth showed a similar logarithmic decrease in conductivity with depth into underlying mineral till (Carey & Quinton, 2005). Specific yield values are within the range reported for peatlands (Rezanezhad et al., 2016), but generally lower than those reported in other undisturbed peatlands (e.g., Price, 1996). Dredge (1979) also observed anomalous hydrophysical peat properties in the Churchill region compared to peatlands in other regions. Peatlands in this region are dominated by (and therefore formed by) a combination of sedges, feather mosses and lichen-heath communities, and there is little *Sphagnum* in the area. This contrast in the primary species forming the peat may produce peat with hydrophysical properties that differ from those of *Sphagnum* peat (Belyea & Baird, 2006). Given the likelihood of a transition towards increased sedge production in Northern peatlands under a changing climate (Potvin et al., 2015; Strack et al., 2006), further study of the key differences in hydrophysical properties between *Sphagnum* and Sedge peats is of increasing relevance.

In additional to the sub-annual seasonal pattern of catchment storage, pond-peatland interactions are tied to inter-annual precipitation variability. The 1980-2010 average Churchill rainfall totals for May to October are 273.1 mm. Generally, 2014 was a wet year (May to October precipitation total of 314.5 mm) although marked by several extended dry periods (e.g., 19 days with 0 mm of precipitation from 9 June to 27 June; 16 days with 0 mm precipitation from 22 July to 6 Aug) punctuated by large storm events, particularly in the early summer post-melt period. Illustrating the importance of moisture storage exceedance for runoff generation, two events similar in magnitude occurred within two weeks of each other during this period (48.1 mm June 28-30, 51.8 mm July 12-14), resulting in major runoff event, where the first served as a “filling” prior to the second as a “spilling” period in terms of peatland-pond runoff response (Figure 3.8).

In addition to the timing of precipitation events controlling catchment moisture storage throughout the season, the mid-summer dry season coincides with the period of greatest radiative energy available for evapotranspiration during the growing season (Rouse et al., 1997). Projections of an earlier melt and prolonged summer growing season (Callaghan et al., 2010) may extend those periods during which ponds are hydrologically disconnected from their catchments, providing a greater window during which pond desiccation is likely. The hydrology of the prolonged summer season will be impacted by changing precipitation regimes (Shook & Pomeroy, 2012), particularly in the timing and state of autumnal precipitation (Spence et al., 2011). As the autumnal season lengthens and precipitation falls in liquid phase during large storm events during a period of reduced available evaporative energy, there is a potential for re-filling of the catchment storage and runoff entering ponds prior to winter freeze-up to offset increased summer desiccation. Thus the future water balance of shallow ponds in this region under a changing climate will likely be determined by the difference in increased evaporation in the summer months and increased precipitation and storage-exceedance runoff generation in the autumnal season.

3.4.2 Hydrochemistry

Throughout 2014, variance between HRU groundwater nutrient chemistry may be explained by variations in topographic position. Early season DON, TDP, and NH_4 concentrations at SL and PP locations were frequently orders of magnitude greater than FC locations. These locations, representing the sloping edge (SL) and footslope (FC) of an upland peat plateau (PP), often are at a much steeper grade (~20%) than most of the surrounding landscape, leading to ephemeral hydrologic connection during early season periods (made possible by a high water table perched on a frost table whose development is stunted in peat plateaus, see Figure 3.6). In addition to hydrologic transport moving nutrient downgradient, the thermal and moisture regime of the SL and FC may function as a biogeochemical hot spot, characteristic of breaks in slope (McClain et al., 2003).

The parabolic seasonal trajectory of both shallow and deep groundwater NH_4 concentrations with dry mid-summer minima may be reflective of efficient uptake during the growing season, both terrestrially and in ponds, in concert with reduced mineralization during cool and saturated periods and increased mineralization during warm and dry periods (Borner et al., 2008; Baumann et al., 2009), or during periods of time in which dry HRUs (PPs and SLs) are hydrologically connected (Figure 3.3). Organic nutrients (reflected in DON and TDP) may be liberated from shallow organic undecomposed peat layers while mineralization is inhibited, in addition to biotic competition for uptake of organic forms of nutrients (Kielland, 1997; Weedon et al., 2012; Schimel & Chapin III, 1996) resulting in a decline terrestrially throughout the growing season. As deeper peat layers thaw seasonally, the degree of peat decomposition increases with depth, the organic nutrient fraction decreases and mineralized material increases (Harms & Jones, 2012) coincident with the distribution of microbial community compositions with depth (Lin et al., 2014). When thawed, deeper mineral soils provide additional adsorption sites for organic materials leached from overlying peat (Petrone et al., 2006; Harms & Jones, 2012), further decreasing the organic fraction of loosely-bound nutrients in deep soils. However, although shallow permafrost mineral layers that are subject to thaw might have a different character of soil chemistry (e.g., Frey & McClelland, 2009; Keuper et al., 2012), this may not be reflected in future runoff chemistry due to the stratigraphy of hydrophysical properties with depth (Figure 3.2).

As well, differences in groundwater chemistry between HRUs (Figure 3.7) may be reflected in transport signatures during periods of hydrologic connection such as elevated DON concentrations from shallow PP groundwater arriving in ponds during a series of runoff-generating storms in June and July 2014 (Figures 3.8 and 3.9). Other mechanisms, such as the vertical redistribution of groundwater from deeper, less conductive layers to the surface, such as through springs, are currently rare in permafrost environments due to the confining nature of the frost table (Woo, 2012). Throughout 2014, there were no measured differences in head at different depths measured within any single piezometer nest within any HRU, suggesting that vertical transport was not a factor, further underscoring the potential hydrological irrelevance of deep peat/shallow permafrost chemical export (or lack thereof).

Rainfall chemistry, and transformations thereof (c.f. Quinton & Pomeroy, 2006), may be an important source of hydrochemical inputs to ponds and catchments, both in direct rainfall, and as transformations of new water that eventually may reach the pond. Although highly variable through time, rainfall chemistry represents an end member rich in inorganic species and poor in organic species relative to groundwater contributions (Means ± standard deviations of 0.182 ± 0.149 mg NH_4-N L^{-1}, 0.184 ± 0.041 mg DON-N L^{-1}, 0.097± 0.014 mg TDP-P L^{-1}). Future work should incorporate a new water/old water approach to flow separation to elucidate both the effect of chemical transformations of new water as it travels through the landscape, and its eventual fate.

Seasonal trajectories of pond nutrient chemistry may be attributed to both transport and internal cycling mechanisms. Increasing DON and TDP concentrations in the early season post-melt period (Figure 2.9) coincide with both (a) periods of three major runoff events occurring when DON and TDP concentrations are greatest in the catchments (Figure 3.7) and (b) seasonal conditions favourable to pond productivity driven by high photosynthetic available radiation and increasing water column temperatures. Thus, the increase in organic species of N and P within the pond over the same period may be a result of transport to the pond, or of biological fixation of inorganic N and P species to an organic fraction. However, concentrations of SRP and NO_3 (Sandwich Pond annual means of <0.001 mg NO_3-N L^{-1} [detection limit] and 0.003 mg SRP-P L^{-1}, Strange Pond annual means <0.001 mg NO_3-N L^{-1} [detection limit] and 0.003 mg SRP-P L^{-1}) are insufficient to provide internal volumes that explain seasonal changes to TDP and DON concentrations as entirely a result of productivity without additional sourcing of N and P species for biological fixation. Another mechanism leading to elevated nutrient concentrations may have been evapoconcentration (Lewis et al., 2015), although the seasonal trend of chloride concentrations as a conservative indicator and the pond stage record were temporally decoupled from seasonal trajectories of nutrient concentration (Figures 3.8 and 3.9). Within this study, surface-water sediment interactions were not considered as a mechanism for additional loading or loss of any chemical species. In other research, biological assimilation of inorganic species by benthic organisms in pond sediments has been shown to be rapid (Eichel et al., 2014), demonstrating bulk assimilation of artificially spiked concentrations in mesocosms occurring within 24 hours of addition. In this study, rapid influxes of inorganic species may not have been captured by the sample design despite sampling within six hours of major runoff-generating runoff events in Strange Pond and Sandwich Pond. Without a direct measure of these individual processes, it is impossible to determine the relative contribution of each for all concentration measurements. Groundwater and pond concentrations represent a snapshot in time, which captures the sum of hydrophysical processes (such as transport, mixing, stratification, and evapoconcentration) and biogeochemical processes (such as mineralization, demobilization through biological fixation, denitrification). In this study, direct measures of biotic and abiotic processes contributing to biogeochemical nutrient cycling were not present. Future work should attempt to determine the relative contributions of both major biogeochemical processes and hydrological transport mechanisms in determining nutrient mobilization through subarctic landscapes.

3.5 Conclusions

Runoff generation is an important consideration for the water balance of subarctic ponds, in which a single runoff event may comprise as much as a third of the total hydrologic inputs for a summer. The water table position in HRUs acts as a runoff threshold and is implicitly tied to the frost table position, particularly in the early season, due to the perched nature of the hydrology of the system. As the frost table migrates downward seasonally, capacity for storage increases and the distance from the base of the frost table to the threshold depth for runoff generation increases in each HRU. If storms occur following a dry period when antecedent moisture is low and soil storage capacity is high (i.e., a low frost table), ponds may receive no contributions from the catchment irrespective of the event size. It is well known that the fate of hydrologic inputs to northern catchments is largely dependent on the perched water table on frost table position; however, this may be confounded by the access of deeper, finer grain materials as previously permanently frozen layers are thawed. In this study, upper, less decomposed portions of the peat profile were rich in organic nitrogen, while ammonium and phosphorus concentrations did not vary with depth. Pond organic nitrogen and phosphorus concentrations increased through the summer period to a mid-summer maxima while ammonium followed the opposite trend, attaining a mid-summer minima. Hydrochemical contributions to ponds may be more reflective of periods of catchment storage exceedance in early- to mid-summer and extended autumnal seasons with increased frequency and intensity of storms with flow primarily through highly-conductive upper peat layers rich in organic forms of nutrients.

3.6 Acknowledgements

This research was funded by the Churchill Northern Studies Centre Northern Research Fund, Earth Rangers, Northern Scientific Training Program, and Cluster for Subarctic Ecosystems in Transition, NSERC Discovery Grants (Macrae and Petrone, and NSERC Northern Supplement, Petrone). Field assistance was provided by A. Goodman, G. Berard, C. Storie, J. Budgen-Storie, D. Gibson, J. Verstege, J. Blossom, C. Pulleyblank, R. Rimas, A. Lester, D. Closey, F. Godineau, P. Dodonov, M. Taverson, L. Koloski, and P. Kumar. Laboratory assistance was provided by V. Lam, C. Wells, R. Bourbonniere, T. Lozier, C. Irvine, G. Holmes, J. Robinson, N. MacDonald, C. Murchison, and J. Perz. Additional logistical support was provided by the staff and volunteers of the Churchill Northern Studies Centre.

Chapter 4: Capturing Temporal and Spatial Variability in the Chemistry of Shallow Permafrost Ponds

4.1 Introduction

Small, shallow freshwater bodies (<1 km^2) across the north are ubiquitous in the landscape (Muster et al., 2013; Dyke & Sladen, 2010; Macrae et al., 2014). In many regions, these features maintain the capacity to store and exchange carbon (C) (Macrae et al., 2004; Abnizova et al., 2012), act as habitat (Smol & Douglas, 2007a), and mediate the landscape energy balance (Chapin et al., 2000). These tundra ponds are highly sensitive to climate change (Schindler & Smol, 2006), which may impact their hydrology and biogeochemistry. This has implications for their ability to support organisms and store or cycle C, which in turn has important feedbacks to climate change. Thus, an improved understanding of pond biogeochemistry is needed. Climate change may impact pond hydrobiogeochemical conditions by modifying pond hydrologic and thermal conditions, as well as pond-catchment connectivity. In permafrost systems, recent work has focused on the impact of climate-induced permafrost thaw on lake and pond chemistry (Vonk et al., 2015) over a timescale of decades, generally showing increasing concentrations of ions indicative of deeper flowpaths and weathering processes (Kokelj et al., 2009). Lougheed et al. (2011) examined changes in tundra pond chemistry over 40 years in Alaska and observed substantial increases in inorganic nutrients, which were attributed to a thaw-based release from shallow permafrost and increased atmospheric nitrogen (N) deposition. In addition to changing chemical contributions from thawing catchments, the water balances of ponds are sensitive to climatic changes that impact the ponds directly as well as indirectly through changing catchment hydromorphology (Walvoord & Kurylyk, 2016).

Adjacent to pond edges, thermokarst expansion acts as a mechanism for lateral seepage and loss (e.g., Yoshikawa & Hinzman, 2003) leading to increased connectivity, potentially modifying seasonal biogeochemical trajectories (Abbott et al., 2015). Elevated levels of nutrients and/or ions may impact the C uptake function of ponds via primary productivity, which has been shown to be nutrient-limited in subarctic and arctic freshwater bodies (Levine & Whalen, 2001; Bergström et al., 2005; Bergström, 2010; Bonilla et al., 2005; Symons et al., 2012). Indeed, increased nutrient loading to ponds may either bring about an increase in pond primary productivity (Levine & Whalen, 2001; O'Brien et al., 2005) or may lead to a decrease through increased turbidity and suboptimal conditions for photosynthesis (northern Sweden, Ask et al., 2009; northern Québec, Roiha et al., 2015), linking nutrient concentrations to biological markers such as chlorophyll (Przytulska et al., 2016).

Although climate change may lead to long-term changes in pond permanence and hydrologic exchange, pond hydrologic storage can also vary greatly over the course of a single season or among different hydrologic years (Morison et al., 2017; Woo & Guan, 2006). Annual changes to pond storage often reflect the highly variable local climatic conditions, and ponds may either desiccate completely (e.g., Bouchard et al., 2013; Smith et al., 2005) or spill over bankfull storage and/or coalesce (Macrae et al., 2014). The chemical concentrations of the water column in ponds are closely tied to hydrology, both directly through physical processes (i.e. dilution and evapoconcentration; Borghini et al., 2013) and indirectly through mediating environmental factors that control the rate of biogeochemical processes (e.g., variable pond depth controlling the diurnal water temperature amplitude; Smol & Douglas, 2007b). Mazurek et al. (2012) sampled shallow ponds over several summer seasons in Svalbard and found ionic concentrations increasing in ponds over the summer months, coincident with pond drying. White et al. (2014) monitored ponds at three time steps over the ice-free season and related pond seasonal biogeochemical trajectories to pond morphology and pond-peatland connectivity. Given the significant control of hydrological processes on pond biogeochemistry, and the highly variable hydrological conditions experienced by ponds within a single season, an improved understanding of seasonal patterns of pond hydrochemistry is needed to better understand potential pond responses to climate change.

The concepts of hydrochemical coherence (or synchrony; Baines et al., 2000) have been employed in temperate lake systems to determine the role of different climatic and hydrological factors in driving lake chemical variations, often by examining correlation of different chemical measures across space (e.g., Magnuson et al., 1990). For instance, Pace and Cole (2002) found in Northern Michigan that changes to dissolved organic carbon and colour were synchronous among lakes while total phosphorus, chlorophyll, and pH were not. Other methods, such as the use of evaporative normalization factors (e.g., Borghini et al., 2013), have allowed for comparisons among different chemical species and the degree to which they are driven by hydrological variation. Both of these methods allow for comparison of relative deviations of values which would otherwise be masked by absolute differences among lakes. Approaches of hydrochemical coherence have been less seldom employed in subarctic permafrost pond and lake settings.

Recent approaches to characterizing shallow pond biogeochemical processes across Arctic, Antarctic, and alpine permafrost settings have used three to four water samples from each lake or pond, taken at different points of the ice-free season to represent “early-season”, “mid-season”, and “late-season” conditions. Other approaches have relied on a single annual sample to characterize various geochemical indicators of ponds, such as nutrient status, carbon dynamics, major ion and metal concentrations, often sampling many ponds and lakes (often 10-100) at that single time period (Appendix B, Table B.1). However, given the variability in pond storage and hydrological conditions over the course of an ice-free season, it is important to frame the results of pond chemical analyses in the proper hydrologic context, and further, to be prudent in generalizing pond geochemical process from samples taken in different hydrological periods. Beyond broad spatial sampling campaigns of many periods at a coarse temporal resolution, less is known about the amplitude, drivers, and total variation in seasonal and event chemographs of shallow ponds in remote northern catchments, despite their importance in driving key ecological functions across the circumpolar north. Further, as large summer storms increase in frequency and magnitude (Sauchyn & Kulshreshtha, 2008; Kaufman et al., 2009), it is important to understand how storm events control short-term water chemistry variation, which can represent a substantial proportion of the annual water balance over a period of hours to days (Macrae et al., 2014).

The objectives of this study were to characterize spatial and temporal patterns in the chemistry of a suite of tundra ponds to determine if: (1) temporal variability exceeded spatial variability throughout the open water season; (2) temporal variability existed, whether all ponds (or groups of ponds) behaved in a similar temporal pattern, linked to season or hydrology; and (3) spatiotemporal variability in pond biogeochemical signatures could be used to make inferences about processes occurring within ponds and between ponds and surrounding peatlands. This information will improve our understanding of hydrobiogeochemical processes in tundra ponds, particularly in terms of seasonal patterns, and, will aid in developing appropriate sampling designs in future. Further, this study provides a geochemical survey of six ponds in the Hudson Bay Lowlands region at two unprecedented temporal scales (bimonthly, spanning an ice-free season, in addition to diurnal samples spanning an intense rainfall-runoff event).

4.2 Methods

4.2.1 Study Site and Sampling Design

This study was completed in the Hudson Bay Lowlands (HBL), approximately 20 km east of the town of Churchill, Manitoba, Canada. The regional climate is strongly influenced by the close proximity to Hudson Bay (Rouse, 1991), with average air temperatures in the region (1980-2010 normal) of -6.5 °C (annually) with a snow-free season from May to October, and maximum temperatures in July (monthly average 12.7 °C; Government of Canada, 2016).

The HBL are the largest contiguous wetland complex in North America, with thousands of lakes and ponds in the landscape (Keller et al., 2014; Dyke & Sladen, 2010) from impeded drainage due to very low topographic gradients (Boudreau & Rouse, 1995) and the presence of permafrost. Ponds have been demonstrated to be stably stratified in the eastern HBL (Deshpande et al., 2015), while the very shallow (<1 m) ponds in the western HBL are assumed to be well mixed by wind action (Bello & Smith, 1990). Ponds in the western HBL have been shown to be nutrient-limited (Eichel et al., 2014; Symons et al., 2012), restricted in surface and groundwater connection (Boudreau and Rouse, 1995), with steep banks and thick, organic sediments with dense mats of benthic blue-green, green and diatomaceous algae (Macrae et al., 2004; Gray, 1987), with the dominant diatom genus being *Denticula* (Macrae et al., 2004). Symons et al. (2012) showed the most abundant phytoplankton communities to be *Chlamydomonas* spp., *Sphaerocystis* spp., *Diatoma* spp. and *Crugienella* spp. Due to their small size and extremely alkaline conditions (8 to 9.8 pH, Macrae et al., 2004; Bos & Pellatt, 2012), stickleback (*Gasterosteidae*) are the only fish species present. *Carex aquatilis* is found along pond perimeters in zones where water is shallow. Eichel et al. (2014) experimentally demonstrated the importance of benthic organisms to the cycling of nutrients in these ponds, showing that mesocosms with sediment removed inorganic nutrients from the water column at a rate orders of magnitude greater than mesocosms without sediment.

The ponds and their catchments are underlain by continuous permafrost, with a seasonal active layer of 40-100 cm thickness. In the catchments, there is a peat layer of 30-40 cm overlying unsorted glaciomarine till. The surface is comprised of patterned polygonal peat plateaus segregated by sedge lawn and narrow fen channel networks. Dry uplands (plateau) are dominated by lichen-heath communities, with sparse tree cover (*Larix* spp. and *Salix* spp.). Transition zones (moderate moisture, sedge lawns) are comprised of hummocks and hollows, dominated by a mixture of lichen-heath communities and *Carex mitis*. Low-lying channel fens (saturated) are dominated by *Carex aquatilis*. Dwarf shrubs (*Betula glandulosa* and *Salix arctica*) are also found in some channel fens and around pond perimeters.

Six study ponds were selected: Erin Pond, Frisbee Pond, Larch Pond, Left Pond, Strange Pond, and Sandwich Pond (Figure 4.1). These ponds were selected for their range in surface areas, perimeter, catchment area, and depth, because they have been the subject of long-term research in the area, and have been shown to be representative of a range of chemical and hydrological properties (Table 4.1; Macrae et al., 2004; White et al., 2014; Wolfe et al., 2011; Bos & Pellatt, 2012). Each pond was sampled regularly (every 14 days) throughout the ice-free season of 2015, from day of year (DOY) 140-300, May to October). Additionally, during an intensive storm during DOY 185-188, ponds were sampled twice per day during the storm and 24 hours following the event to determine the hydrochemical impacts of a storm event, including the inputs of both direct precipitation and runoff water. Pond stage (water column depth) data were recorded hourly with pressure transducers (HOBO U20, Onset Ltd) installed in PVC (50 mm inner diameter) slotted pipes located within 1m of the shore of each pond (with the exception of Erin pond) and corrected with a barometric logger housed in an identical PVC pipe to minimize temperature-related artifacts in pressure differences between barometric and level loggers (McLaughlin & Cohen, 2011). Precipitation data were taken from the Environment Canada "Churchill" station (20 km west of the study site). Runoff was determined as the residual change in pond storage exceeding the input from direct precipitation during and up to 24 h. following a rain event, after Morison et al. (2017). The perimeter and area of each pond were surveyed with a Trimble Juno SB GPS unit, with a differentially corrected horizontal accuracy of ±5m.

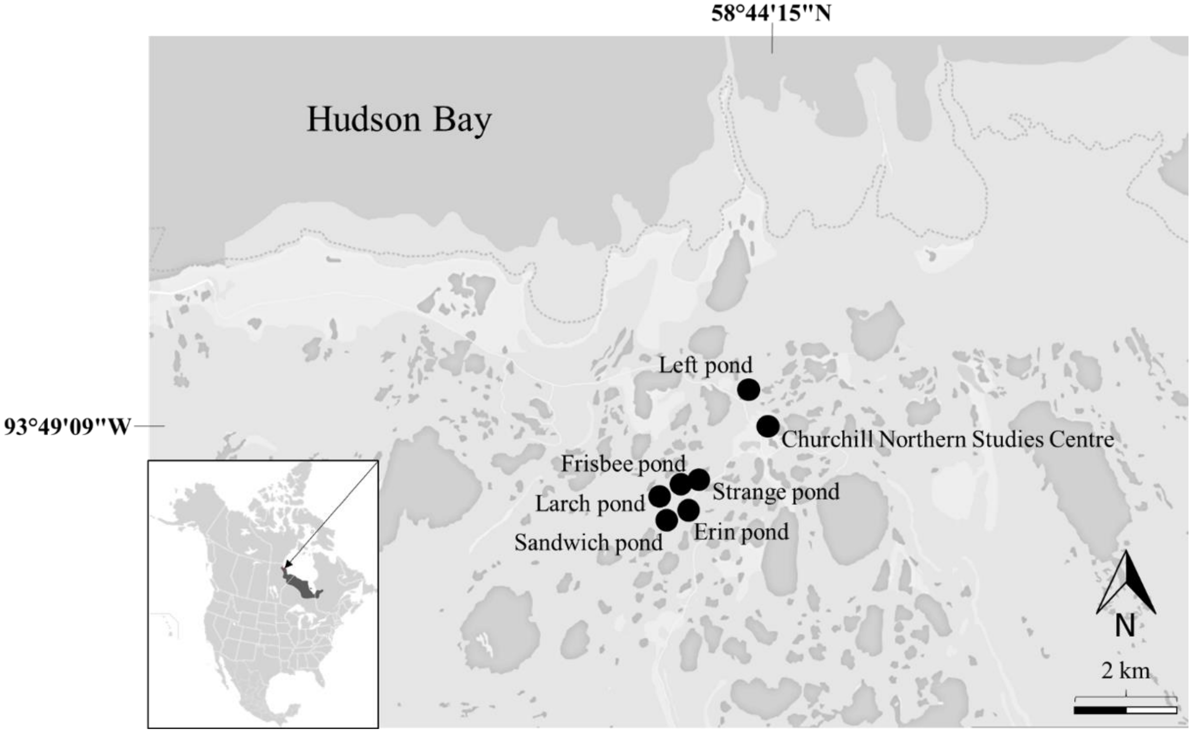

Figure 4.1 Site map of the general near-coastal tundra region with the catchment areas containing Frisbee, Larch, Strange, Sandwich, Left, and Erin Ponds. Inset map highlights the entire Hudson Bay Lowlands (dark-coloured region to the south of Hudson Bay) and the Churchill study region (indicated with an arrow). Map data: Google, Digital Globe, 2017.

Table 4.1 Physical characteristics and locations of study ponds near Churchill, Manitoba. *Shoreline development, D_L, is the ratio of measured shoreline perimeter, P, of a given pond to the shoreline perimeter of a perfectly circular pond of equal area, A, such that $D_L = \frac{P}{2\sqrt{\pi A}}$ (Aronow, 1982).

Pond	Area (m^2)	Perimeter (m)	Shoreline development* (m^1 m^{-1})	Average depth, μ ± σ (cm)	Catchment area (m^2)	Coordinates
Erin	8479	448	1.37	No data	108160	58°43'14.3"N 93°50'20.2"W
Left	752	130	1.34	30.0 ± 6.8	5737	58°44'44.2"N 93°49'20.6"W
Strange	6307	424	1.51	22.2 ± 10.0	20441	58°43'36.8"N 93°50'20.6"W
Sandwich	17146	548	1.18	19.6 ± 4.8	34638	58°43'24.2"N 93°50'34.4"W

Frisbee	4416	258	1.10	14.2 ± 2.8	31128	58°43'35.5"N 93°50'33.9"W
Larch	4066	333	1.47	14.2 ± 4.9	15228	58°43'26.9"N 93°50'41.5"W

4.2.2 Water Chemistry Sampling and Analysis

Samples of pond water were collected manually as a depth-integrated profile of the water column, approximately 3 m from the pond edge, and placed in sterile, triple-primed 50 ml polyethylene containers. Care was taken to not disturb pond sediments when samples were being collected. Samples were preserved on ice in the field and passed through a 0.45 μm cellulose acetate filter within two hours of collection. A 50 ml subsample was acidified to a final concentration of 0.2% H_2SO_4 and stored until digestion. Non-acidified samples were immediately frozen. All samples were shipped to the Biogeochemistry Lab at the University of Waterloo for analysis. In the lab, acidified samples were digested (Kjeldahl digestions, Seal Analytical Hot Block Digestion System BD50, Seattle, USA) for the analysis of dissolved Kjeldahl N (DKN). Digested samples and non-acidified subsamples were analyzed for N species using colorimetric methods: (Bran-Luebbe AutoAnalyzer III, Seal Analytical: Methods G-102-93, [ammonium; NH_4^+-N]; G-103-93 [SRP-P], G-109-94 [nitrate; NO_3^--N], G-189-97 [DKN]). Results for NH_4^+ and NO_3^- have a detection limit of 0.001 mg N L^{-1}. Dissolved organic nitrogen (DON) concentrations were determined as the difference between DKN and NH_4^+ concentrations. Samples were analyzed for other major ions: chloride (Cl^-), sulphate (SO_4^{2-}), sodium (Na^+), potassium (K^+), magnesium (Mg^{2+}), and calcium (Ca^{2+}) using ion chromatography (DIONEX ICS 3000, IonPac AS18 and CS16 analytical columns).

4.2.3 Statistical Techniques

Due to large variability (spatial and temporal) in absolute values of concentration across the data set, values were normalized as deviations from mean values to permit their comparison (Schoenfeld & Numberger, 2007; Viner, 1984). This was accomplished by examining the departure of each sampling point from the mean of either temporal or spatial groups. More specifically, for each measurement, proportional deviations from either spatial or temporal means were determined as the absolute difference from unity of either the ratio of the measured sample concentration at a particular date and pond, $[x]_{st}$, to the mean concentration of the species from all ponds sampled that date, $\overline{[x]_t}$; to examine spatial deviations, Eq. (3.1), or the ratio of the measured sample concentration to the mean concentration of the species from all samples taken from that pond over the entire study period, $\overline{[x]_s}$; to examine temporal deviations, Eq. (3.2).

$$\left|\frac{[x]_{st}}{\overline{[x]_t}} - 1\right| = \text{Spatial Deviation Score} \qquad \text{(Eq. 3.1)}$$

$$\left|\frac{[x]_{st}}{\overline{[x]_s}} - 1\right| = \text{Temporal Deviation Score} \qquad \text{(Eq. 3.2)}$$

Thus, each sample (n = 72; 12 samples from each of 6 ponds) is associated with both a temporal deviation score and spatial deviation score for each chemical species. Once a set of deviation scores was computed for each species, a Mann-Whitney U test was used to determine if there was a significant difference between the medians of the set of spatial deviation scores and the set of temporal deviation scores for each chemical species.

To determine the relationship between pond volume and concentrations of different chemical species, a power function (Eq. 3.3) was fit to the spatially normalized concentration (the ratio of each concentration to the mean concentration $\overline{[x]_t}$) and stage data to represent the geometry of conical bathymetry, based on observations and measurements of several sediment basins, in the non-linear pond stage-volume relationship.

$$[x] = \beta_1(\text{stage})^{\beta_2} \qquad \text{(Eq. 3.3)}$$

The parameter β_2 is invariant under linear translation, such as spatial-normalization, and is expected to maintain a negative value with the magnitude depending on the bathymetry of the pond (with a theoretical value of 0 for a cylindrical flat-bottomed pond, and highly negative for a steep conically-shaped pond basin). The fit of each power function was assessed for each chemical species in each pond with the root mean square error, as the coefficient of determination R^2 is inappropriate for the nonlinear case (Spiess & Neumeyer, 2010). Since the pond mean-normalized concentrations are dimensionless and not scale-dependent, the root mean square error term is also dimensionless and can be compared across ponds and chemical species. The degree of hydrologic control on different nutrient species concentrations was manually determined by the goodness of fit of a power curve to each set of normalized concentration data against pond stage for each of the five instrumented ponds. In each pond, chemical species with a constant pond-specific value of β_2 (the slope of the power curve) with low root mean square error (S) were categorized as hydrologically driven, where species with either (1) a β_2 value inconsistent with other hydrologically driven species or (2) poor performance (greater root mean square error) were categorized as non-hydrologically driven.

A principal component analysis (PCA; Dunteman, 1989) was employed on logarithmically-transformed hydrochemistry data, using singular value decomposition scaled to have unit variance. PCA has been used before in explorations of pond chemical trajectories over a scale of months to years (White et al., 2014, Sokal et al., 2010, Wiklund et al., 2012).

Coherence was assessed by Pearson correlation following the approach of Magnuson et al. (1990), both among lakes for each chemical species as well as for each chemical species in all lakes combined. All statistical analyses were conducted with R software (version 3.3.2, R Development Core Team, 2016).

4.3 Results

4.3.1 Spatial and Temporal Variability of Pond Chemistry

Medians of temporal deviation scores significantly exceeded the median spatial deviation scores in several chemical species (Cl^-, SO_4^{2-}, Na^+, K^+, Ca^{2+}; Figure 4.2) but there was no significant difference between the median spatial and temporal deviation scores for DON, Mg^{2+}, NH_4^+, and NO_3^-. For species that were significantly more temporally variable than spatially variable, concentrations among ponds, despite differences in magnitude, tended to be strongly positively correlated with each other ($p < 0.01$) with the notable exception of DON (Table 4.2). NO_3^- and NH_4^+ were not significantly correlated to any other species ($p > 0.01$) (Table 4.3) while all other species tended to be strongly positively correlated with each other ($p < 0.01$), although there were some exceptions. Spatial deviations did not significantly exceed temporal deviations for any chemical species.

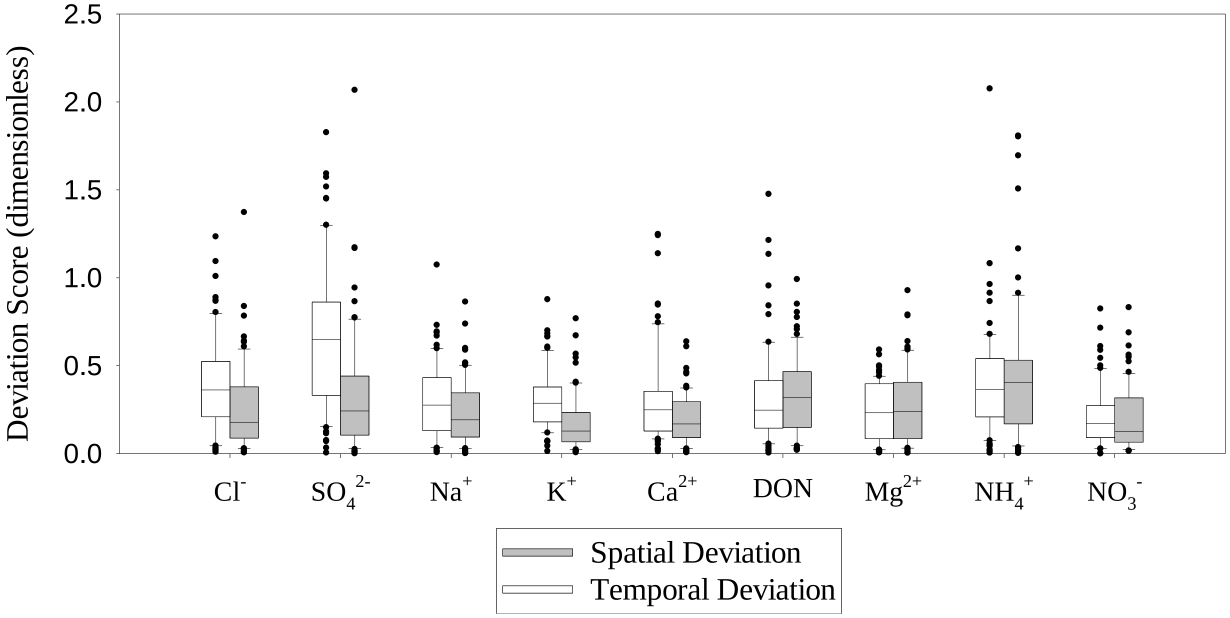

Figure 4.2 Boxplots of spatial and temporal proportional deviations for each chemical species. Significant differences between medians ($p < 0.01$) are present for all species on the left side of the panel (Cl^-, SO_4^{2-}, Na^+, K^+, Ca^{2+}), and no significant difference is present for species on the right (DON, Mg^{2+}, NH_4^+, NO_3^-).

Table 4.2 Correlation coefficients among ponds for all chemical species. Values are bolded when the correlation is significant at the $p < 0.01$ level.

Species/Pond	Erin	Frisbee	Larch	Left	Sandwich
DON					
Frisbee	**0.761**				
Larch	**0.802**	**0.687**			
Left	**0.794**	**0.912**	**0.846**		
Sandwich	**0.860**	**0.689**	**0.965**	**0.829**	
Strange	**0.763**	**0.904**	0.659	**0.900**	**0.688**
Cl^-					
Frisbee	**0.859**				
Larch	**0.762**	**0.751**			
Left	**0.875**	**0.787**	**0.884**		
Sandwich	**0.649**	0.539	**0.941**	**0.851**	
Strange	**0.774**	**0.680**	**0.751**	**0.889**	**0.746**
SO_4^{2-}					
Frisbee	**0.745**				
Larch	-0.056	-0.007			
Left	**0.740**	**0.836**	-0.271		

Sandwich	-0.415	-0.388	0.134	-0.285	
Strange	**0.731**	**0.728**	-0.133	**0.958**	-0.318
Na^+					
Frisbee	**0.863**				
Larch	**0.667**	**0.625**			
Left	**0.875**	**0.765**	**0.818**		
Sandwich	**0.777**	**0.643**	**0.920**	**0.948**	
Strange	**0.843**	**0.682**	**0.711**	**0.963**	**0.897**
K^+					
Frisbee	**0.847**				
Larch	0.561	0.490			
Left	0.401	0.261	**0.584**		
Sandwich	0.428	0.562	**0.794**	**0.523**	
Strange	**0.614**	0.563	**0.834**	**0.734**	**0.725**
Mg^{2+}					
Frisbee	**0.935**				
Larch	**0.830**	**0.881**			
Left	**0.912**	**0.944**	**0.878**		
Sandwich	**0.904**	**0.905**	**0.946**	**0.952**	
Strange	**0.929**	**0.905**	**0.831**	**0.979**	**0.939**
Ca^{2+}					
Frisbee	0.138				
Larch	**0.700**	0.330			
Left	0.278	0.571	0.102		
Sandwich	0.226	0.433	0.354	0.274	
Strange	**0.772**	0.419	**0.723**	0.340	0.566
NH_4^+					
Frisbee	**0.715**				
Larch	**0.605**	**0.619**			
Left	-0.135	-0.250	0.261		
Sandwich	0.000	-0.003	-0.256	-0.103	
Strange	-0.449	-0.040	-0.277	-0.024	-0.325
NO_3^-					
Frisbee	0.000				
Larch	-0.087	0.320			
Left	0.404	-0.346	-0.366		
Sandwich	0.136	-0.011	0.295	-0.289	
Strange	-0.294	-0.133	0.353	-0.504	0.292

Table 4.3 Correlation coefficients among chemical species for all ponds. Values are bolded when the correlation is significant at the $p < 0.01$ level.

Species	DON	Cl^-	SO_4^{2-}	Na^+	K^+	Mg^{2+}	Ca^{2+}	NH_4^+
Cl^-	**0.710**							
SO_4^{2-}	**0.594**	**0.827**						
Na^+	**0.615**	**0.971**	**0.802**					
K^+	0.276	**0.504**	**0.462**	**0.595**				
Mg^{2+}	**0.563**	**0.892**	**0.787**	**0.940**	**0.585**			
Ca^{2+}	**0.605**	**0.408**	**0.531**	**0.285**	0.000	0.166		
NH_4^+	-0.097	0.034	0.039	0.000	-0.163	0.027	-0.082	
NO_3^-	-0.134	-0.201	-0.143	-0.207	-0.076	-0.158	-0.078	0.218

4.3.2 Seasonal Patterns in Pond Water Chemistry

Pond water chemistry varied among ponds, but also throughout the season (Figure 4.3). Throughout 2015, the temporal trend of pond mean-normalized concentrations in the six ponds appeared to have a spatial coherency in DON, Cl^-, SO_4^{2-}, Na^+, K^+ and Mg^{2+} concentrations. There was a gradual increase in concentrations of these species from DOY 140-260, punctuated by small decline in concentrations following a large storm on DOY 185-188, followed by a gradual decrease from DOY 260 to the end of the season. Ca^{2+} displayed a contrasting temporal trajectory to the other chemical species, decreasing from DOY 190 to the end of the season, while NO_3^- and NH_4^+ appeared to have no coherent pattern relative to the other chemical species. Generally, ponds were closest to their mean values during the mid-season (DOY 200-250) and pond-mean normalized concentrations differed the least among ponds during this time, being more divergent earlier (DOY 140-200) and later (DOY 250-300) in the season.

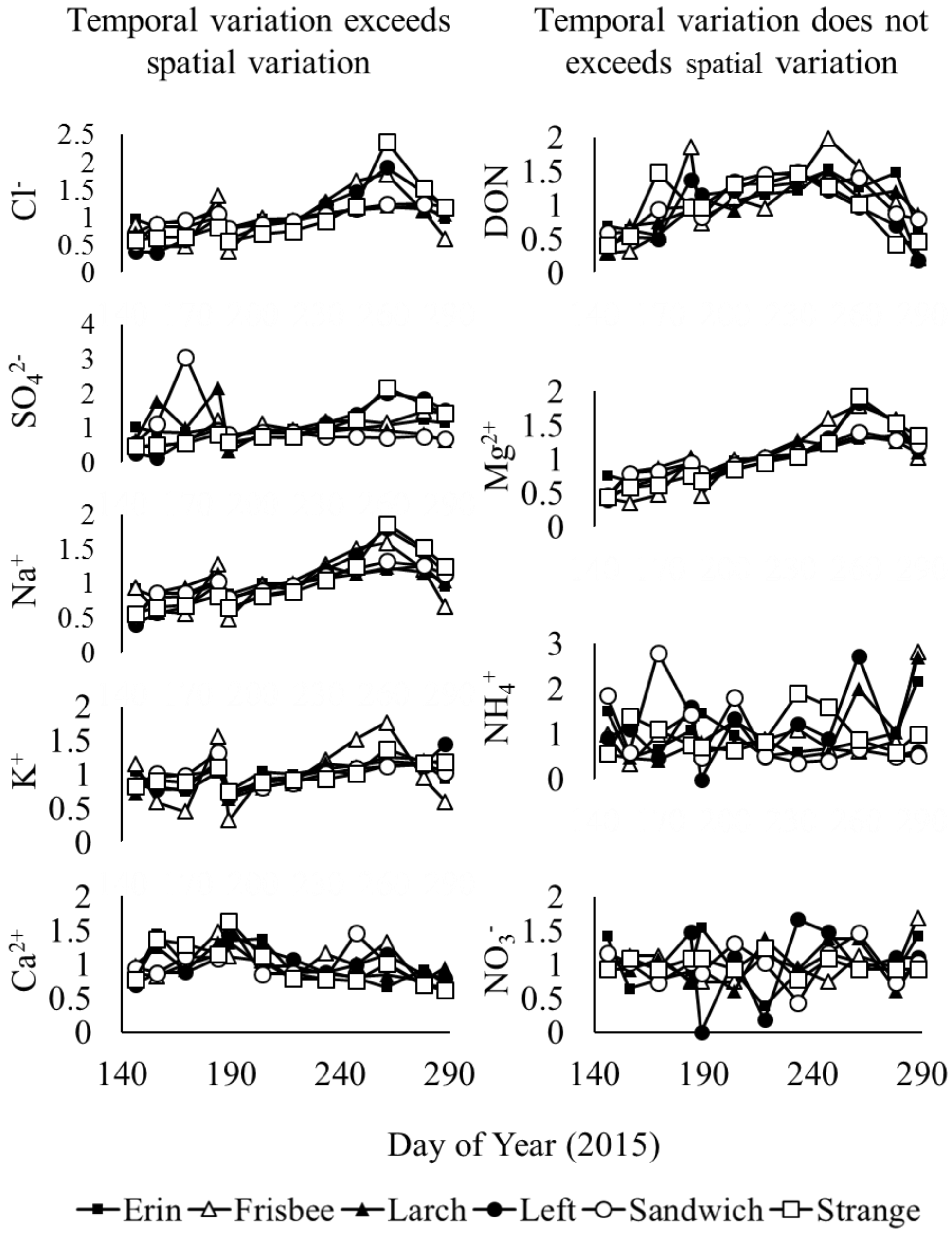

Figure 4.3 Pond normalized concentrations of all measured chemical species in each pond and precipitation for the 2015 snow-free season. In chemical species on left side of the panel (Cl^-, SO_4^{2-}, Na^+, K^+, Ca^{2+}) temporal variation exceeds spatial variation, and no significant difference is present for species on the right (DON, Mg^{2+}, NH_4^+, NO_3^-).

4.3.3 Pond Hydrology and Linkages with Water Chemistry

As was observed for water chemistry, there was also a seasonal pattern in pond hydrologic storage (Figure 4.4). In general, ponds were full following snowmelt, with water levels generally declining throughout the season and eventually rising again in late summer. Catchments showed synchronous runoff responses to two major rain events on DOY 166 and DOY 185 and three smaller rain events between DOY 260 and 290, although the magnitude of response varied. Following the early-season rain events, Left Pond and Strange Pond experienced prolonged summer drawdown while this drawdown was less pronounced in Larch, Frisbee and Sandwich Ponds. At DOY 250 all ponds began a gradual increase in stage continuing to the end of season, but did not return to post-snowmelt levels. Within these five study ponds with recorded depth, there appeared to be no clear relationship between variation in stage and pond geometry (depth, shoreline development, area, or perimeter; Table 4.1).

Generally, DON, Cl^-, Na^+, K^+ .and Mg^{2+} were classified as the hydrologically driven chemical species and Ca^{2+}, NH_4^+, NO_3^-, and SO_4^{2-} were classified as non-hydrologically driven (Table 4.4; Figure 4.5). There were few exceptions to this general classification, most notably, DON and K^+ tended to slightly poorer fits (larger S; slightly less hydrologically driven) in Sandwich Pond, whereas SO_4^{2-} may have been hydrologically driven in Strange Pond. Slight differences in β_2 values among ponds for hydrologically driven species are influenced by the differences in bathymetry which dictates the stage-volume relationship.

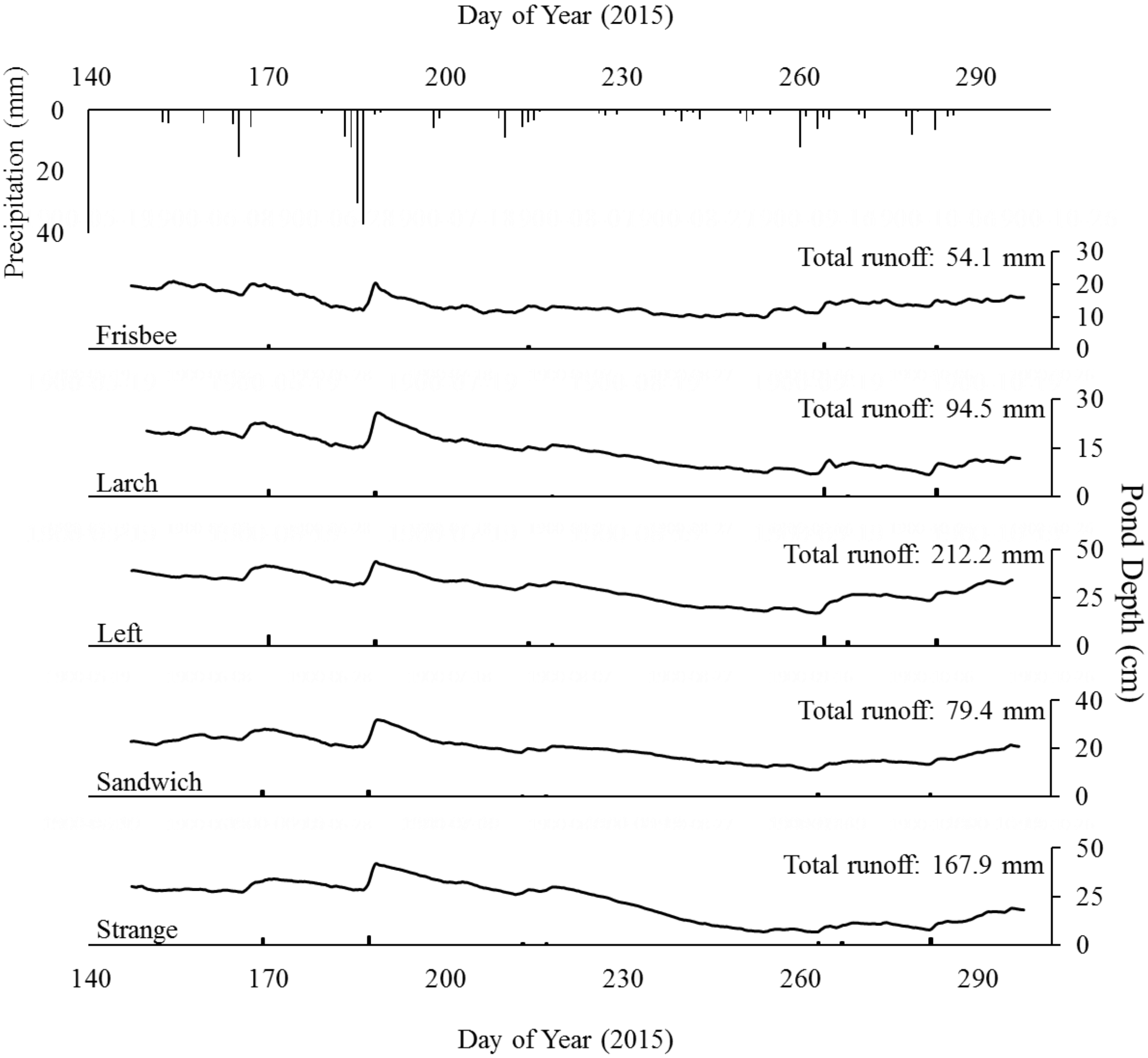

Figure 4.4 Precipitation (vertical bars, top panel), as well as depth of water column (continuous line) and runoff depths (vertical bars) in each of the instrumented study ponds over the 2015 ice-free season.

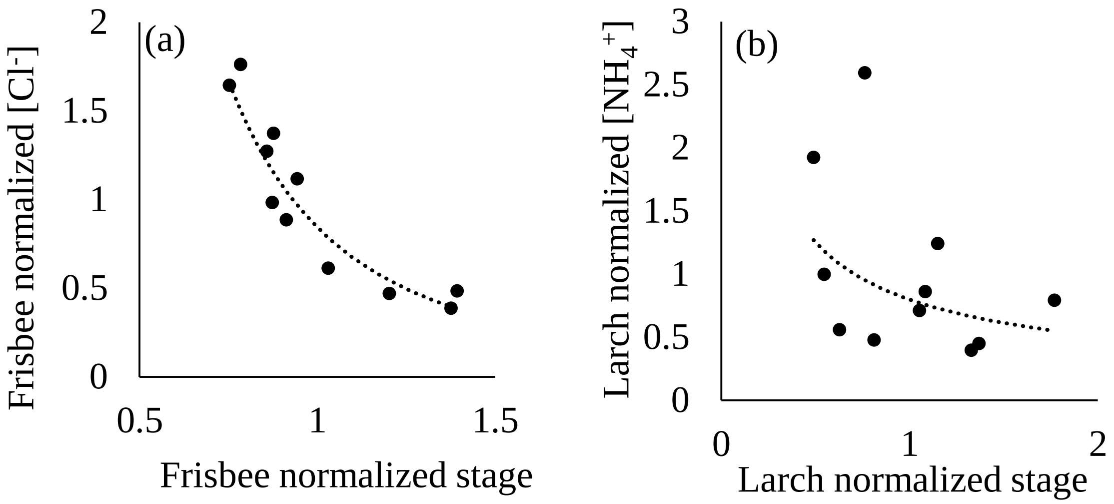

Figure 4.5 Comparison of the stage-concentration relationship in a (a) hydrologically driven chemical species (Cl$^-$, in Frisbee Pond), and (b) a non-hydrologically driven species (NH$_4^+$, in Larch Pond).

Table 4.4 Values of β_2 and root mean square error (S) from the curve $[\boldsymbol{x}] = \frac{[x_{st}]}{[x_s]} = \boldsymbol{\beta_1}(\textbf{stage})^{\beta_2}$ for each set of normalized concentration data, $[\boldsymbol{x}]$. Chemical species were manually classified as hydrologically driven if they shared a common (approximate) $\boldsymbol{\beta_2}$ value within a pond with a low S relative to other species in the same pond. Notable exceptions to the general classification in the table heading are bolded.

	Hydrologically driven					Not hydrologically driven			
	DON	Cl$^-$	Na$^+$	K$^+$	Mg^{2+}	Ca^{2+}	NH$_4^+$	NO$_3^-$	SO$_4^{2-}$
Frisbee									
β_2	-2.61	-2.63	-2.01	-2.52	-2.15	-0.38	-0.23	0.23	-1.11
S	0.27	0.16	0.15	0.22	0.23	0.25	0.70	0.29	0.24
Larch									
β_2	-0.35	-0.28	-0.29	-0.38	-0.44	0.39	-0.73	-0.18	0.08
S	0.16	0.06	0.09	0.09	0.08	0.14	0.65	0.29	0.52
Left									
β_2	-0.70	-1.20	-1.07	-0.21	-1.05	-0.12	-1.44	-0.29	-1.30
S	0.28	0.19	0.14	0.19	0.16	0.15	0.52	0.38	0.35
Sandwich									
β_2	**-0.47**	-0.43	-0.53	**-0.28**	-0.63	0.36	0.82	-0.35	0.85
S	**0.19**	0.08	0.05	**0.15**	0.07	0.30	0.78	0.28	0.66
Strange									

β_2	-0.16	-0.75	-0.55	-0.23	-0.57	0.42	-0.08	0.07	**-0.71**
S	0.37	0.18	0.11	0.11	0.15	0.24	0.45	0.13	**0.18**

4.3.4 Principal Component Analysis

PCA allowed for a reduction in the redundancy of species that are highly correlated (Table 4.3) and the clustering of samples from each pond in PC space (Figure 4.6). The analysis also shows a clustering of chemical species along the PC axes. A collection of the hydrologically driven chemical species (Table 4.4; DON, Mg^{2+}, K^+, Na^+, Cl^-) closely follows the PC1 axis with slightly negative scores for PC2. Two other non-hydrologically driven chemical species have positive scores along PC1 with slightly negative (SO_4^{2-}) and positive (Ca^{2+}) scores along PC2. Inorganic nitrogen species, (NO_3^- and NH_4^+), also non-hydrologically driven, have negative scores along the PC2 axis and slightly negative scores along PC1. The spread of data points for Strange Pond, Left Pond and Frisbee Pond are more elongate along the PC1 axis where the spread of data from Larch Pond, Erin Pond and Sandwich Pond are aligned along the PC2 axis. Temporally, the data tend to move from the upper-left quadrant (positive scores for PC2, negative scores for PC1) to the lower-right quadrant (positive scores for PC1, negative scores for PC2) over the course of the season. Chemical species which were classified as hydrologically driven (Table 4.4) were not necessarily the same species which showed that temporal variance exceeded spatial variance (Figure 4.2). DON and Mg^{2+} were classified as hydrologically driven but did not have the same degree of temporal coherence displayed by Cl^-, Na^+, and K^+. Conversely, Ca^{2+} and SO_4^{2-} displayed significantly greater temporal variability than spatial variability, but were not classified as hydrologically driven constituents. Strange, Left, and Frisbee ponds were elongated with respect to the PC1 axis, which corresponds closely with the group of chemical species that are hydrologically driven. Strange and Left Ponds showed the greatest variation in pond stage (Table 4.1; Figure 4.4), linking the hydrological variation with the variation in concentrations of chemical species controlled by stage. Frisbee pond showed less variation in stage but was elongate with respect to the axis of the hydrologically driven species cluster, suggesting that variation in pond stage alone does not necessarily dictate which species are most chemodynamic within a pond. Larch and Sandwich Ponds, which showed lesser variation in stage, were elongated with respect to PC2, orthogonal to the cluster of hydrologically driven species along PC1. The redundancy in the original dataset is primarily due to the clustering of the hydrologically driven species along PC1, and the very close clustering of Na^+ and Cl^- in PC space (indicating the marine halite influence on these ponds; Bos and Pellatt, 2012). In addition, the decoupling of Mg^{2+} and Ca^{2+} trajectories (Figure 4.3) and in PC space (Figure 4.6) indicate the potential role of Ca^{2+} in either carbonate cycling associated with productivity and carbon dioxide intake (Macrae et al., 2004), precipitation, or cation substitution (Wetzel, 2001). Further, not only are the hydrologically driven species (Table 4.4) correlated among ponds (Table 4.2), but they are also correlated among species (Table 4.3). The apparent redundancy of several of these chemical trajectories is observed in the normalized time series of concentration data, with many of the species which align along PC1 axis showing similar concentration trajectories at the seasonal (Figure 4.3) and event (Figure 4.7) scales.

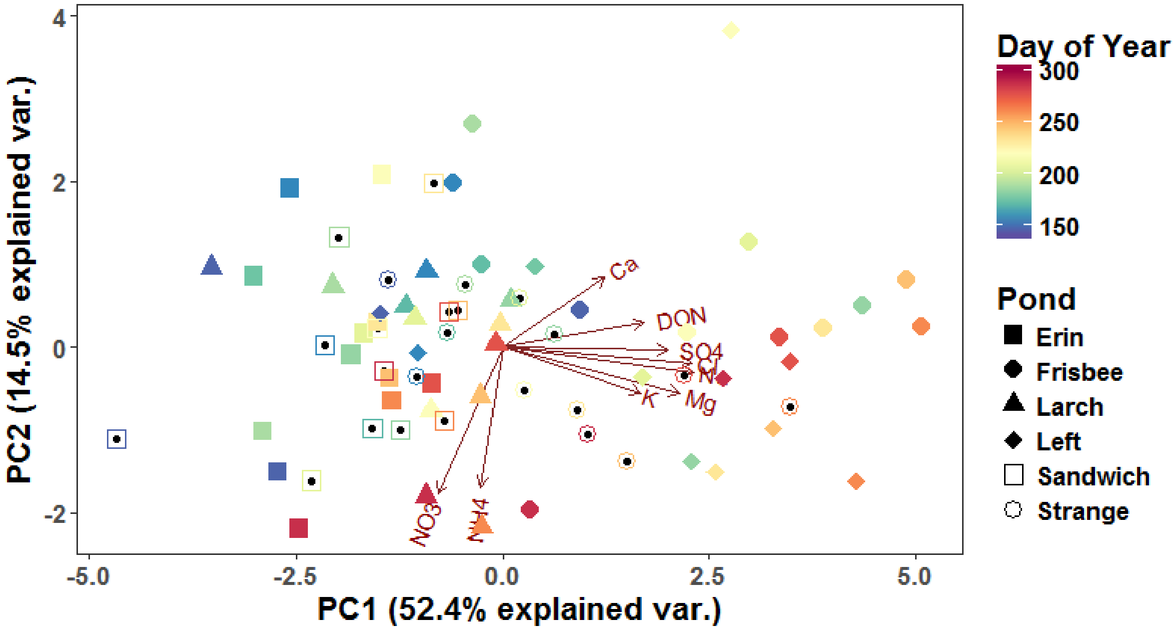

Figure 4.6 Principal components analysis of chemical concentrations in all ponds throughout the 2015 snow-free season. The sampling date corresponds to the colour ramp with earlier dates in blue and later dates in red. PC1 primarily corresponds with the hydrologically driven chemical species while PC2 corresponds to inorganic nitrogen species (NO_3^-, NH_4^+). The hollow symbols are highlighted with solid points.

4.3.5 Event-Scale Variation in Pond Chemistry

In addition to being highly chemodynamic over the course of an ice-free season, pond chemistry varied greatly over the course of a single storm-runoff event (Figure 4.7). For samples taken during and following the storm event in Strange Pond on DOY 185-188, concentrations of some chemical species varied by the same magnitude over the course of several days as they did over the period of the entire ice-free season (DON, K^+, Ca^{2+}, NO_3^-); other species varied but not to the same extent (Cl^-, SO_4^{2-}, Na^+, Mg^{2+}, NH_4^+; Appendix B, Table B.2). In Frisbee pond, chemical species tended to vary by a similar magnitude over the storm period as they did over the entire season, and this was not restricted to DON, K^+, and Ca^{2+}.

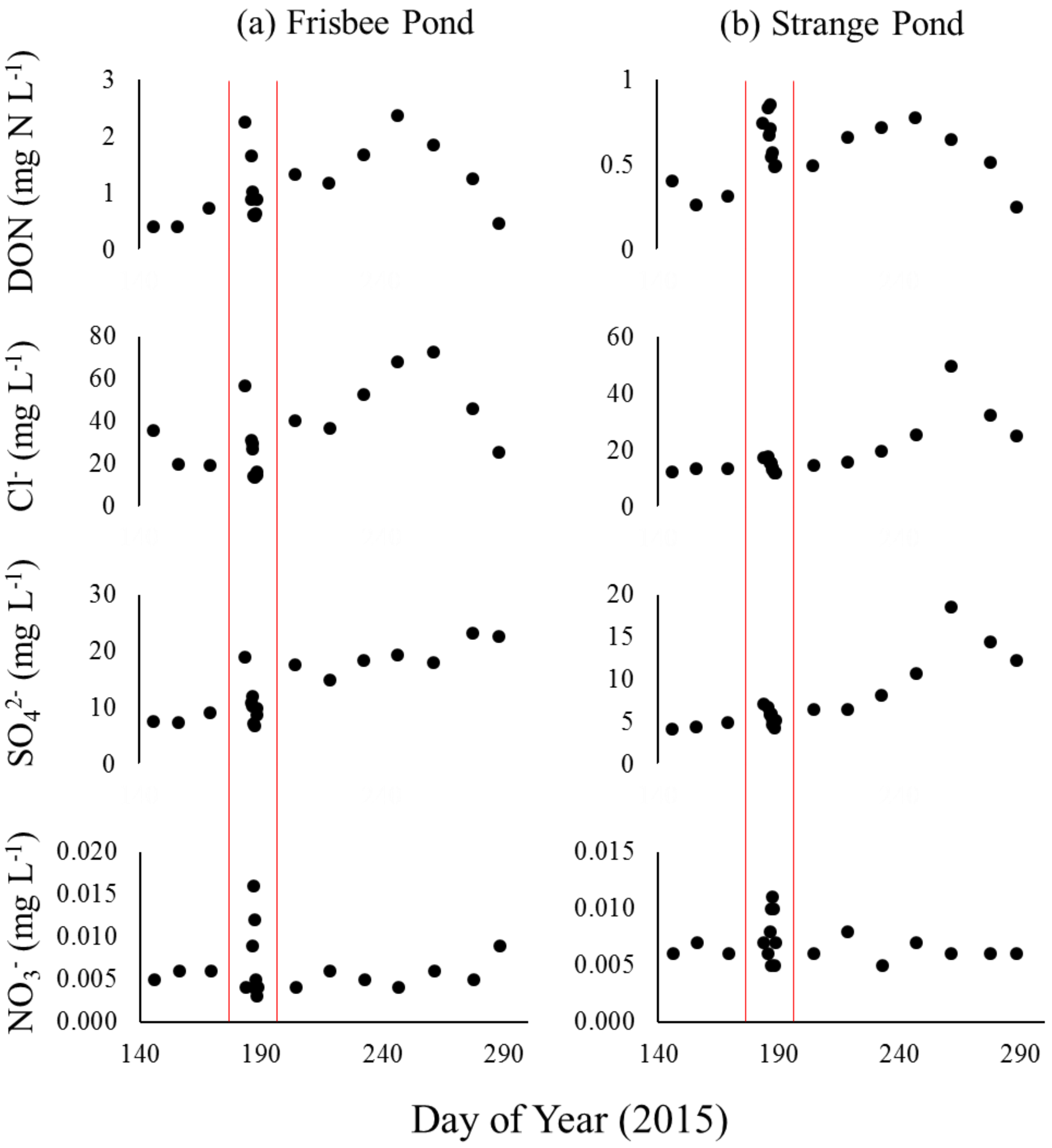

Figure 4.7 Short term variation in DON, Cl^{-}, SO$_4^{2-}$, and NO$_3^{-}$ concentrations in (a) Frisbee pond and (b) Strange Pond during a rain event on July 3rd to 6th, 2015 (DOY 185-188, highlighted with red bars).

4.4 Discussion

4.4.1 Seasonal and Spatial Variability in Pond Chemistry

Ponds in this study displayed a coherent trend in several chemical concentrations over an ice-free season, despite differences in pond geometry, catchment characteristics, and absolute magnitude of chemical concentrations. Landscape scale factors, such as climate, are controlling hydrological processes, which in turn control concentrations of chemical species (specifically, Cl^-, Na^+, K^+, Mg^{2+}, and dissolved organic nitrogen). Magnuson et al. (1990) and Baines et al. (2000) reported Ca^{2+} to be temporally coherent among groups of large lakes in Wisconsin, USA, consistent with our findings, while Magnuson et al. (1990) found K^+ or SO_4^{2-} to lack coherence, contrasting with our results. However, the absolute magnitudes of different chemical species concentrations varied among ponds despite similar trajectories of mean-normalized concentrations. This suggests that influences such as runoff inputs, evapoconcentration, bathymetry, and internal processes (sediment-water interaction and biological cycling) may be driving these absolute differences while preserving seasonal trajectories relative to a pond mean value. Other authors have reported on local spatial heterogeneity of biogeochemical properties of ponds, such as the conditions of nutrient limitation of primary productivity in different lakes (Hogan et al., 2014; Symons et al., 2012) or the impact of localized catchment-scale sedimentation processes on mercury accumulation (Burke et al., 2018). This work suggests that the seasonal trajectory of concentration of at least some chemical species are not reflective of this spatial variability and instead more reflective of landscape-level processes.

The importance of biogeochemical and hydrological processes can be informed by the location of (a) clusters of samples from individual ponds and (b) ordination of chemical species in PCA space. In many of the same study ponds as this work, White et al. (2014) found similar clustering of Cl^-, Na^+, K^+, and Mg^{2+} along their first PC axis (most variance explained) and another cluster including NH_4^+ and NO_3^- along their second axes. In contrast, total nitrogen was approximately orthogonal to both those clusters, instead of being aligned with the other species which were identified as hydrologically driven in our analysis. Differences between the findings of White et al. (2014) and this work may be explained by the inclusion of additional limnological measurements into the PCA, the greater number of lakes in their study (20), the smaller number of samples taken at each lake per year (3), and the reporting of total N as opposed to the dissolved fraction. Sokal et al. (2012) did not report a similar clustering of chemical species in PC space, with TKN, Cl^-, Na^+, Mg^{2+}, and K+ showing great variation relative to the tight clustering found in this study in the Slave River Delta and with less separation from the non-hydrologically driven chemical species in our study (Ca, SO_4). This could be due to larger and deeper lakes studied in the region (~10^6 m^2 surface area; 1.5 m deep) in addition to additional limnological and isotopic measurements into the PCA. However, this difference in species clustering may not be region-specific, as Wiklund et al. (2012) found a clustering of Na^+, Cl^-, TKN, K^+ and Mg^{2+} in PC space from lakes in the Peace Athabasca Delta region. Wiklund et al. (2012) also reported approximately equal angles between vectors of (a) the cluster of hydrologically driven chemical species and (b) Ca^{2+} and SO_4^{2-}, as was found in this study.

4.4.2 Event-Scale Variation in Pond Chemistry

Short-term variation in concentrations during a storm was pronounced in Frisbee pond during the storm of DOY 185-188, 2015. This is likely due to the difference in the proportion of new water entering the pond relative to the volume of old water in the pond. In Frisbee pond, the rainfall inputs represented a much greater fraction of the total pond water at the conclusion of the event (nearly one-half), compared to Strange Pond, which was larger and more full of water pre-event, where event water represented a smaller proportion of the total post-event water (approximately one-quarter) despite the lesser runoff amount (Figure 4.4). This led to the dampening of the storm-based concentration variability in Strange Pond. Those species that may have elevated concentrations in event water relative to lower concentrations in pond water, such as DON (Morison et al., 2017), showed a heightened response in terms of pond concentrations in both Frisbee Pond and Strange Pond. Species which had event water concentrations which were similar to background pond water concentrations showed a dampened response. Although the volume of event runoff water that was added may not have represented a great fraction of the total water in the pond, that new water was enriched in species that occur naturally in rainwater or through primary runoff pathways (shallow, organic subsurface material). This finding agrees with the findings of Abnizova (2013) which showed that the ionic composition at the event scale of runoff water to ponds in high Arctic wetlands was caused by the vegetative structure of the catchment (related to dissolved organic material) and bedrock composition.

4.4.3 Inferring Hydrological and Biogeochemical Process from Patterns in Pond Chemistry

This study does not aim to present direct measurements of any biogeochemical process, including the magnitude and direction of physiochemical transformations. Each chemical species measured in this study is subject to differing degrees of reactivity/conservativism. Future research is needed to elucidate the individual or coupled cycling processes of these elements in subarctic freshwater ecosystems. Chemical species which appear to be driven primarily by non-hydrological processes (Table 4.4) are likely those which are most reactive. However, our results can be contextualized within the existing body of knowledge of hydrobiogeochemical processes which have been measured in similar environments, to determine if our observations are consistent with the explanations for temporal patterns of chemical concentration data in previous findings.

Biogeochemical variations large in magnitude also often occur on short time scales, which are typically associated with the movement of water across geochemical boundaries (McClain et al., 2003). Previous work in tundra and high Arctic environments have shown pathways for transformations of runoff water through the catchments, including biological incorporation of nutrients (Thompson & Woo, 2009) and geochemical processes of weathering and ion exchange (Quinton & Pomeroy, 2006), which impact the quality of the runoff water arriving at the pond. Once the runoff water is delivered to the ponds, rapid biological incorporation and sedimentary burial of nitrogen and phosphorus (< 72 hours of return to pre-event levels) was demonstrated experimentally by Eichel et al. (2014). These observations are consistent with the increase in nutrient concentrations followed by rapid uptake to pre-event levels which was observed during and following the storm event around DOY 185 (Figure 4.7) in this study. These mechanisms of runoff contributions to pond chemical variability are important for future studies that aim to use seasonal and interannual variations in pond and lake chemistries to examine changing flowpaths in thawing permafrost environments. The relative change of concentrations in ponds and lakes over events, seasons, and years will be a product of the difference in concentrations between new and old water and the degree of dilution of new water arriving at the pond. If the concentration of a constituent in old water is not significantly different from that in new water, future work which infers changing flow paths from changing chemical concentrations over time may significantly underestimate the degree of change to the movement of water and solutes due to thawing permafrost (Lougheed et al., 2011). Conversely, it also possible to overestimate the change in flowpaths delivering solutes which are radically different in concentration from old water. In this work, no clear relationship between chemical trajectory (Figure 4.3) and runoff (Figure 4.4) was observed, nor were either related specifically to total catchment area (Table 4.1). However, this may be a result of the variable source area concept applying in this fill-and-spill system (Spence et al., 2010; Morison et al., 2017), in which substantial portions of the catchment are not contributing runoff to the ponds for certain storms which do not provide requisite overfilling of the catchment storage capacity threshold. This effect renders estimates of total catchment area which are delineated by topography less useful without additional knowledge of total subsurface storage capacity and effective contributing area for each runoff event.

The method of fitting curves to stage-concentration relations to manually determine the degree to which evapoconcentration and dilution dictates chemical concentrations may not capture all of the complex dynamics related to hydrological controls. For example, pond volume controls diurnal temperature fluctuation amplitude, and indirectly the rate of biogeochemical processes. In northern tundra environments, low temperatures limit the rates at which biogeochemical processes occur (Stark, 2007). Microbial decomposition remains the crucial bottleneck (rate limiting step) in nutrient cycling (Stark, 2007; Andersen et al., 2013). Temperatures are often the most important factor limiting the rate of microbial decomposition of organic matter in cold region aquatic and terrestrial ecosystems (Wallenstein et al., 2009; Vonk et al., 2015, Wickland et al., 2012). On the North shore of Alaska, Koch et al. (2014) showed that the chemical dynamics were less pronounced in larger ponds with greater storage capacity which maintained lower temperatures, limiting evaporation (and therefore evapoconcentration) as well as retarding biological uptake. Some of these processes may explain some discrepancies between the classified hydrologically driven chemical species and those species for which temporal variability exceeded spatial variability.

4.4.4 Implications for Sampling Design in Future Studies

Generally, the current standard of infrequent measurements per annum are unlikely to be sufficient to capture the variability in highly chemodynamic systems, such as shallow ponds in which storage varies by up to 80% of the mean value over the course of the ice-free season. In contrast, sampling campaigns that are temporally coarse but spatially intensive are applicable for larger volume (less chemodynamic) lakes and ponds, in which total water inputs and outputs represent a much smaller proportion of the total water storage. Further, the synchrony in the chemical behaviour of some species (Cl^-, Na^+, K^+, SO_4^{2-}, Ca^{2+}) in these ponds suggests potential redundancy in the sampling of a great deal of lakes if the research goals are related to the measurement of these chemical species. This study may be subject to different limitations by observing water column chemistry in only six ponds over the ice-free season. However, it appears these six ponds capture a representative range of chemical concentrations, spanning 1-2 orders of magnitude (Appendix B, Table B.2), which are representative of much wider spatial surveys in much of the work outlined in Table B.1 (Appendix B), and, more specifically, in line with the variance observed by other authors who have studied ponds in our specific region (Bos & Pellatt, 2012; White et al., 2014; Jacques et al., 2016). The fact that these ponds are closely spatially clustered may remove effects of microclimates on the scales of 10-100 kilometres which may reduce the degree of synchrony observed in chemical concentrations, due to different precipitation, runoff, and evaporative drawdown regimes. Further, the very shallow and small nature of these ponds in this work, although comprising the majority of surface water features in permafrost landscapes (Muster et al., 2013), may not reflect the chemostatic nature of larger lakes in permafrost regions. Larger lakes, with a much greater total volumetric storage capacity, would be generally subject to hydrologic fluxes (evaporation, precipitation, inflows) which represent a much smaller proportion of total water storage on both annual and individual rain event timescales. This would result in the hydrodynamics and associated changes to hydrochemical concentrations to be dampened in these larger lakes relative to our highly chemodynamic systems.

Future biogeochemical research must consider the relative terms in the water balance in a pond to determine periods of greatest variability (such as snowmelt versus rainwater dominated ponds, e.g., Bouchard et al., 2013). A water budget approach should be incorporated into future studies which attempt to use changing solute concentrations as a proxy for changes to ensure that appropriate hydrological weighting to changes of concentrations in surface water are properly represented. Alternately, approaches characterizing total mass depletion of different ions and nutrients (e.g., Koch et al., 2014), an evaporative normalization factor (e.g., Borghini et al., 2013), the use of the Shannon index in a hydrochemical context (Thompson & Woo, 2009), hydrologic inference through isotopic composition (e.g., White et al., 2014) may provide a hydrologic context to concentration measurements which is lacking otherwise.

4.5 Conclusions

This study reported on the degree of hydrologic control on nutrient and major ion chemistry of a set of six of small (<1 ha), shallow permafrost ponds in the Hudson Bay Lowlands. Generally speaking, temporal variability exceeds spatial variability in pond chemistry in this landscape. Five chemical species (Cl^-, SO_4^{2-}, Na^+, K^+ and Ca^{2+}) showed a temporal coherence in six different ponds over the course of an ice-free season (Figure 4.8). No pond demonstrated a spatial coherence in concentration trajectory which was distinct from any other pond. A set of species was determined to be hydrologically controlled (DON, Cl^-, Na^+, K^+ and Mg^{2+}), either directly through processes of evapoconcentration and inflow/precipitation dilution, or indirectly through pond hydrology exerting an influence on other environmental controls such as temperature regimes, which influence biogeochemical characteristics. Approaches of PCA and coherence/correlation showed that these hydrologically driven chemical species are strongly correlated to each other and among ponds. This evidence suggests that landscape level controls on pond hydrology may reduce the spatial heterogeneity in pond chemical trajectories for the hydrologically driven chemical species, but not for those species that are not hydrologically controlled (Ca^{2+}, SO_4^{2-}, NO_3^-, NH_4^+). Further, at the event scale, variation over the course of days during, and following precipitation events may be on equal order as the variation over the course of months. This longer period variation is also not limited to the hydrologically driven species, indicating the importance of biogeochemically active periods coinciding with periods of water movement across boundaries (catchment-pond interactions). This work has important implications for understanding the highly chemodynamic behavior of small, shallow permafrost ponds through over both short-term and long-term temporal scales while remaining spatially synchronous. Our findings indicate the design of future sampling regimes, which continue to rely on inference from broad spatial sampling at coarse temporal scales must consider the hydrologic context of the samples taken. In particular, the proximity of recent rain events and the trajectory of pond water balance are important considerations for interpreting pond chemical concentration data for the purpose of inferring landscape level changes to permafrost environments.

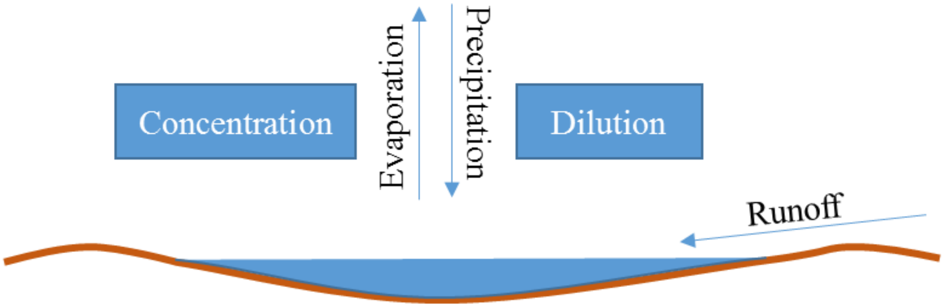

(a) Pond concentrations of DON, Cl^-, Na^+, K^+ and Mg^{2+} are hydrologically controlled

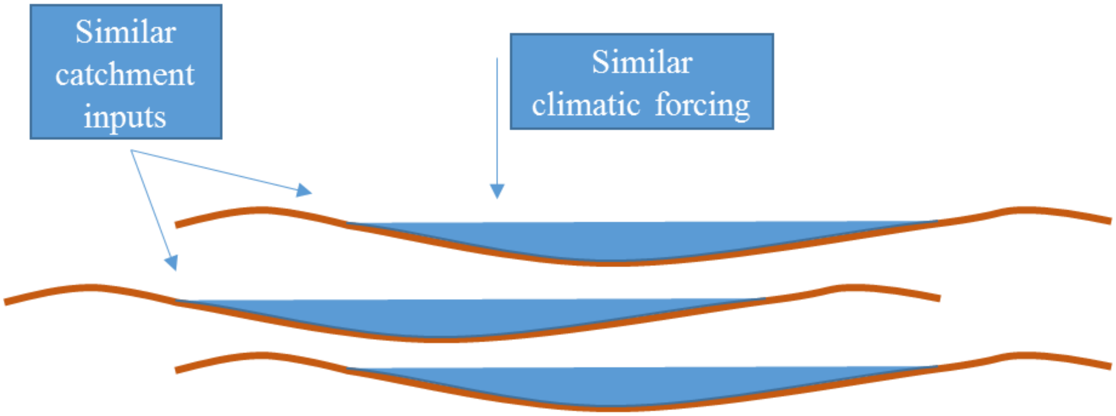

(b) Adjacent ponds experience synchronous variation of Cl^-, SO_4^{2-}, Na^+, K^+ and Ca^{2+}

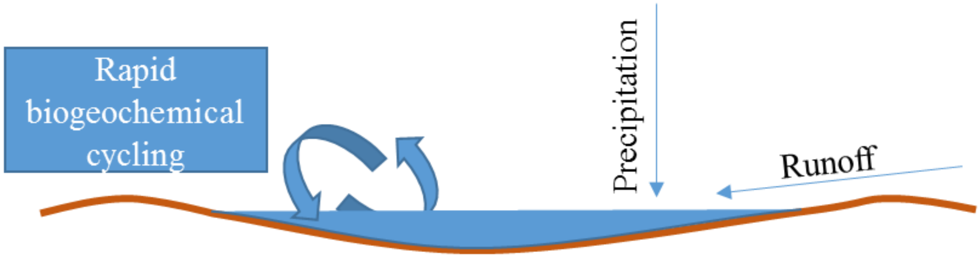

(c) Short-term variability of hydrochemistry during and following storm events may exceed seasonal-term variability

Figure 4.8 Graphical summation of major findings from this study: (a) factors driving hydrological control of particular chemical species in ponds, (b) hypothesized factors driving temporal coherence in chemical species in ponds, and (c) short-term variation in hydrochemistry can exceed seasonal-scale variation despite the large difference in timescales.

4.6 Acknowledgments

The funding for this research came from NSERC Discovery Grants (Macrae, Petrone), NSERC Northern Supplement (Petrone), the Northern Scientific Training Program, and Northern Research Fund (Churchill Northern Studies Centre). Field assistance with sample collection was provided by Matt Webb and Kimberly Thompson. Laboratory assistance was provided by Vito Lam. Additional logistical support was provided by the staff and volunteers of the Churchill Northern Studies Centre. I thank Dr. Genevieve Ali and Dr. Janina Plach for helpful discussions on statistical analyses of the data, the editorial team of Biogeosciences led by Dr. Helge Niemann, as well as Dr. Maciej Bartosiewicz and other anonymous referees for their helpful comments and insight towards improving the final draft of the manuscript.

Chapter 5: Effects of Contemporary Thermokarst Shoreline Expansion on Nutrient Dynamics and Diatom Ecology in a Subarctic Tundra Pond

5.1 Introduction

Within the next century, up to 70% of existing terrestrial permafrost could be thawed through different modes of degradation due to climatic changes (Schaefer et al., 2011; Schuur et al., 2013; Lawrence et al., 2012). Thermokarst-driven collapse of shoreline features and expansion of lakes in permafrost regions has important implications for lake drainage and disappearance (Yoshikawa & Hinzman, 2003), methane dynamics (Walter et al., 2007), and colonization of thaw-lake basins by terrestrial vegetation (Schuur et al., 2007). Thawing permafrost has been shown to modify nutrient export from catchments, resulting in changing stream chemistry (Frey & McLelland, 2009), including a shift from organic nitrogen sources to inorganic (Walvoord & Striegl, 2007) and elevated concentrations of ammonium, nitrate, and phosphate (Bowden et al., 2008).

Previous work focusing on effects of thermokarst slumps in the Northwest Territories on chemistry of adjacent lakes have shown elevated concentrations of calcium, magnesium, sulphate, and decreased dissolved organic carbon in thermokarst lakes relative to undisturbed basins (Kokelj et al., 2005). The evaluated concentrations were attributed to the release of soluble materials from degrading permafrost, with the magnitude of increase in concentrations related to the proportion of catchment area that has been disturbed (Kokelj & Burn, 2005). In particular, lakes and ponds with small surface areas (< 1 ha), which are abundant in the landscape (Muster et al., 2013), are more susceptible and sensitive to inputs of allochthonous matter than larger lakes, as the total volume of these lakes may be small relative to the mass loading of nutrients and carbon of terrestrial origin due to thermokarst lake expansion processes.

In contrast to gradual active layer deepening, in which dissolved export fluxes of nutrients and solutes increase, mass wasting (resulting in transport of particular matter) is enhanced by thermokarst processes (Lewkowicz & Kokelj, 2002; Gooseff et al., 2009). The transport of dissolved and particulate phases of nutrients are distinct for several reasons, including the hydrological transit time, as well as the biogeochemical transformations that the nutrient is subject to. For instance, the flux of phosphorus in sediment form (as opposed to dissolved phases) through a catchment is subject to fewer biogeochemical transformations in transport, as particulate phosphorus is less reactive in transport than dissolved phosphates (Dornblaser & Striegl, 2007; Lobbes et al., 2000; Dittmar & Kattner, 2003). Given that many aquatic systems in cold-region are nutrient limited (Levine & Whalen, 2001; Bergström, 2010; Bonilla et al., 2005), the addition of bioavailable nitrogen and phosphate from thermokarst slumping events to downstream ponds could have important implications for productivity (and associated carbon storage) and community structure of lentic biota. Indeed, experimental additions of nutrients to shallow ponds have resulted in increases in productivity (Eichel et al., 2014; Symons et al., 2012). Thus, an improved understanding of how thermokarst processes will affect lake nutrient cycling is needed to anticipate future ecological changes in permafrost systems.

In tandem with changing nutrient concentrations and stoichiometry, freshwater ecosystems across the circumpolar arctic have experienced unprecedented diatom regime shifts associated with climatic warming during the past 150 years, with generally higher productivity and greater diversity of diatoms (Smol et al., 2005). Comprehensive evidence across many northern environments indicates that important ecological thresholds have been crossed since 1850 (Smol & Douglas, 2007) and that diatom ecology is strongly influenced by water surface temperature (Pienitz et al., 1995). The impact of thermokarst activity also impacts diatom abundance and composition through changes to hydrochemistry, water level and habitat arability, such as in the Siberian Arctic through the Late Holocene (Biskaborn et al., 2013) and the eastern Hudson Bay Lowlands through the past two centuries (Bouchard et al., 2013). However, the shorter-term responses of diatom communities to present-day catastrophic thaw and shoreline erosion disturbance events require further study in shallow freshwater permafrost systems.

A recent (2006-2008) thermokarst shoreline expansion in a shallow subarctic peatland pond in the Hudson Bay Lowlands is examined in this study, as it presents a unique opportunity to assess the extent of changes to sediment nutrient accumulation, nutrient isotopic signatures and diatom community structure due to thermokarst slumping. I hypothesized that thermokarst expansion would result in increased allochthonous organic matter supply, which would be reflected in a shift in nutrient origin and deposition flux, and isotopic signatures towards that of terrestrial material in the pond sediment. These processes, as well as enhanced productivity due to nutrient inputs in a nitrogen and phosphorous-limited system, would lead to an increased sedimentation rate and greater bulk diatom productivity.

5.2 Materials and Methods

5.2.1 Study Site

Frisbee pond (58.727° N, 93.843° W) is located in the western Hudson Bay Lowlands, a transition zone between open tundra and the northern edge of the boreal forest. The regional climate is strongly influenced by the proximity of Hudson Bay (Rouse, 1991) and is a continuous permafrost zone with an active layer depth of 0.4 to 1 m (Dyke & Sladen, 2010). The landscape is poorly drained due to low relief (~ 1 m km^{-1}) and the confining nature of permafrost, which leads to the prevalence of small closed-basin shallow pond and lake systems (Keller et al., 2014). Recent climatic changes have resulted in enhanced thermokarst processes in the region (Payette et al., 2004). The contemporary nutrient status in surface sediment and water chemistry of small tundra ponds in this region has been investigated across several spatial and temporal scales (White et al., 2011; Paterson et al., 2014; Macrae et al., 2004; Morison et al., 2017). As well, recent work has investigated disturbance to ponds in this region from factors not directly related to permafrost degradation or warming air temperatures, such as increased nutrient loading due to increasing influence of lesser snow geese in the region (MacDonald et al., 2015). Frisbee pond has undergone thermokarst-driven shoreline expansion throughout the period 2006 – 2008, the extent of which is visible from satellite imagery (Figure 5.1). This event led to the inundation of formally terrestrial material becoming incorporated into the total lake area. The perimeter increased from 250 to 700 m, and the pond area increased from 3,400 to 10,800 m^2, estimated from historical imagery and surveys of previous shorelines of the pond.

Air temperature and precipitation data for the region were acquired from Environment and Climate Change Canada (2017) stations “Churchill A” (58.74º N, 94.07º W; data for 1947 to 2007) and “Churchill Climate” (58.73º N, 94.07º W; data for 2008 to 2015), and the data for each station were assumed to be representative of conditions at Frisbee pond given the proximity of the stations and their similar elevation (less than 1 m elevation difference).

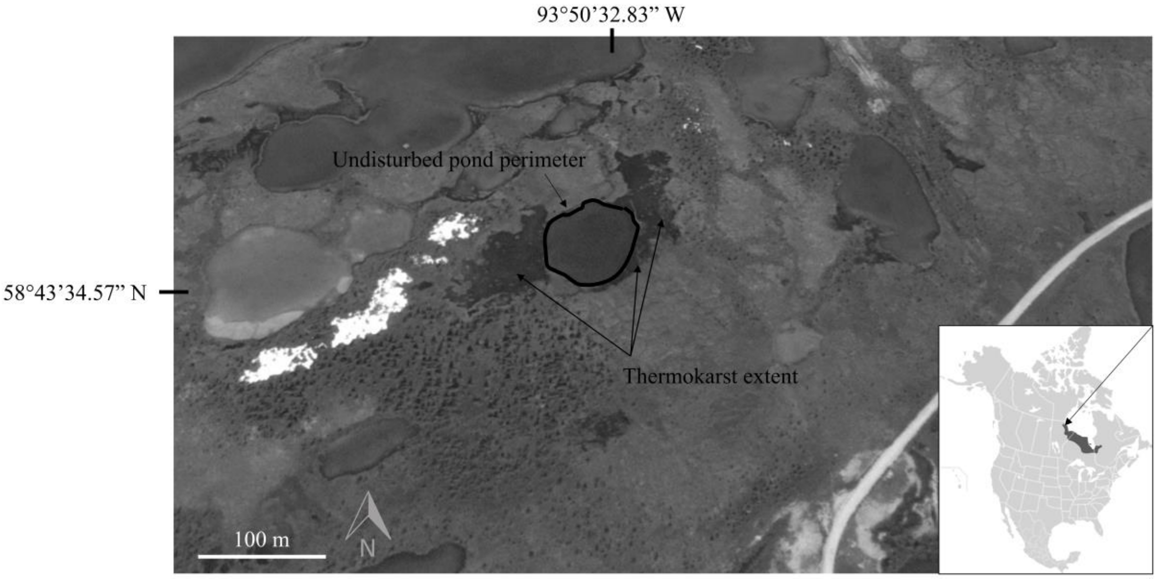

Figure 5.1 Frisbee pond basin; the undisturbed pond perimeter prior to the thermokarst event is highlighted in a thick black outline while the extent of the thermokarst shoreline slump is evident in the photo Imagery was obtained from DigitalGlobe, and was collected on July 29, 2014. Inset map highlights the entire Hudson Bay Lowlands (dark coloured region to the south of Hudson Bay) and the location of Frisbee pond (indicated with an arrow).

5.2.2 Sediment Core Collection

A 7.62 cm inner diameter cylindrical gravity corer was used to retrieve a 29-cm long core from Frisbee pond in September, 2015, approximately 7-9 years after thermokarst expansion. The sediment core was sectioned into 0.5-cm intervals using an upright extruder (Glew, 1988), and stored in sealed plastic bags at 4 °C in a dark environment until analysis. Gravimetric moisture content, organic matter content, and carbonate content were determined by sequential mass loss following oven treatments of 90 °C for 24 hours, 550 °C for 4 hours, and 950 °C for 1 hour, respectively (Heiri et al. 2001). Bulk density was determined as the total dry mass of sample contained in the volume of each 0.5-cm section.

5.2.3 Core Chronology

A ^{210}Pb constant rate of supply (CRS) chronology was constructed for the Frisbee Lake sediment core using standard methods (Appleby & Oldfield, 1978; Binford, 1990; Appleby 2001; Sanchez-Cabeza & Ruiz-Fernandez, 2012; Figure 5.2). Freeze dried subsamples (n=11; 0.8 – 2.2 g per interval) spanning the top 13 cm of the core were packed into plastic tubes and sealed with a silicone septum and epoxy resin and allowed to equilibrate for ≥2 weeks before analysis of ^{210}Pb, ^{226}Ra and ^{137}Cs activity via gamma ray spectroscopy (HPGe ORTEC digital gamma ray spectrometer). Excess ^{210}Pb activities (total ^{210}Pb – ^{226}Ra activity) corrected to coring date in conjunction with cumulative dry sediment mass (g cm^{-2}) was used to construct the CRS age model and interval specific sedimentation rates (g cm^{-2} year^{-1}) for the sediment core where total ^{210}Pb – (^{226}Ra + pooled Standard deviation of ^{210}Pb and ^{226}Ra activities) was > 0 as in Binford (1990) and Appleby (2001), which comprised the 10 cm of the Frisbee core. Total inventory of excess ^{210}Pb activity utilized by the CRS age model was corrected for in the manner described in Appleby (2001). The artificial fallout radionuclide (^{137}Cs) was used to verify the ^{210}Pb age model as peak North American ^{137}Cs fallout occurred in 1963 due to atmospheric nuclear weapons testing. The ^{210}Pb determined age-depth of the Frisbee Lake sediment core interval containing the most ^{137}Cs activity was congruent with the known timing of peak ^{137}Cs fallout.

5.2.4 Sediment Core Nutrient Analysis

A subsample of each 0.5-cm section was freeze-dried, ball-milled, and treated with 10% HCl to remove carbonate minerals, and then rinsed with deionized water repeatedly until the pH of sediment slurries returned to neutral. Dried subsamples (1 mg to 0.2 g dry mass, dependant on instrument signal strength) were analyzed for bulk composition of total organic carbon and nitrogen at the University of Waterloo Environmental Isotope Laboratory (Costech Instruments 4010 Elemental Analyzer). Carbon stable and nitrogen isotopic composition were measured with a continuous flow isotope ratio mass spectrometer (CF-IRMS) at the University of Waterloo Environmental Isotope Laboratory. The stable carbon isotope ratio is reported as $\delta^{13}C_{org}$ values in per mil (‰) units relative to the Vienna – Peedee Belemnite (VPDB) standard, while $\delta^{15}N$ values are in per mil units (‰) relative to atmospheric abundance. As carbonate content was very low (0.6 ± 0.3 mass percent) throughout the upper 10 cm of the core, and thus organic carbon values are reported as total carbon or total $\delta^{13}C$. A second dried and milled subsample (0.2 ± 0.01 g dry mass) of each core section was digested in H_2SO_4 and H_2O_2 for the determination of total phosphorus through the method of Parkinson and Allen (1975), with subsequent analysis of digested phosphorus as phosphate through standard colorimetric methods at the University of Waterloo Biogeochemistry Laboratory (Bran-Luebbe AutoAnalyzer III system, Seal Analytical, Method G-188-097). Nutrient sediment accumulation rates were then determined as the product of the concentration of each nutrient in the sediment and the sedimentation rate.

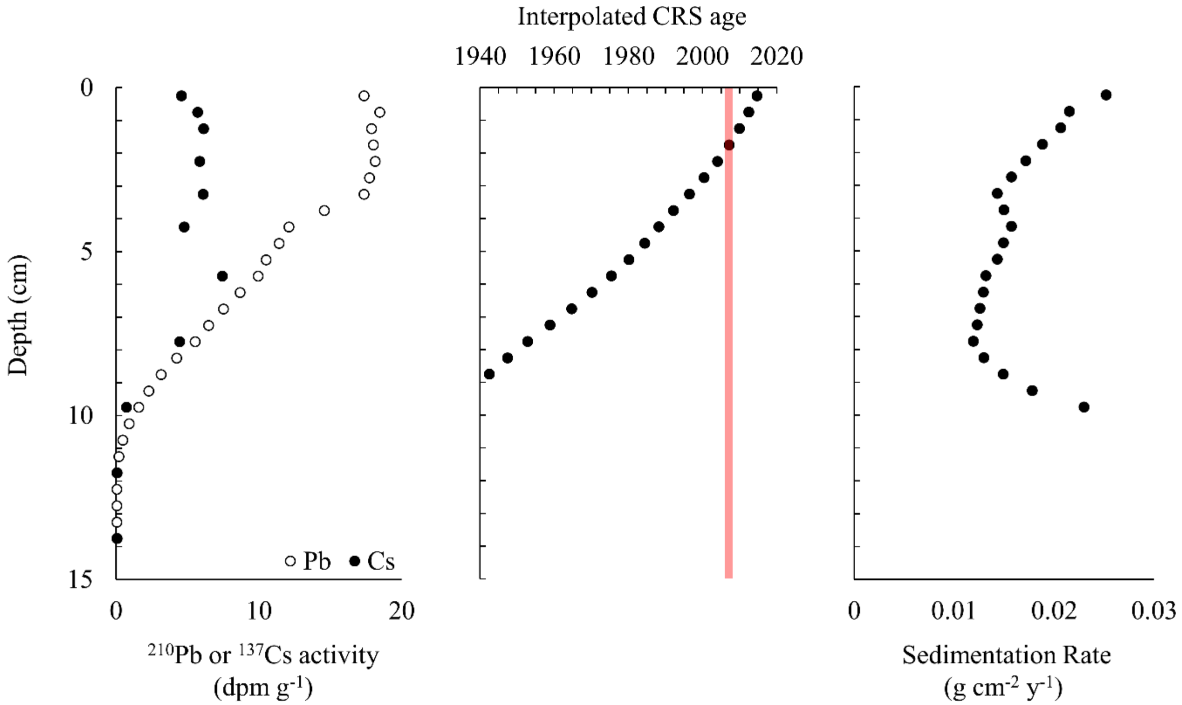

Figure 5.2 ^{137}Cs activity and ^{210}Pb activity through depth, interpolated CRS age-depth model, and sedimentation rate through time for the Frisbee Pond core. The timing of the thermokarst event is highlighted with a red outline.

5.2.5 Diatom Analysis

A subsample (0.2 ± 0.05 g wet mass) of each 0.5-cm core section was digested in a 1:1 volumetric mixture of H_2SO_4 and HNO_3 to remove organic material, following standard methods (Battarbee et al., 2001). Following digestion, diatom slurries were rinsed repeatedly with deionized water until returning to their initial pH. A known quantity of marker microspheres was added in order to quantify the diatom concentration. Diatom slurries were dried onto glass coverslips and mounted onto slides using Naphrax (refraction index 1.7), and diatom identification was performed at 1000x magnification following taxonomic information in Spaulding et al. (2010). At least 400 valves were counted in each sample, and relative abundance and total diatom concentration values were calculated following the methods of Battarbee et al. (2001).

5.3 Results

5.3.1 Hydroclimatic Conditions Preceding the Thermokarst Event

Summer air temperatures were relatively constant during 1947-1990, with a mean June, July, and August (JJA) temperature of 9.9 ± 1.0 ºC (Figure 5.3). From 1991-2015, mean JJA air temperature increased to 11.1 ± 1.4 ºC. This warming prior to the thermokarst shoreline expansion includes all of the thirteen warmest years since 1947. This period also corresponded with an increase in the cumulative precipitation departure from the long term (1946 – 2016) annual mean (427.0 mm), including a cumulative surplus of +821.5 mm above the long term mean during the period 1996 – 2006. This cumulative surplus represents almost two years equivalent of average precipitation (427.0 mm) over the decade preceding the thermokarst event in Frisbee pond.

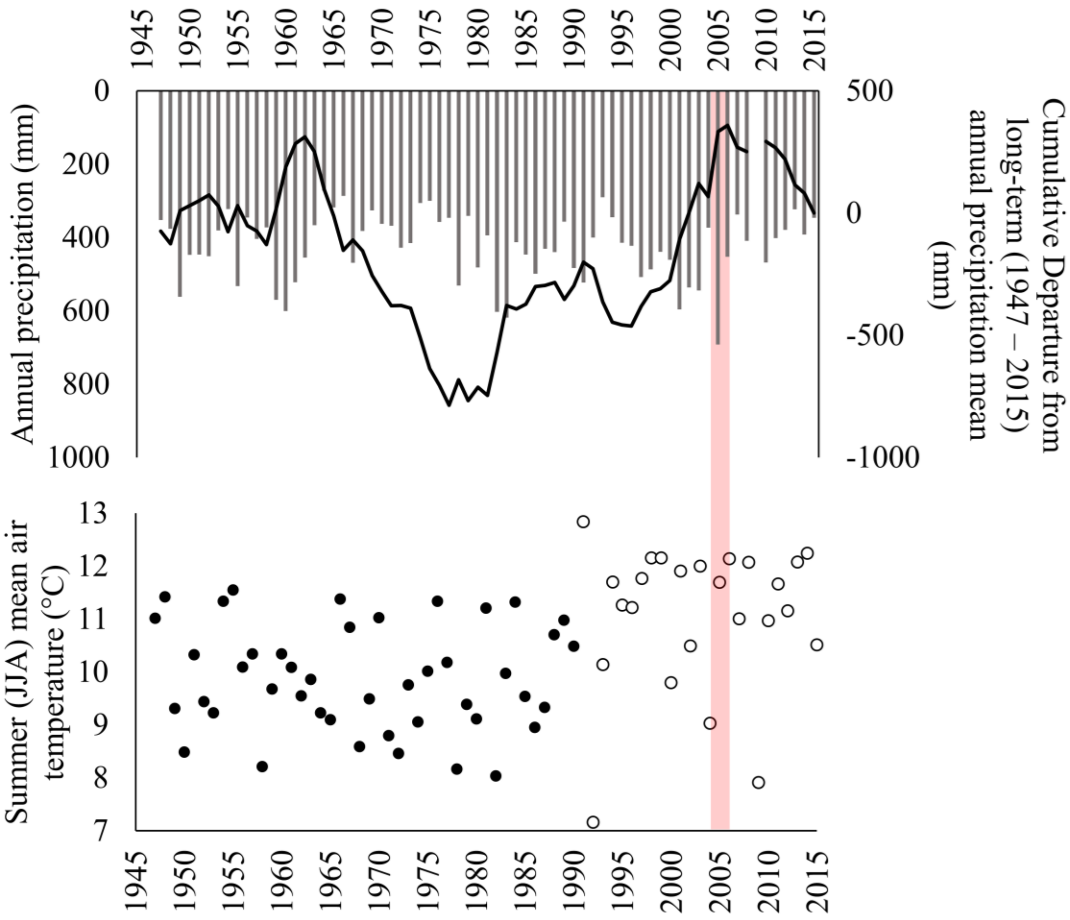

Figure 5.3 Summer (June, July and August; JJA) air temperature and annual precipitation in the Churchill region, 1947 - 2015. Total annual precipitation is shown as bars, while the cumulative departure from the long-term (1947 – 2015) precipitation mean (167.0 mm) is shown as a solid line. Mean annual air temperatures 1946 – 1990 are shown as black dots, while temperatures 1990 – 2016 are shown as open circles. The thermokarst event is highlighted with a red outline.

5.3.2 Sediment Composition and Nutrients

Carbon, nitrogen, and phosphorus sedimentation rates all increased leading up to, during, and following the thermokarst shoreline slump event (Figure 5.4). Carbon accumulation increased from ~0.8 mg C cm^{-2} y^{-1} (2004) to 0.13 mg C cm^{-2} y^{-1} (2014), nitrogen accumulation increased from 4.8 µg N cm^{-2} y^{-1} (2004) to 7.0 µg N cm^{-2} y^{-1} (2014), and phosphorus accumulation increased from 11.2 ng P cm^{-2} y^{-1} (2004) to 21.4 ng P cm^{-2} y^{-1} (2014). No obvious “shift” in sedimentation rates or C,N or P accumulation was observed during or following the thermokarst slumping event. However, the isotopic composition of the deposited sediment appeared to shift following the thermokarst event (Figure 5.4), where δ^{13}C decreased from -23.0 ‰ (2007) to -23.9 ‰ (2014) and δ^{15}N increased from -0.6 ‰ (2007) to 0.1 ‰ (2014). The total organic content of the sediment did not change substantially from ~1930 to 2015 (88.1 ± 0.7 percent by mass).

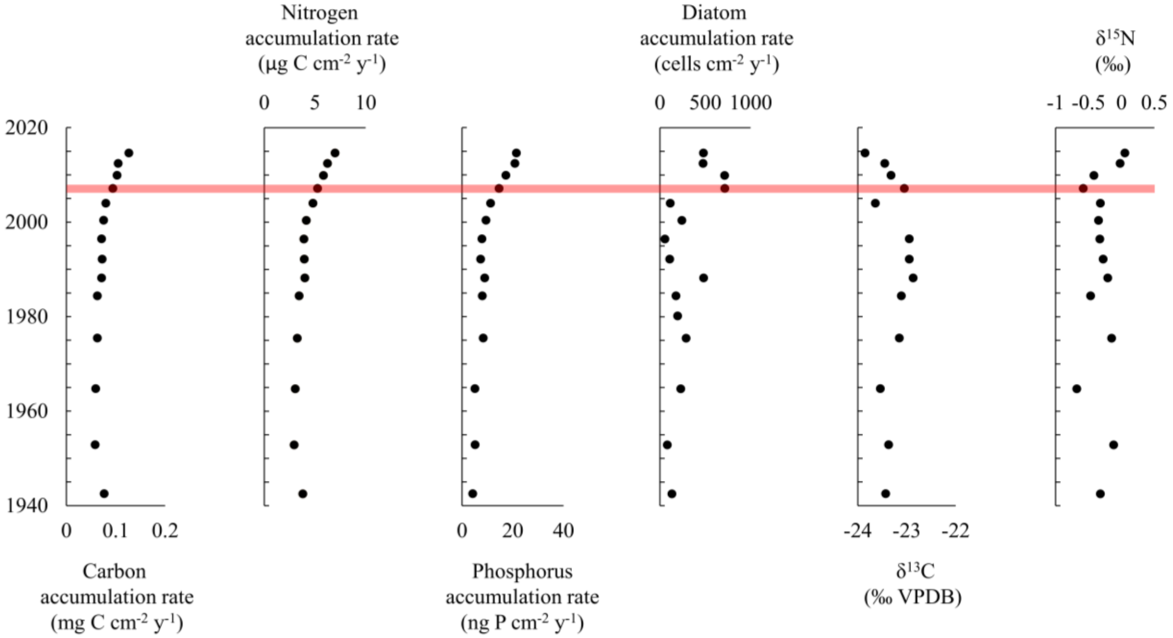

Figure 5.4 Carbon, nitrogen, phosphorus, and diatom accumulation rates in the sediment core from Frisbee pond (~1940 to 2015), with isotopic composition of carbon and nitrogen. The thermokarst event of 2006-2008 is highlighted with a red outline.

5.3.3 Diatom Assemblages

Twenty-nine species were identified in the sediment core samples analyzed, but only 11 species were present at maximum abundance of >1%, and only those species were included in further analyses. Immediately following the thermokarst event, total accumulation increased to 715 cells cm^{-2} y^{-1}, outside of the range of pre-disturbance conditions, before decreasing to ~478 cells cm^{-2} y^{-1} over the seven-year period following disturbance. Total diatom accumulation was relatively low (<150 cells cm^{-2} y^{-1}) in the core record prior to ~1960, before approximately doubling to ~200 to 300 cells cm^{-2} y^{-1} during the period ~1960 - 1980 (Figure 4). Following this increase, diatom accumulation was highly variable between 1980 and 2005, reaching a maximum of 480 cells cm^{-2} y^{-1} in 1988. Prior to ~1960, diatom assemblages were dominated by *Navicula vulpina*, *Navicula pupula* and *Stauroneis fluminopsis* (Figure 5.5), taxa that are common in water bodies with a wide range of trophic conditions (from dystrophic to eutrophic). The decades ~1960 to ~1980 were characterized by the dominance by *N. vulpina, S. fluminopsis* and *Navicula tuscula*, with a prominent rise in relative abundance of *Denticula kuetzingii.* After ~1980, the diatom assemblages become dominated by *D. kuetzingii,* coupled with increases in mesotrophic taxa (*N. vulpina, S. fluminopsis, N. pupula* and *Navicula cryptocephala;* Denys, 2011).

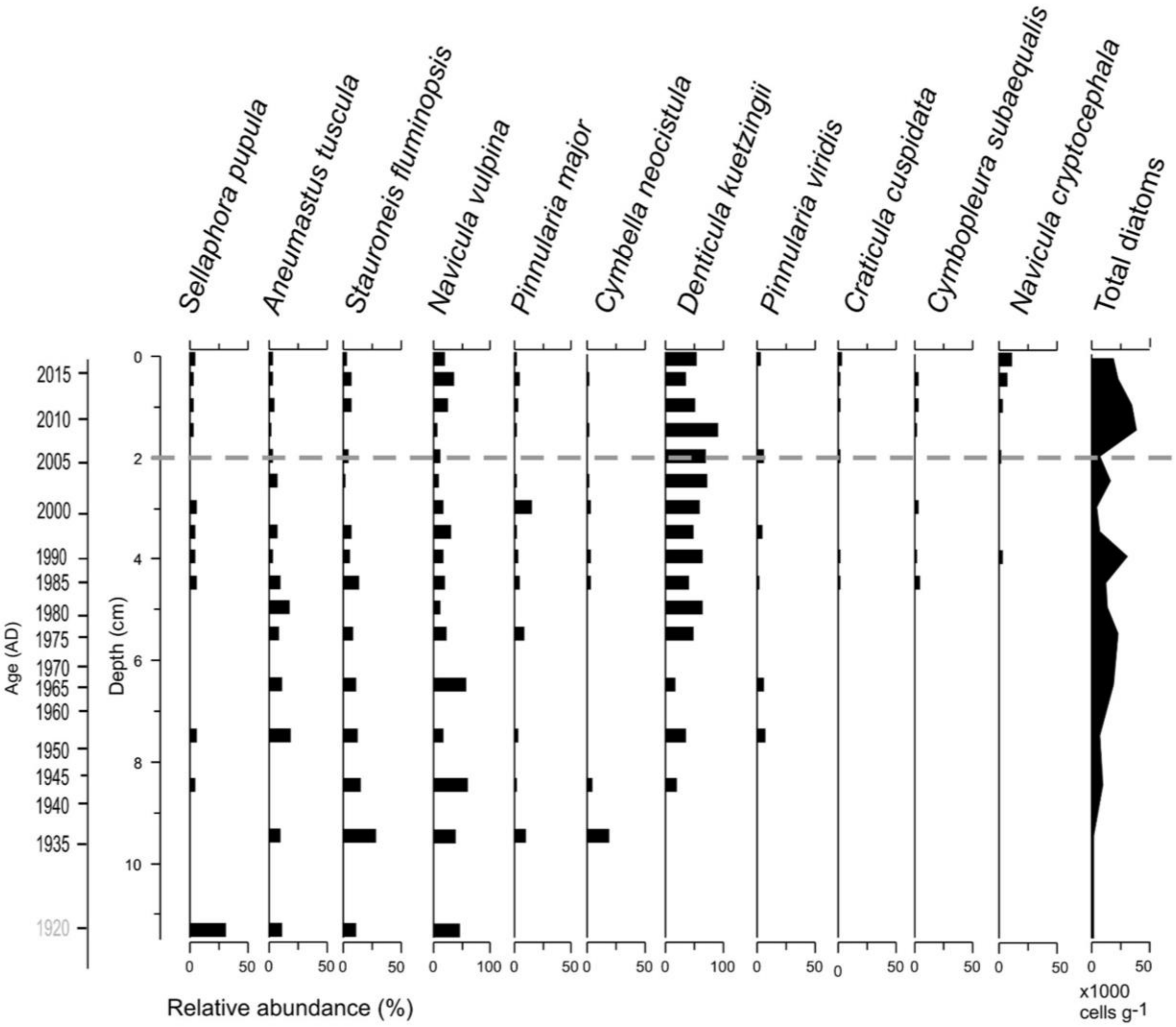

Figure 5.5 Relative diatom abundance through the sediment core, with the thermokarst event highlighted as the gray dotted line at the 2 cm depth. Only species with relative abundance of >1% are shown.

5.4 Discussion

The evidence from the core of the shallow thermokarst-impacted Frisbee pond suggests that thaw-driven shoreline slumping has the potential to increase nutrient sedimentation rate coupled with an increase in total diatom accumulation. The increased nutrient sedimentation appears to initiate prior to the slumping although is enhanced through the slumping event.

Shifts in diatom community composition began several decades prior to the thermokarst event and appear to not substantially change immediately prior to, or as a result of, the shoreline slump. Bulk sedimentation rate increased several years prior to the event (~2000 to 2004), while the proportion of mineral/organic sediment did not change in the primarily organic (mean 88% ± 0.6% from 0 cm to 10 cm depth) pond sediment. Changing isotopic signatures of carbon and nitrogen (a decrease in $\delta^{13}C$ and increase in $\delta^{15}N$) following the disturbance indicate a shift in the sources of these elements in the settling sediment towards terrestrially-derived carbon and atmospheric nitrogen inputs. The trend in increased sedimentation appears to continue increasing for up to 7 years following disturbance whereas the increase in diatom accumulation peaked shortly after disturbance and stabilized in the surface sediment.

Previous work focusing on the effects of thermokarst disturbance on lake chemistry has shown increase in sediment delivery to lake bottoms, but the composition of that sediment has been reflective of the mineral-dominated shoreline material in non-organic covered catchments. MacDonald et al. (2012) found that shoreline erosion around a thermokarst lake in the Old Crow Flats, Canada, resulted in declining organic matter, carbon, nitrogen, and depleted organic carbon isotope values, associated with an input of mineral sediment, and subsequent decline in aquatic productivity. Medeiros et al. (2014) found that thermokarst disturbance in the Southern Seward Peninsula, Alaska resulted in increasing sedimentation of inorganic carbon and nitrogen from shoreline erosional processes, associated with a decline in $\delta^{13}C$. These findings from mineral-dominated basins differ from those of our peatland study, in which total organic content did not shift following thermokarst expansion, although the isotopic signature of recent sediments indicated a change in nutrient sources as well as increased nutrient sedimentation. This contrast indicates the potential importance of the thermokarst sediment origin (mineral/organic) in determining lake hydroecological disturbance trajectory.

The reduction in $\delta^{13}C$ values following disturbance indicates a change in carbon source and a shift towards allochthonous material with proportionally reduced contributions from modern atmospheric carbon inputs. Several samples taken from the shoreline material adjacent to slumping zones show average peat (-27.9 ‰) and vegetation (-25.8 ‰) $\delta^{13}C$ values which are depleted relative to the pond sediment record, consistent with peat-vegetative $\delta^{13}C$ offsets from a peatland in Alaska (Jones et al., 2010). In a reference pond in the Hudson Bay Lowlands, (undisturbed by apparent shoreline thaw processes or avian influence), MacDonald et al. (2015) found a static δ^{13} C value of ~ -22 ‰ from 1900 to present. This differs from our results (a depletion of $\delta^{13}C$ and the prevalence of terrestrial/shoreline material in deposited sediment), whereas MacDonald et al. (2015) found a maintenance of the ratio between carbon derived from of atmospheric carbon dioxide invasion and allochthonous inputs in a pond unperturbed by shoreline inputs over the same period. While δ^{13} C becomes increasingly depleted following slumping, δ^{15} N becomes increasingly enriched, showing a marked increase from -0.5 ‰ to values near 0 ‰ by 2015, indicating a shift towards atmospherically-sourced nitrogen (Esmeijer-Liu et al., 2012), which initiates five years following disturbance. These shifts in inferred nitrogen source material to Frisbee pond following thermokarst disturbance contrast to the findings of Light (2011) who examined a core from a pristine (non-thermokarst impacted) pond in a nearby catchment (< 1 km) adjacent to Frisbee pond in the Hudson Bay Lowlands. Light (2011) reported depletion of δ^{15} N (approaching -0.8‰ in 2009) throughout the period ~1965 – 2009, and attribute this to the dominance of blue-green algae under nitrogen limiting conditions (Light, 2011; Vreca & Muri, 2010).

Following increases to nutrient sedimentation, diatom accumulation increased to the maximum values within the core record in 2009, indicating an increase in diatom production immediately following the thermokarst event. Diatom accumulation then began to decrease after four years post-disturbance until 2015, although it remained above pre-disturbance levels. During this period, increased nutrient inputs were also evident from the diatom assemblages, including increased abundance of species preferring eutrophic to mesotrophic conditions (Denys, 1991), while contemporary surface water chemistry measurements show average total dissolved nitrogen and phosphorus concentrations of 1.07 mg N L^{-1} and 44.5 µg P L^{-1}. The change in diatom assemblages in the post-thermokarst period are also indicative of slightly alkaline conditions (Denys, 2011), which are consistent with measurements of contemporary surface water chemistry in the region (Bos & Pellatt, 2012).

Our study showed shoreline disturbance resulting in increased nutrient sedimentation trend persisting for seven years following disturbance (and initiating several years prior to disturbance), but the increase in diatom accumulation stabilized relatively shortly (2-3 years) afterward. Other work that has focused on the impact of thaw disturbance has resulted in a range of outcomes of the longevity and severity of effects on nutrient export from catchments to aquatic fates. Bowden et al. (2008) compared two areas upstream and downstream of a thermokarst disturbance in the Alaskan North Slope and found that the thermokarst occurrences delivered inorganic nutrient loads orders of magnitude greater than historical pre-disturbance flows, which persisted for several years' post-disturbance. In contrast, at another

Alaskan tundra site, nutrient export was resilient to thermokarst disturbance, showing rapid ecosystem stabilization in terms of export fluxes returning to pre-disturbance levels on a subannual time scale (Larouche et al., 2015). Other, more catastrophic modes of permafrost degradation may also control the relative longevity and severity of altered nutrient fluxes. In a high Arctic catchment, Lafrenière & Lamoureux (2013) observed an initial abrupt, short lived sediment flux, followed by a gradual change to discharge and turbidity as a result of massive active layer detachment disturbance. In the same catchment, Lamhonwah et al. (2016) found the impacts of increased sediment flux from active layer detachment to persist over a 7-year study post-disturbance, whereas gentler modes of permafrost degradation (thermal perturbation) resulted in changes to sediment flux which persisted over shorter timescales (only up to two years following disturbance).

I hypothesized that nutrient supply, sedimentation rate, and diatom community composition would all change dramatically to thermokarst erosion of the shoreline of Frisbee pond. However, the results from our suggest that instead, trends towards increased C, N and P flux began about 5 years before the slump, and continued during and after the event. Further, although increases to diatom accumulation coincide with the timing of the slump event, the most substantial changes to diatom community composition occur several decades prior. Thus, the role of general climatic forcing in the decades prior may be the larger driver of pond hydroecoloigcal response. In this study, the thermokarst event was preceded by a decade of warming temperatures in addition to sustained increased precipitation, a trend in the regional climate previously documented by Macrae et al. (2014). The combined signals from both of these disturbances may be present in the sediment record, however, the effects of each may be distinct given the relatively gradual nature of climate change relative to the rapid impacts of shoreline disturbance. Permafrost thaw and thermokarst processes have been attributed to similar hydroclimatic conditions in several other northern catchments, commonly interpreted as the capacity to thermally disturb permafrost and hydrologically connect near-shore material to the pond, respectively. Thus, the extent of thermal permafrost disturbance on nutrient dynamics could be limited by the hydrologic connection of the disturbed area to larger hydrologic transport networks, as supported by evidence from other thermally-perturbed landscapes. Lamhonwah et al. (2016) found that warming increased total solute availability in a high Arctic catchment, while rainfall controlled the timing and longevity of the export from the catchment as ions released from ground thaw were available for export through a flushing. In addition to thawing resulting in changing hydrologic pathways, warming may also result in increased mineralisation of exposed and thawed recalcitrant material (Stark, 2007), further contributing to nutrient fluxes to the pond prior to shoreline collapse.

As the diatom community composition shifted several decades prior to the thermokarst event in Frisbee Pond, results from other studies may assist in determining the extent of which is driven by general climatic forcing. In the Hudson Bay Lowlands, MacDonald et al. (2014) suggest recent climate warming is responsible for both changes in dominance from episammic to benthic mat-dwelling taxa (specifically *Fragilaria pinnata* to *Denticula kuetzingii*) with a new habitat regime as well as increasing organic content with increased productivity, synchronous with our findings, beginning around 1975. Bouchard et al. (2016) summarize both the effects of general (relatively long-term) climate forcing as well as the effects of more catastrophic (relatively short-term) shoreline thermokarst thaw slumping on ponds and lakes.

This summary of hydroecological changes due to thaw slumping are in close agreement with our results, such as an increase in sedimentation, increase in diatom accumulation, the prevalence of *Denticula kuetzingii*, and an increase in allochthonous-derived carbon sources.

5.5 Conclusions

This study has examined the potential for thermokarst processes to modify nutrient dynamics and the aquatic ecology of subarctic ponds. The increase in nutrient sedimentation from the slumping of terrestrial material into the pond appears to have led to an increase in total diatom accumulation, although the rise in sedimentation imitated some years prior to the shoreline slump. Shifts in diatom assemblages prior to and during the disturbance is similar to changes reported in other northern environments due to general climatic forcing, which may mask the signal of thermokarst activity on diatom ecology. The source of organic carbon shifted strongly towards allochthonous origin following the thermokarst event which persisted throughout the seven-year period and did not return to pre-disturbance composition. The hydroclimatic conditions preceding the thermokarst expansion are consistent with those conditions that resulted in catastrophic thaw in other permafrost catchments of sustained higher than average precipitation coupled with warming temperatures. Further research should include investigations into the relationship between the spatial extent and the longevity of that disturbance, as this work presents the response of only one small catchment to thermokarst disturbance, which is projected to occur and continue across many spatial scales within the next century.

5.6 Acknowledgments

The funding for this research came from Natural Sciences and Engineering Research Council Discovery Grants (Macrae, Petrone), Natural Sciences and Engineering Research Council Northern Supplement (Petrone) and the Northern Scientific Training Program. I thank H. White and D. Gibson for field assistance and J. Telford and J. Cober for lab assistance.

Chapter 6: Conclusions

This thesis presents a broad assessment of the hydrology and nutrient biogeochemistry of pond-peatland complexes of the Hudson Bay Lowlands. It both (a) represents a benchmark of the state of the landscape's hydrochemical status and function in a region experiencing rapid geomorphic and climatic change, as well as (b) provides insight into the potential trajectories permafrost organic-covered landscapes and small aquatic bodies may follow under a thawing and warming climate. This thesis demonstrates the sensitivity of this landscape to climatic change through both observational and experimental studies. This encompassed hydrological and biogeochemical processes occurring both within the catchments (further subdividing the catchment into discrete landscape units), within the ponds, and the hydrologic dynamics between the two through runoff pathways.

Under a changing climate, modified nutrient cycling processes may result in altered nutrient availability, both in terms of magnitude and timing. The impacts of changing nutrient dynamics within the catchment will be directly realized by an associated change in productivity, given that the vegetation is nutrient limited, particularly given the substantial observed increase in nitrification observed in thermokarst material under oxic and warming conditions. In addition to direct effects on the catchment, this also represents a change in bioavailable nutrients that may be transported to ponds (also nutrient-limited) via runoff pathways. However, the timing of the activation of these runoff pathways is closely tied to the evolution of the frost table, which will likely migrate downward more rapidly, earlier in the season, reducing the optimal window for runoff generation. In addition to changing runoff hydrochemical contributions to ponds, changing hydrometerological regimes will further influence pond chemistry trajectories, as evapoconcentration and dilution processes are key drivers of several chemical concentrations. These controls result in synchronous behavior in adjacent ponds, which are subject to similar climatological forcing. Across all of these hydrologic and biogeochemical processes which are subject to alteration due to climate change, the inclusion of thermokarst dynamics may further and more rapidly disturb the natural functioning of these systems both within and between catchments and ponds. However, I show examples of distinct impacts of (1) general climatic change on ponds (such as changes to relative abundance diatom communities coincident with warming temperatures) and (2) catastrophic thermokarst shoreline impacts (such as rapid increases in nutrient sedimentation) which will likely both continue to occur and increase in intensity.

In addition to the scientific findings of this thesis, several novel approaches in methodology offer opportunities for further study and potential application to wider environments. An approach to quantify measures of synchronous hydrochemical behavior beyond linear regression through single-factor (temporal, spatial) normalization was developed. As well, this study highlighted the importance of either high-temporal frequency sampling or at least the importance of determining the hydrologic context in which a sample was collected when reviewing chemical concentration data, as these values are highly sensitive in these chemodynamic systems.

Implicit in all of this work is a degree of regional specificity of this work which must be considered with regards to the transferability the findings of this thesis. The peatland permafrost landscape varies not only from mineral soils comprising much of the arctic and subarctic but also from other peatland ecosystems across temperate and permafrost landscapes.

It is essential to recall the definition of permafrost as the state of a soil remaining at subzero temperatures of a minimum period of two years, a definition which makes no reference to the chemical and hydrophysical properties of the soil. However, it is exactly these properties that will determine the hydroecological impacts of permafrost thaw. This work provides an overview of these changes in the western Hudson Bay Lowlands and the context of these changes while simultaneously yet cautiously providing potential transferability to other regions. More concretely, this thesis has identified major comparative and contrasting results from other regions and extensively hypothesized to determine the key regional differences which may result in future divergence in responses to climatic change and permafrost loss across the global landscape. Generalizations are often made of the effects of permafrost thaw across region and landform; however it is the chemical and hydrophysical quality of material that will determine the regionally-specific impacts of such thaw. Future worldwide permafrost research may benefit from careful concern with regional relevance and transferability, given the diverse range of environments and conditions in which permafrost peatlands are situated.

Bibliography

Abbott, B. W., Jones, J. B., Godsey, S. E., Larouche, J. R., & Bowden, W. B. (2015). Patterns and persistence of hydrologic carbon and nutrient export from collapsing upland permafrost. *Biogeosciences*, *12*(12), 3725-3740.

Abnizova, A. (2013). Hydrology, carbon dynamics and hydrochemical properties of ponds in an extensive low gradient High Arctic wetland, Polar Bear Pass, Bathurst Island, Nunavut, Canada. Ph.D. thesis, York University, Canada.

Abnizova, A., Siemens, J., Langer, M., & Boike, J. (2012). Small ponds with major impact: The relevance of ponds and lakes in permafrost landscapes to carbon dioxide emissions. *Global Biogeochemical Cycles*, *26*(2).

Aerts, R., & Ludwig, F. (1997). Water-table changes and nutritional status affect trace gas emissions from laboratory columns of peatland soils. *Soil Biology and Biochemistry*, *29*(11-12), 1691-1698.

Ali, G., Tetzlaff, D., McDonnell, J. J., Soulsby, C., Carey, S., Laudon, H., ... & Shanley, J. (2015). Comparison of threshold hydrologic response across northern catchments. *Hydrological Processes*, *29*(16), 3575-3591.

Allan, C. J., Roulet, N. T., & Hill, A. R. (1993). The biogeochemistry of pristine, headwater Precambrian shield watersheds: an analysis of material transport within a heterogeneous landscape. *Biogeochemistry*, *22*(1), 37-79.

Andersen, R., Wells, C., Macrae, M., & Price, J. (2013). Nutrient mineralization and microbial functional diversity in a restored bog approach natural conditions 10 years post restoration. *Soil biology and Biochemistry*, *64*, 37-47.

Andresen, L. C., Jonasson, S., Ström, L., & Michelsen, A. (2008). Uptake of pulse injected nitrogen by soil microbes and mycorrhizal and non-mycorrhizal plants in a species-diverse subarctic heath ecosystem. *Plant and Soil*, *313*(1-2), 283-295.

Appleby, P. G., & Oldfield, F. (1978). The calculation of lead-210 dates assuming a constant rate of supply of unsupported ^{210}Pb to the sediment. *Catena*, *5*(1), 1-8.

Appleby, P.G. (2001). Chronostratigraphic techniques in recent sediments. In: Last, W.M., Smol, J.P., (Eds.). *Tracking Environmental Change Using Lake Sediments: Vol. 1: Basin Analysis, Coring, and Chronological Techniques*. Kluwer Academic Publishers, Dordrecht.

Archer, S. D., McDonald, I. R., Herbold, C. W., Lee, C. K., Niederberger, T. S., & Cary, C. (2016). Temporal, regional and geochemical drivers of microbial community variation in the melt ponds of the Ross Sea region, Antarctica. *Polar Biology*, *39*(2), 267-282.

Aronow, S. (1982). Beaches and Coastal Geology. Springer, United States.

Arunachalam, A., Pandey, H. N., Tripathi, R. S., & Maithani, K. (1996). Fine root decomposition and nutrient mineralization patterns in a subtropical humid forest following tree cutting. *Forest Ecology and Management*, *86*(1-3), 141-150.

Ask, J., Karlsson, J., Persson, L., Ask, P., Byström, P., & Jansson, M. (2009). Terrestrial organic matter and light penetration: Effects on bacterial and primary production in lakes. *Limnology and Oceanography*, *54*(6), 2034-2040.

Austin, A. T., & Vitousek, P. M. (1998). Nutrient dynamics on a precipitation gradient in Hawai'i. *Oecologia*, *113*(4), 519-529.

Baddeley, J. A., Woodin, S. J., & Alexander, I. J. (1994). Effects of increased nitrogen and phosphorus availability on the photosynthesis and nutrient relations of three arctic dwarf shrubs from Svalbard. *Functional Ecology*, 676-685.

Baines, S. B., Webster, K. E., Kratz, T. K., Carpenter, S. R., & Magnuson, J. J. (2000). Synchronous behavior of temperature, calcium, and chlorophyll in lakes of northern Wisconsin. *Ecology, 81*(3), 815-825.

Balasubramaniam, A. M., Hall, R. I., Wolfe, B. B., Sweetman, J. N., & Wang, X. (2015). Source water inputs and catchment characteristics regulate limnological conditions of shallow subarctic lakes (Old Crow Flats, Yukon, Canada). *Canadian Journal of Fisheries and Aquatic Sciences*, *72*(7), 1058-1072.

Battarbee, R. W., Jones, V. J., Flower, R. J., Cameron, N. G., Bennion, H., Carvalho, L.,& Juggins, S. (2001). Diatoms. In: Smol, J. P., Birks, H. J., & Last, W. M. (Eds.). *Tracking environmental change using lake sediments: Volume 3: Terrestrial, algal, and siliceous indicators* (Vol. 3). Springer Science & Business Media, United States.

Baumann, F., HE, J. S., Schmidt, K., Kuehn, P., & Scholten, T. (2009). Pedogenesis, permafrost, and soil moisture as controlling factors for soil nitrogen and carbon contents across the Tibetan Plateau. *Global Change Biology*, *15*(12), 3001-3017.

Bayley, S. E., Thormann, M. N., & Szumigalski, A. R. (2005). Nitrogen mineralization and decomposition in western boreal bog and fen peat. *Ecoscience*, *12*(4), 455-465.

Bello, R., & Smith, J. D. (1990). The effect of weather variability on the energy balance of a lake in the Hudson Bay Lowlands, Canada. *Arctic and Alpine Research*, 98-107.

Belyea, L. R., & Baird, A. J. (2006). Beyond “the limits to peat bog growth”: Cross-scale feedback in peatland development. *Ecological Monographs*, *76*(3), 299-322.

Bergström, A. K. (2010). The use of TN: TP and DIN: TP ratios as indicators for phytoplankton nutrient limitation in oligotrophic lakes affected by N deposition. *Aquatic Sciences*, *72*(3), 277-281.

Bergström, A. K., Blomqvist, P., & Jansson, M. (2005). Effects of atmospheric nitrogen deposition on nutrient limitation and phytoplankton biomass in unproductive Swedish lakes. *Limnology and Oceanography*, *50*(3), 987-994.

Binford, M. W. (1990). Calculation and uncertainty analysis of 210 Pb dates for PIRLA project lake sediment cores. *Journal of Paleolimnology*, *3*(3), 253-267.

Bintanja, R., & Andry, O. (2017). Towards a rain-dominated Arctic. *Nature Climate Change*, *7*(4), 263.

Biskaborn, B. K., Herzschuh, U., Bolshiyanov, D., Savelieva, L., Zibulski, R., & Diekmann, B. (2013). Late Holocene thermokarst variability inferred from diatoms in a lake sediment record from the Lena Delta, Siberian Arctic. *Journal of Paleolimnology*, *49*(2), 155-170.

Bonilla, S., Villeneuve, V., & Vincent, W. F. (2005). Benthic and planktonic algal communities in a high arctic lake: pigment structure and contrasting responses to nutrient enrichment. *Journal of Phycology*, *41*(6), 1120-1130.

Boone, R. D., Grigal, D. F., Sollins, P., Ahrens, R. J., & Armstrong, D. E. (1999). Soil sampling, preparation, archiving, and quality control. In: *Standard Soil Methods for Long-term Ecological Research.* Oxford University Press, New York, 3-28.

Borghini, F., Colacevich, A., Loiselle, S. A., & Bargagli, R. (2013). Short-term dynamics of physico-chemical and biological features in a shallow, evaporative antarctic lake. *Polar Biology*, *36*(8), 1147-1160.

Borner, A. P., Kielland, K., & Walker, M. D. (2008). Effects of simulated climate change on plant phenology and nitrogen mineralization in Alaskan Arctic tundra. *Arctic, Antarctic, and Alpine Research*, *40*(1), 27-38.

Bos, D. G., & Pellatt, M. G. (2012). The water chemistry of shallow ponds around Wapusk national park of Canada, Hudson Bay Lowlands. *Canadian Water Resources Journal*, *37*(3), 163-175.

Bouchard, F., MacDonald, L. A., Turner, K. W., Thienpont, J. R., Medeiros, A. S., Biskaborn, B. K., ... & Wolfe, B. B. (2016). Paleolimnology of thermokarst lakes: a window into permafrost landscape evolution. *Arctic Science*, *3*(2), 91-117.

Bouchard, F., Pienitz, R., Ortiz, J. D., Francus, P., & Laurion, I. (2013). Palaeolimnological conditions inferred from fossil diatom assemblages and derivative spectral properties of sediments in thermokarst ponds of subarctic Quebec, Canada. *Boreas*, *42*(3), 575-595.

Bouchard, F., Turner, K. W., MacDonald, L. A., Deakin, C., White, H., Farquharson, N., ... & Edwards, T. W. D. (2013). Vulnerability of shallow subarctic lakes to evaporate and desiccate when snowmelt runoff is low. *Geophysical Research Letters*, *40*(23), 6112-6117.

Boudreau, L. D., & Rouse, W. R. (1995). The role of individual terrain units in the water balance of wetland tundra. *Climate Research*, 31-47.

Bouwman, A. F., Lee, D. S., Asman, W. A. H., Dentener, F. J., Van Der Hoek, K. W., & Olivier, J. G. J. (1997). A global high-resolution emission inventory for ammonia. *Global Biogeochemical Cycles*, *11*(4), 561-587.

Bowden, W. B., Gooseff, M. N., Balser, A., Green, A., Peterson, B. J., & Bradford, J. (2008). Sediment and nutrient delivery from thermokarst features in the foothills of the North Slope, Alaska: Potential impacts on headwater stream ecosystems. *Journal of Geophysical Research: Biogeosciences*, *113*(G2).

Breton, J., Vallieres, C., & Laurion, I. (2009). Limnological properties of permafrost thaw ponds in northeastern Canada. *Canadian Journal of Fisheries and Aquatic Sciences*, *66*(10), 1635-1648.

Bridgham, S. D., Updegraff, K., & Pastor, J. (1998). Carbon, nitrogen, and phosphorus mineralization in northern wetlands. *Ecology*, *79*(5), 1545-1561.

Brown, R. D., & Braaten, R. O. (1998). Spatial and temporal variability of Canadian monthly snow depths, 1946–1995. *Atmosphere-Ocean*, *36*(1), 37-54.

Burke, S. M., Zimmerman, C. E., Branfireun, B. A., Koch, J. C., & Swanson, H. K. (2018). Patterns and controls of mercury accumulation in sediments from three thermokarst lakes on the Arctic Coastal Plain of Alaska. *Aquatic Sciences,* 80(1), 1.

Burpee, B., Saros, J. E., Northington, R. M., & Simon, K. S. (2016). Microbial nutrient limitation in Arctic lakes in a permafrost landscape of southwest Greenland. *Biogeosciences*, *13*(2), 365.

Callaghan, T. V., Bergholm, F., Christensen, T. R., Jonasson, C., Kokfelt, U., & Johansson, M. (2010). A new climate era in the sub-Arctic: Accelerating climate changes and multiple impacts. *Geophysical Research Letters*, *37*(14).

Canadian Cryopsheric Information Network. (2017). Permafrost. <https://www.ccin.ca/home/ccw/permafrost/current>, Accessed 07/11/2017.

Carey, S. K., & Quinton, W. L. (2005). Evaluating runoff generation during summer using hydrometric, stable isotope and hydrochemical methods in a discontinuous permafrost alpine catchment. *Hydrological Processes*, *19*(1), 95-114.

Cargill, S. M., & Jefferies, R. L. (1984). Nutrient limitation of primary production in a sub-arctic salt marsh. *Journal of Applied Ecology*, 657-668.

Chambers, C., Marshall, J. D., & Danehy, R. J. (2004). Nitrogen uptake and turnover in riparian woody vegetation. *Oecologia*, *140*(1), 125-134.

Chapin, F. S., McGuire, A. D., Randerson, J., Pielke, R., Baldocchi, D., Hobbie, S. E., ... & Zimov, S. A. (2000). Arctic and boreal ecosystems of western North America as components of the climate system. *Global Change Biology, 6*(S1), 211-223.

Chasmer, L., Kenward, A., Quinton, W., & Petrone, R. (2012). CO2 exchanges within zones of rapid conversion from permafrost plateau to bog and fen land cover types. *Arctic, Antarctic, and Alpine Research*, *44*(4), 399-411.

Cohen, J., Screen, J. A., Furtado, J. C., Barlow, M., Whittleston, D., Coumou, D., ... & Jones, J. (2014). Recent Arctic amplification and extreme mid-latitude weather. *Nature Geoscience*, *7*(9), 627.

Connon, R. F., Quinton, W. L., Craig, J. R., & Hayashi, M. (2014). Changing hydrologic connectivity due to permafrost thaw in the lower Liard River valley, NWT, Canada. *Hydrological Processes*, *28*(14), 4163-4178.

Davies, G. M., & Gray, A. (2015). Don't let spurious accusations of pseudoreplication limit our ability to learn from natural experiments (and other messy kinds of ecological monitoring). *Ecology and Evolution*, *5*(22), 5295-5304

DeBusk, W. F., & Reddy, K. R. (1998). Turnover of detrital organic carbon in a nutrient-impacted Everglades marsh. *Soil Science Society of America Journal*, *62*(5), 1460-1468.

Denys, L. (1991). A check-list of the diatoms in the holocene deposits of the Western Belgian coastal plain with a survey of their apparent ecological requirements. I. Introduction, ecological code and complete list. *Ministère des Affaires Economiques – Service Geologique de Belgique*. Brussels, Belgium.

Deshpande, B. N., MacIntyre, S., Matveev, A., & Vincent, W. F. (2015). Oxygen dynamics in permafrost thaw lakes: Anaerobic bioreactors in the Canadian subarctic. *Limnology and Oceanography*, *60*(5), 1656-1670.

Dittmar, T., & Kattner, G. (2003). The biogeochemistry of the river and shelf ecosystem of the Arctic Ocean: a review. *Marine Chemistry*, *83*(3-4), 103-120.

Dore, J. E., & Priscu, J. C. (2001). Phytoplankton phosphorus deficiency and alkaline phosphatase activity in the McMurdo Dry Valley lakes, Antarctica. *Limnology and Oceanography*, 46(6), 1331-1346.

Dornblaser, M. M., & Striegl, R. G. (2007). Nutrient (N, P) loads and yields at multiple scales and subbasin types in the Yukon River basin, Alaska. *Journal of Geophysical Research: Biogeosciences*, *112*(G4).

Dredge, L.A. (1979). Thaw Depths and Permafrost in Polygonal Peat Terrain, Hudson Bay Lowland, Manitoba. *Current Research*, *Part C, Geological Survey of Canada*, *79-1C*, 27-30.

Dunteman, G. H. (1989). *Principal components analysis*. Sage, California, United States.

Dyke, L. D., & Sladen, W. E. (2010). Permafrost and peatland evolution in the northern Hudson Bay Lowland, Manitoba. *Arctic*, 429-441.

Eaton, A. K., Rouse, W. R., Lafleur, P. M., Marsh, P., & Blanken, P. D. (2001). Surface energy balance of the western and central Canadian subarctic: Variations in the energy balance among five major terrain types. *Journal of Climate*, 14(17), 3692-3703.

Eichel, K. A., Macrae, M. L., Hall, R. I., Fishback, L., & Wolfe, B. B. (2014). Nutrient uptake and short-term responses of phytoplankton and benthic algal communities from a subarctic pond to experimental nutrient enrichment in microcosms. *Arctic, Antarctic, and Alpine Research*, *46*(1), 191-205.Elberling, B., Christiansen, H. H., & Hansen, B. U. (2010). High nitrous oxide production from thawing permafrost. *Nature Geoscience*, *3*(5), 332.

Elbert, W., Weber, B., Burrows, S., Steinkamp, J., Büdel, B., Andreae, M. O., & Pöschl, U. (2012). Contribution of cryptogamic covers to the global cycles of carbon and nitrogen. *Nature Geoscience*, *5*(7), 459.

Environment and Climate Change Canada. (2017). Daily Data Report for “Churchill A” and “Churchill Climate” stations. Meteorological Service of Canada. <http://climate.weather.gc.ca/climate_data>, Accessed online: 08/25/2017.

Eppinga, M. B., Rietkerk, M., Belyea, L. R., Nilsson, M. B., Ruiter, P. C. D., & Wassen, M. J. (2010). Resource contrast in patterned peatlands increases along a climatic gradient. *Ecology*, *91*(8), 2344-2355.

Esmeijer-Liu, A. J., Kürschner, W. M., Lotter, A. F., Verhoeven, J. T., & Goslar, T. (2012). Stable carbon and nitrogen isotopes in a peat profile are influenced by early stage diagenesis and changes in atmospheric CO 2 and N deposition. *Water, Air, & Soil Pollution*, *223*(5), 2007-2022.

Fellman, J. B., & D'Amore, D. V. (2007). Nitrogen and phosphorus mineralization in three wetland types in southeast Alaska, USA. *Wetlands*, *27*(1), 44-53.

Fisher, J., & Acreman, M. C. (2004). Wetland nutrient removal: a review of the evidence. *Hydrology and Earth System Sciences Discussions*, *8*(4), 673-685.

Frey, K. E., & McClelland, J. W. (2009). Impacts of permafrost degradation on arctic river biogeochemistry. *Hydrological Processes*, *23*(1), 169-182.

Golovchenko, A. V., Tikhonova, E. Y., & Zvyagintsev, D. G. (2007). Abundance, biomass, structure, and activity of the microbial complexes of minerotrophic and ombrotrophic peatlands. *Microbiology*, *76*(5), 630-637.

Gooseff, M. N., Balser, A., Bowden, W. B., & Jones, J. B. (2009). Effects of hillslope thermokarst in northern Alaska. *Eos, Transactions American Geophysical Union*, *90*(4), 29-30.

Gorham, E. (1991). Northern peatlands: role in the carbon cycle and probable responses to climatic warming. *Ecological Applications*, *1*(2), 182-195.

Gray, I. M. (1987). Factors regulating phytoplankton populations at Churchill, Manitoba. M.Sc. thesis, University of Windsor, Canada.

Haag, R. W. (1974). Nutrient limitations to plant production in two tundra communities. *Canadian Journal of Botany*, *52*(1), 103-116.

Harms, T. K., & Jones, J. B. (2012). Thaw depth determines reaction and transport of inorganic nitrogen in valley bottom permafrost soils. *Global Change Biology*, *18*(9), 2958-2968.

Heiri, O., Lotter, A. F., & Lemcke, G. (2001). Loss on ignition as a method for estimating organic and carbonate content in sediments: reproducibility and comparability of results. *Journal of paleolimnology*, *25*(1), 101-110.

Hinkel, K. M., Arp, C. D., Townsend-Small, A., & Frey, K. E. (2017). Can Deep Groundwater Influx be Detected from the Geochemistry of Thermokarst Lakes in Arctic Alaska?. *Permafrost and Periglacial Processes*, *28*(3), 552-557.

Hinzman, L. D., Bettez, N. D., Bolton, W. R., Chapin, F. S., Dyurgerov, M. B., Fastie, C. L., ... & Jensen, A. M. (2005). Evidence and implications of recent climate change in northern Alaska and other arctic regions. *Climatic Change*, *72*(3), 251-298.

Hogan, E. J., McGowan, S., & Anderson, N. J. (2014). Nutrient limitation of periphyton growth in arctic lakes in south-west Greenland. *Polar Biology*, *37*(9), 1331-1342.

Houben, A. J., French, T. D., Kokelj, S. V., Wang, X., Smol, J. P., & Blais, J. M. (2016). The impacts of permafrost thaw slump events on limnological variables in upland tundra lakes, Mackenzie Delta region. *Fundamental and Applied Limnology/Archiv für Hydrobiologie*, *189*(1), 11-35.

Jacques, O., Bouchard, F., MacDonald, L. A., Hall, R. I., Wolfe, B. B., & Pienitz, R. (2016). Distribution and diversity of diatom assemblages in surficial sediments of shallow lakes in Wapusk National Park (Manitoba, Canada) region of the Hudson Bay Lowlands. *Ecology and Evolution*, *6*(13), 4526-4540.

Jones, D. L., Kielland, K., Sinclair, F. L., Dahlgren, R. A., Newsham, K. K., Farrar, J. F., & Murphy, D. V. (2009). Soil organic nitrogen mineralization across a global latitudinal gradient. *Global Biogeochemical Cycles*, *23*(1).

Jones, M. C., Peteet, D. M., & Sambrotto, R. (2010). Late-glacial and Holocene $\delta^{15}N$ and $\delta^{13}C$ variation from a Kenai Peninsula, Alaska peatland. *Palaeogeography, Palaeoclimatology, Palaeoecology*, *293*(1-2), 132-143.

Jorgenson, M. T., & Osterkamp, T. E. (2005). Response of boreal ecosystems to varying modes of permafrost degradation. *Canadian Journal of Forest Research*, *35*(9), 2100-2111.

Jorgenson, M. T., Shur, Y. L., & Pullman, E. R. (2006). Abrupt increase in permafrost degradation in Arctic Alaska. *Geophysical Research Letters*, *33*(2).

Kaufman, D. S., Schneider, D. P., McKay, N. P., Ammann, C. M., Bradley, R. S., Briffa, K. R., ... & Lakes, A. (2009). Recent warming reverses long-term Arctic cooling. *Science*, *325*(5945), 1236-1239.

Keller, W., Paterson, A. M., Rühland, K. M., & Blais, J. M. (2014). Introduction—environmental change in the Hudson and James Bay Region. *Arctic, Antarctic, and Alpine Research*, *46*(1), 2-5.

Kelley, A. M., Epstein, H. E., Ping, C. L., & Walker, D. A. (2012). Soil Nitrogen Transformations Associated with Small Patterned-Ground Features along a North American Arctic Transect. *Permafrost and Periglacial Processes*, *23*(3), 196-206.

Keuper, F., Bodegom, P. M., Dorrepaal, E., Weedon, J. T., Hal, J., Logtestijn, R. S., & Aerts, R. (2012). A frozen feast: Thawing permafrost increases plant-available nitrogen in subarctic peatlands. *Global Change Biology*, *18*(6), 1998-2007.

Kielland, K. (1997). Role of free amino acids in the nitrogen economy of arctic cryptogams. *Ecoscience*, *4*(1), 75-79.

Kling, G. W., Kipphut, G. W., Miller, M. M., & O'Brien, W. J. (2000). Integration of lakes and streams in a landscape perspective: the importance of material processing on spatial patterns and temporal coherence. *Freshwater Biology*, *43*(3), 477-497.

Koch, J. C., Fondell, T. F., Laske, S., & Schmutz, J. A. (2018). Nutrient dynamics in partially drained arctic thaw lakes. *Journal of Geophysical Research: Biogeosciences*, *123*(2), 440-452.

Koch, J. C., Gurney, K., & Wipfli, M. S. (2014). Morphology-Dependent Water Budgets and Nutrient Fluxes in Arctic Thaw Ponds. *Permafrost and Periglacial Processes*, *25*(2), 79-93.

Kokelj, S. V., & Burn, C. R. (2005). Geochemistry of the active layer and near-surface permafrost, Mackenzie delta region, Northwest Territories, Canada. *Canadian Journal of Earth Sciences*, *42*(1), 37-48.

Kokelj, S. V., Jenkins, R. E., Milburn, D., Burn, C. R., & Snow, N. (2005). The influence of thermokarst disturbance on the water quality of small upland lakes, Mackenzie Delta region, Northwest Territories, Canada. *Permafrost and Periglacial Processes*, *16*(4), 343-353.

Kokelj, S. V., Zajdlik, B., & Thompson, M. S. (2009). The impacts of thawing permafrost on the chemistry of lakes across the subarctic boreal-tundra transition, Mackenzie Delta region, Canada. *Permafrost and Periglacial Processes*, *20*(2), 185-199.

Kuhry, P., & Turunen, J. (2006). The postglacial development of boreal and subarctic peatlands. *In* Wieder, R.K., and Vitt, D.H. (eds.), *Boreal Peatland Ecosystems.* Berlin Heidelberg: Springer, 25-46.

Lafrenière, M. J., & Lamoureux, S. F. (2013). Thermal perturbation and rainfall runoff have greater impact on seasonal solute loads than physical disturbance of the active layer. *Permafrost and Periglacial Processes*, *24*(3), 241-251.

Lamhonwah, D., Lafrenière, M. J., Lamoureux, S. F., & Wolfe, B. B. (2016). Multi-year impacts of permafrost disturbance and thermal perturbation on High Arctic stream chemistry. *Arctic Science*, *3*(2), 254-276.

Lamhonwah, D., Lafrenière, M. J., Lamoureux, S. F., & Wolfe, B. B. (2017). Evaluating the hydrological and hydrochemical responses of a High Arctic catchment during an exceptionally warm summer. *Hydrological Processes*, *31*(12), 2296-2313.

Lamoureux, S. F., & Lafrenière, M. J. (2014). Seasonal fluxes and age of particulate organic carbon exported from Arctic catchments impacted by localized permafrost slope disturbances. *Environmental Research Letters*, *9*(4), 045002.

Larouche, J. R., Abbott, B. W., Bowden, W. B., & Jones, J. B. (2015). The role of watershed characteristics, permafrost thaw, and wildfire on dissolved organic carbon biodegradability and water chemistry in Arctic headwater streams. *Biogeosciences*, *12*(14), 4221-4233.

Larsen, A. S., O'Donnell, J. A., Schmidt, J. H., Kristenson, H. J., & Swanson, D. K. (2017). Physical and chemical characteristics of lakes across heterogeneous landscapes in arctic and subarctic Alaska. *Journal of Geophysical Research: Biogeosciences*, *122*(4), 989-1008.

Lawrence, D. M., Slater, A. G., & Swenson, S. C. (2012). Simulation of present-day and future permafrost and seasonally frozen ground conditions in CCSM4. *Journal of Climate*, *25*(7), 2207-2225.

Levine, M. A., & Whalen, S. C. (2001). Nutrient limitation of phytoplankton production in Alaskan Arctic foothill lakes. *Hydrobiologia*, *455*(1-3), 189-201.

Lewis, T. L., Lindberg, M. S., Schmutz, J. A., Heglund, P. J., Rover, J., Koch, J. C., & Bertram, M. R. (2015). Pronounced chemical response of Subarctic lakes to climate-driven losses in surface area. *Global Change Biology*, *21*(3), 1140-1152.

Lewis, T., Lafrenière, M. J., & Lamoureux, S. F. (2012). Hydrochemical and sedimentary responses of paired High Arctic watersheds to unusual climate and permafrost disturbance, Cape Bounty, Melville Island, Canada. *Hydrological Processes*, *26*(13), 2003-2018.

Lewkowicz, A. G., & Kokelj, S. V. (2002). Slope sediment yield in arid lowland continuous permafrost environments, Canadian Arctic Archipelago. *Catena*, *46*(4), 261-283.

Light, E. L. D. (2011). Characterizing the present and past hydrology of shallow ponds in the Churchill area using isotopic methods. M.Sc. thesis, Wilfrid Laurier University, Canada.

Liljedahl, A. K., Boike, J., Daanen, R. P., Fedorov, A. N., Frost, G. V., Grosse, G., ... & Necsoiu, M. (2016). Pan-Arctic ice-wedge degradation in warming permafrost and its influence on tundra hydrology. *Nature Geoscience*, *9*(4), 312.

Lim, D. S., Douglas, M. S., Smol, J. P., & Lean, D. R. (2001). Physical and chemical limnological characteristics of 38 lakes and ponds on Bathurst Island, Nunavut, Canadian High Arctic. *International Review of Hydrobiology*, *86*(1), 1-22.

Lin, X., Tfaily, M. M., Steinweg, J. M., Chanton, P., Esson, K., Yang, Z. K., ... & Kostka, J. E. (2014). Microbial community stratification linked to utilization of carbohydrates and phosphorus limitation in a boreal peatland at Marcell Experimental Forest, Minnesota, USA. *Applied and Environmental Microbiology*, *80*(11), 3518-3530.

Lipson, D. A., Zona, D., Raab, T. K., Bozzolo, F., Mauritz, M., & Oechel, W. C. (2012). Water-table height and microtopography control biogeochemical cycling in an Arctic coastal tundra ecosystem. *Biogeosciences*, *9*(1), 577.

Lobbes, J. M., Fitznar, H. P., & Kattner, G. (2000). Biogeochemical characteristics of dissolved and particulate organic matter in Russian rivers entering the Arctic Ocean. *Geochimica et Cosmochimica Acta*, *64*(17), 2973-2983.

Long, M. S., Litton, C. M., Giardina, C. P., Deenik, J., Cole, R. J., & Sparks, J. P. (2017). Impact of nonnative feral pig removal on soil structure and nutrient availability in Hawaiian tropical montane wet forests. *Biological Invasions*, *19*(3), 749-763.

Lougheed, V. L., Butler, M. G., McEwen, D. C., & Hobbie, J. E. (2011). Changes in tundra pond limnology: Re-sampling Alaskan ponds after 40 years. *AMBIO: A Journal of the Human Environment*, *40*(6), 589-599.

Lyons, W. B., Welch, K. A., Gardner, C. B., Jaros, C., Moorhead, D. L., Knoepfle, J. L., & Doran, P. T. (2012). The geochemistry of upland ponds, Taylor Valley, Antarctica. *Antarctic Science*, *24*(1), 3-14.

MacDonald, L. A., Farquharson, N., Hall, R. I., Wolfe, B. B., Macrae, M. L., & Sweetman, J. N. (2014). Avian-driven modification of seasonal carbon cycling at a tundra pond in the Hudson Bay Lowlands (northern Manitoba, Canada). *Arctic, Antarctic, and Alpine Research*, *46*(1), 206-217.

MacDonald, L. A., Farquharson, N., Merritt, G., Fooks, S., Medeiros, A. S., Hall, R. I., ... & Sweetman, J. N. (2015). Limnological regime shifts caused by climate warming and Lesser Snow Goose population expansion in the western Hudson Bay Lowlands (Manitoba, Canada). *Ecology and Evolution*, *5*(4), 921-939.

MacDonald, L. A., Turner, K. W., Balasubramaniam, A. M., Wolfe, B. B., Hall, R. I., & Sweetman, J. N. (2012). Tracking hydrological responses of a thermokarst lake in the Old Crow Flats

(Yukon Territory, Canada) to recent climate variability using aerial photographs and paleolimnological methods. *Hydrological Processes*, *26*(1), 117-129.

Mack, M. C., Schuur, E. A., Bret-Harte, M. S., Shaver, G. R., & Chapin III, F. S. (2004). Ecosystem carbon storage in arctic tundra reduced by long-term nutrient fertilization. *Nature*, *431*(7007), 440.

MacLeod, J., Keller, W. B., Paterson, A. M., Dyer, R. D., & Gunn, J. M. (2016). Scale and watershed features determine lake chemistry patterns across physiographic regions in the far north of Ontario, Canada. *Journal of Limnology*, *76*(1).

Macrae, M. L., Bello, R. L., & Molot, L. A. (2004). Long-term carbon storage and hydrological control of CO2 exchange in tundra ponds in the Hudson Bay Lowland. *Hydrological Processes*, *18*(11), 2051-2069.

Macrae, M. L., Brown, L. C., Duguay, C. R., Parrott, J. A., & Petrone, R. M. (2014). Observed and projected climate change in the Churchill region of the Hudson Bay Lowlands and implications for pond sustainability. *Arctic, Antarctic, and Alpine Research, 46(1),* 272-285.

Macrae, M. L., Devito, K. J., Strack, M., & Waddington, J. M. (2013). Effect of water table drawdown on peatland nutrient dynamics: implications for climate change. *Biogeochemistry*, *112*(1-3), 661-676.

Magnuson, J. J., Benson, B. J., & Kratz, T. K. (1990). Temporal coherence in the limnology of a suite of lakes in Wisconsin, USA. *Freshwater Biology*, *23*(1), 145-159.

Mallory, M. L., Fontaine, A. J., Smith, P. A., Wiebe Robertson, M. O., & Gilchrist, H. G. (2006). Water chemistry of ponds on Southampton Island, Nunavut, Canada: effects of habitat and ornithogenic inputs. *Archiv für Hydrobiologie*, *166*(3), 411-432.

Malmer, N., & Nihlgård, B. (1980). Supply and transport of mineral nutrients in a subarctic mire. *Ecological Bulletins*, 63-95.

Mamet, S. D., & Kershaw, G. P. (2013). Environmental influences on winter desiccation of Picea glauca foliage at treeline, and implications for treeline dynamics in northern Manitoba. *Arctic, Antarctic, and Alpine Research*, *45*(2), 219-228.

Manasypov, R. M., Pokrovsky, O. S., Kirpotin, S. N., & Shirokova, L. S. (2014). Thermokarst lake waters across the permafrost zones of western Siberia. *The Cryosphere*, *8*(4), 1177-1193.

Marushchak, M. E., Pitkämäki, A., Koponen, H., Biasi, C., Seppälä, M., & Martikainen, P. J. (2011). Hot spots for nitrous oxide emissions found in different types of permafrost peatlands. *Global Change Biology*, *17*(8), 2601-2614.

Mazurek, M., Paluszkiewicz, R., Rachlewicz, G., & Zwoliński, Z. (2012). Variability of water chemistry in tundra lakes, Petuniabukta coast, Central Spitsbergen, Svalbard. *The Scientific World Journal*, *2012*.

McClain, M. E., Boyer, E. W., Dent, C. L., Gergel, S. E., Grimm, N. B., Groffman, P. M., ... & McDowell, W. H. (2003). Biogeochemical hot spots and hot moments at the interface of terrestrial and aquatic ecosystems. *Ecosystems*, *6*(4), 301-312.

McGuire, A. D., Anderson, L. G., Christensen, T. R., Dallimore, S., Guo, L., Hayes, D. J., ... & Roulet, N. (2009). Sensitivity of the carbon cycle in the Arctic to climate change. *Ecological Monographs*, *79*(4), 523-555.

McLaughlin, D. L., & Cohen, M. J. (2011). Thermal artifacts in measurements of fine-scale water level variation. *Water Resources Research*, *47*(9).

Medeiros, A. S., Taylor, D. J., Couse, M., Hall, R. I., Quinlan, R., & Wolfe, B. B. (2014). Biological and nutrient responses to catchment disturbance and warming in small lakes near the Alaskan tundra–taiga boundary. *The Holocene*, *24*(10), 1308-1319.

Mettrop, I. S., Cusell, C., Kooijman, A. M., & Lamers, L. P. (2014). Nutrient and carbon dynamics in peat from rich fens and Sphagnum-fens during different gradations of drought. *Soil Biology and Biochemistry*, *68*, 317-328.

Michelutti, N., Douglas, M. S., Lean, D. R., & Smol, J. P. (2002). Physical and chemical limnology of 34 ultra-oligotrophic lakes and ponds near Wynniatt Bay, Victoria Island, Arctic Canada. *Hydrobiologia*, *482*(1-3), 1-13.

Moore, T. R., Trofymow, J. A., Siltanen, M., & Kozak, L. M. (2008). Litter decomposition and nitrogen and phosphorus dynamics in peatlands and uplands over 12 years in central Canada. *Oecologia*, *157*(2), 317-325.

Morison, M. Q., Macrae, M. L., Petrone, R. M., & Fishback, L. (2017). Capturing temporal and spatial variability in the chemistry of shallow permafrost ponds. *Biogeosciences*, *14*(23), 5471.

Morison, M. Q., Macrae, M. L., Petrone, R. M., & Fishback, L. (2017). Seasonal dynamics in shallow freshwater pond-peatland hydrochemical interactions in a subarctic permafrost environment. *Hydrological Processes*, *31*(2), 462-475.

Muster, S., Heim, B., Abnizova, A., & Boike, J. (2013). Water body distributions across scales: a remote sensing based comparison of three arctic tundra wetlands. *Remote Sensing*, *5*(4), 1498-1523.

Nadelhoffer, K. J., Giblin, A. E., Shaver, G. R., & Laundre, J. A. (1991). Effects of temperature and substrate quality on element mineralization in six arctic soils. *Ecology*, *72*(1), 242-253.

Natali, S. M., Schuur, E. A., Trucco, C., Hicks Pries, C. E., Crummer, K. G., & Baron Lopez, A. F. (2011). Effects of experimental warming of air, soil and permafrost on carbon balance in Alaskan tundra. *Global Change Biology*, *17*(3), 1394-1407.

Niu, F., Lin, Z., Liu, H., & Lu, J. (2011). Characteristics of thermokarst lakes and their influence on permafrost in Qinghai–Tibet Plateau. *Geomorphology*, *132*(3-4), 222-233.

Niu, F., Lin, Z., Lu, J., Luo, J., & Wang, H. (2015). Assessment of terrain susceptibility to thermokarst lake development along the Qinghai–Tibet engineering corridor, China. *Environmental Earth Sciences*, *73*(9), 5631-5642.

O'Brien, W., Barfield, M., Bettez, N., Hershey, A. E., Hobbie, J. E., Kipphut, G., ... & Miller, M. C. (2005). Long-term response and recovery to nutrient addition of a partitioned arctic lake. *Freshwater Biology*, *50*(5), 731-741.

O'Kelly, B. C., & Sivakumar, V. (2014). Water content determinations for peat and other organic soils using the oven-drying method. *Drying Technology*, *32*(6), 631-643.

Olefeldt, D., Goswami, S., Grosse, G., Hayes, D., Hugelius, G., Kuhry, P., ... & Turetsky, M. R. (2016). Circumpolar distribution and carbon storage of thermokarst landscapes. *Nature Communications*, *7*, 13043.

Osborne, T. Z., & DeLaune, R. D. (2013). Soil and sediment sampling of inundated environments. *In* DeLaune, R.D., Reddy, K.R., Richardson, C.J., and Megonigal, J.P. (eds.), *Methods in Biogeochemistry of Wetlands.* Madison: Soil Science Society of America, 21-40.

Oswald, C. J., Richardson, M. C., & Branfireun, B. A. (2011). Water storage dynamics and runoff response of a boreal Shield headwater catchment. *Hydrological Processes*, *25*(19), 3042-3060.

Pace, M. L., & Cole, J. J. (2002). Synchronous variation of dissolved organic carbon and color in lakes. *Limnology and Oceanography*, *47*(2), 333-342.

Parkinson, J. A., & Allen, S. E. (1975). A wet oxidation procedure suitable for the determination of nitrogen and mineral nutrients in biological material. *Communications in Soil Science and Plant Analysis*, *6*(1), 1-11.

Paterson, A. M., Keller, W., Rühland, K. M., Jones, F. C., & Winter, J. G. (2014). An exploratory survey of summer water chemistry and plankton communities in lakes near the Sutton River, Hudson Bay Lowlands, Ontario, Canada. *Arctic, Antarctic, and Alpine research*, *46*(1), 121-138.

Payette, S., & Delwaide, A. (2000). Recent permafrost dynamics in a subarctic floodplain associated with changing water levels, Québec, Canada. *Arctic, Antarctic, and Alpine Research*, 316-323.

Payette, S., Delwaide, A., Caccianiga, M., & Beauchemin, M. (2004). Accelerated thawing of subarctic peatland permafrost over the last 50 years. *Geophysical Research Letters*, *31*(18).

Petrone, K. C., Jones, J. B., Hinzman, L. D., & Boone, R. D. (2006). Seasonal export of carbon, nitrogen, and major solutes from Alaskan catchments with discontinuous permafrost. *Journal of Geophysical Research: Biogeosciences*, *111*(G2).

Phillips, R. W., Spence, C., & Pomeroy, J. W. (2011). Connectivity and runoff dynamics in heterogeneous basins. *Hydrological Processes*, *25*(19), 3061-3075.

Pienitz, R., Smol, J. P., & Birks, H. J. B. (1995). Assessment of freshwater diatoms as quantitative indicators of past climatic change in the Yukon and Northwest Territories, Canada. *Journal of Paleolimnology*, *13*(1), 21-49.

Pienitz, R., Smol, J. P., & Lean, D. R. (1997). Physical and chemical limnology of 59 lakes located between the southern Yukon and the Tuktoyaktuk Peninsula, Northwest Territories (Canada). *Canadian Journal of Fisheries and Aquatic Sciences*, *54*(2), 330-346.

Pietroniro, A., Prowse, T., Hamlin, L., Kouwen, N., & Soulis, R. I. C. (1996). Application of a grouped response unit hydrological model to a northern wetland region. *Hydrological Processes*, *10*(10), 1245-1261.

Pokrovsky, O. S., Shirokova, L. S., Kirpotin, S. N., Audry, S., Viers, J., & Dupré, B. (2011). Effect of permafrost thawing on organic carbon and trace element colloidal speciation in the thermokarst lakes of western Siberia. *Biogeosciences*, *8*(3), 565-583.

Potvin, L. R., Kane, E. S., Chimner, R. A., Kolka, R. K., & Lilleskov, E. A. (2015). Effects of water table position and plant functional group on plant community, aboveground production, and peat properties in a peatland mesocosm experiment (PEATcosm). *Plant and Soil*, 387(1-2), 277-294.

Price, J. S. (1996). Hydrology and microclimate of a partly restored cutover bog, Quebec. *Hydrological Processes*, *10*(10), 1263-1272.

Przytulska, A., Comte, J., Crevecoeur, S., Lovejoy, C., Laurion, I., & Vincent, W. F. (2016). Phototrophic pigment diversity and picophytoplankton in permafrost thaw lakes. *Biogeosciences*, *13*(1), 13.

Quinton, W. L., & Pomeroy, J. W. (2006). Transformations of runoff chemistry in the Arctic tundra, Northwest Territories, Canada. *Hydrological Processes*, *20*(14), 2901-2919.

Quinton, W. L., Hayashi, M., & Pietroniro, A. (2003). Connectivity and storage functions of channel fens and flat bogs in northern basins. *Hydrological Processes*, *17*(18), 3665-3684.

R Development Core Team, 2016: R: A language and environment for statistical computing, R Foundation for Statistical Computing. Vienna, Austria. <http://www.R-project.org>, Accessed 01/10/2017.

Rautio, M., Dufresne, F., Laurion, I., Bonilla, S., Vincent, W. F., & Christoffersen, K. S. (2011). Shallow freshwater ecosystems of the circumpolar Arctic. *Ecoscience*, *18*(3), 204-222.

Reaney, S. M., Bracken, L. J., & Kirkby, M. J. (2007). Use of the connectivity of runoff model (CRUM) to investigate the influence of storm characteristics on runoff generation and connectivity in semi-arid areas. *Hydrological Processes*, *21*(7), 894-906.

Reddy, K. R., & DeLaune, R. D. (2008). *Biogeochemistry of Wetlands: Science and Applications*. CRC press.

Repo, M. E., Susiluoto, S., Lind, S. E., Jokinen, S., Elsakov, V., Biasi, C., ... & Martikainen, P. J. (2009). Large N 2 O emissions from cryoturbated peat soil in tundra. *Nature Geoscience*, *2*(3), 189.

Rezanezhad, F., Price, J. S., Quinton, W. L., Lennartz, B., Milojevic, T., & Van Cappellen, P. (2016). Structure of peat soils and implications for water storage, flow and solute transport: A review update for geochemists. *Chemical Geology*, *429*, 75-84.

Richardson, C. J. (1985). Mechanisms controlling phosphorus retention capacity in freshwater wetlands. *Science*, *228*(4706), 1424-1427.

Robinson, C. H. (2002). Controls on decomposition and soil nitrogen availability at high latitudes. *Plant and Soil*, *242*(1), 65-81.

Roiha, T., Laurion, I., & Rautio, M. (2015). Carbon dynamics in highly heterotrophic subarctic thaw ponds. *Biogeosciences*, *12*(23), 7223-7237.

Rosswall, T., & Granhall, U. (1980). Nitrogen cycling in a subarctic ombrotrophic mire. *Ecological Bulletins*, 209-234.

Roulet, N. T. (2000). Peatlands, carbon storage, greenhouse gases, and the Kyoto Protocol: Prospects and significance for Canada. *Wetlands*, *20*(4), 605-615.

Roulet, N., Moore, T. M., Bubier, J., & Lafleur, P. (1992). Northern fens: methane flux and climatic change. *Tellus B*, *44*(2), 100-105.

Rouse, W. R. (1991). Impacts of Hudson Bay on the terrestrial climate of the Hudson Bay Lowlands. *Arctic and Alpine Research*, 24-30.

Rühland, K., Priesnitz, A., & Smol, J. P. (2003). Paleolimnological evidence from diatoms for recent environmental changes in 50 lakes across Canadian Arctic treeline. *Arctic, Antarctic, and Alpine Research*, *35*(1), 110-123.

Rustad, L., Campbell, J., Marion, G., Norby, R., Mitchell, M., Hartley, A., ... & Gurevitch, J. (2001). A meta-analysis of the response of soil respiration, net nitrogen mineralization, and aboveground plant growth to experimental ecosystem warming. *Oecologia*, *126*(4), 543-562.

Sanchez-Cabeza, J.A. & Ruiz-Fernandez, A.C. (2012). ^{210}Pb sediment radiochronology: an integrated formulation and classification of dating models. *Geochimica et Cosmochimica Acta*, *(82),* 183-200.

Sannel, A. B. K., & Kuhry, P. (2009). Holocene peat growth and decay dynamics in sub-arctic peat plateaus, west-central Canada. *Boreas*, *38*(1), 13-24.

Sauchyn, D. & Kulshreshtha, S. (2008). *Prairies*. In *From Impacts to Adaptation: Canada in a Changing Climate 2007*. Government of Canada, Ottawa.

Schaefer, K., Zhang, T., Bruhwiler, L., & Barrett, A. P. (2011). Amount and timing of permafrost carbon release in response to climate warming. *Tellus B*, *63*(2), 165-180.

Schimel, J. P., & Chapin, F. S. (1996). Tundra plant uptake of amino acid and NH_4^+ nitrogen in situ: plants complete well for amino acid N. *Ecology*, *77*(7), 2142-2147.

Schimel, J. P., Bilbrough, C., & Welker, J. M. (2004). Increased snow depth affects microbial activity and nitrogen mineralization in two Arctic tundra communities. *Soil Biology and Biochemistry*, *36*(2), 217-227.

Schindler, D. W., & Smol, J. P. (2006). Cumulative effects of climate warming and other human activities on freshwaters of Arctic and subarctic North America. *AMBIO: A Journal of the Human Environment*, *35*(4), 160-168.

Schlesinger, W.H., & Berhhardt, E.S. (2012). *Biogeochemistry: An Analysis of Global Change*. Oxford: Academic Press.

Schmidt, I. K., Jonasson, S., & Michelsen, A. (1999). Mineralization and microbial immobilization of N and P in arctic soils in relation to season, temperature and nutrient amendment. *Applied Soil Ecology*, *11*(2-3), 147-160.

Schuur, E. A. G., Abbott, B. W., Bowden, W. B., Brovkin, V., Camill, P., Canadell, J. G., ... & Crosby, B. T. (2013). Expert assessment of vulnerability of permafrost carbon to climate change. *Climatic Change*, *119*(2), 359-374.

Schuur, E. A. G., McGuire, A. D., Schädel, C., Grosse, G., Harden, J. W., Hayes, D. J., ... & Natali, S. M. (2015). Climate change and the permafrost carbon feedback. *Nature*, *520*(7546), 171-179.

Schuur, E. A., Bockheim, J., Canadell, J. G., Euskirchen, E., Field, C. B., Goryachkin, S. V., ... & Mazhitova, G. (2008). Vulnerability of permafrost carbon to climate change: Implications for the global carbon cycle. *AIBS Bulletin*, *58*(8), 701-714.

Schuur, E. A., Crummer, K. G., Vogel, J. G., & Mack, M. C. (2007). Plant species composition and productivity following permafrost thaw and thermokarst in Alaskan tundra. *Ecosystems*, *10*(2), 280-292.

Serreze, M. C., Walsh, J. E., Chapin, F. S., Osterkamp, T., Dyurgerov, M., Romanovsky, V., ... & Barry, R. G. (2000). Observational evidence of recent change in the northern high-latitude environment. *Climatic Change*, *46*(1-2), 159-207.

Shaver, G. R., & Chapin, F. S. (1980). Response to fertilization by various plant growth forms in an Alaskan tundra: nutrient accumulation and growth. *Ecology*, *61*(3), 662-675.

Shook, K., & Pomeroy, J. (2012). Changes in the hydrological character of rainfall on the Canadian prairies. *Hydrological Processes*, *26*(12), 1752-1766.

Skrzypek, G., Wojtuń, B., Richter, D., Jakubas, D., Wojczulanis-Jakubas, K., & Samecka-Cymerman, A. (2015). Diversification of nitrogen sources in various tundra vegetation types in the high Arctic. *PLoS One*, *10*(9), e0136536.

Smith, L. C., Sheng, Y., MacDonald, G. M., & Hinzman, L. D. (2005). Disappearing arctic lakes. *Science*, *308*(5727), 1429-1429.

Smol, J. P., & Douglas, M. S. (2007a). Crossing the final ecological threshold in high Arctic ponds. *Proceedings of the National Academy of Sciences*, *104*(30), 12395-12397.

Smol, J. P., & Douglas, M. S. (2007b). From controversy to consensus: making the case for recent climate change in the Arctic using lake sediments. *Frontiers in Ecology and the Environment*, *5*(9), 466-474.

Smol, J. P., Wolfe, A. P., Birks, H. J. B., Douglas, M. S., Jones, V. J., Korhola, A., ... & Brooks, S. J. (2005). Climate-driven regime shifts in the biological communities of arctic lakes. *Proceedings of the National Academy of Sciences of the United States of America*, *102*(12), 4397-4402.

Sokal, M. A., Hall, R. I., & Wolfe, B. B. (2010). Inter-annual and seasonal effects of flooding on the water chemistry, diatom phytoplankton communities and macrophyte biomass of lakes in the Slave River Delta (Northwest Territories, Canada). *Ecohydrology*, *3*, 41-54.

Song, K. Y., Zoh, K. D., & Kang, H. (2007). Release of phosphate in a wetland by changes in hydrological regime. *Science of the Total Environment*, *380*(1-3), 13-18.

Spaulding, S. A., Lubinski, D. J., & Potapova, M. (2010). Diatoms of the United States. <http://westerndiatoms.colorado.edu> Accessed online: 07/21/2017.

Spence, C., & Woo, M. K. (2003). Hydrology of subarctic Canadian shield: soil-filled valleys. *Journal of Hydrology*, *279*(1-4), 151-166.

Spence, C., Guan, X. J., Phillips, R., Hedstrom, N., Granger, R., & Reid, B. (2010). Storage dynamics and streamflow in a catchment with a variable contributing area. *Hydrological Processes*, *24*(16), 2209-2221.

Spiess, A. N., & Neumeyer, N. (2010). An evaluation of R^2 as an inadequate measure for nonlinear models in pharmacological and biochemical research: a Monte Carlo approach. *BMC Pharmacology*, *10*(1), 6.

Stark, S. (2007). *Nutrient cycling in the tundra.* In: Marschner, P. & Rengel, Z. (eds) *Nutrient Cycling in Terrestrial Ecosystems.* Springer, Berlin Heidelberg.

Strack, M., & Waddington, J. M. (2007). Response of peatland carbon dioxide and methane fluxes to a water table drawdown experiment. *Global Biogeochemical Cycles*, 21(1).

Symons, C. C., Arnott, S. E., & Sweetman, J. N. (2012). Nutrient limitation of phytoplankton communities in Subarctic lakes and ponds in Wapusk National Park, Canada. *Polar Biology*, *35*(4), 481-489.

T Weedon, J., A Kowalchuk, G., Aerts, R., Van Hal, J., Van Logtestijn, R., Taş, N., ... & Van Bodegom, P. (2012). Summer warming accelerates sub-arctic peatland nitrogen cycling without changing enzyme pools or microbial community structure. *Global Change Biology*, *18*(1), 138-150.

Thompson, D. K., & Woo, M. K. (2009). Seasonal hydrochemistry of a high Arctic wetland complex. *Hydrological Processes*, *23*(10), 1397-1407.

Thompson, M. S., Wrona, F. J., & Prowse, T. D. (2012). Shifts in plankton, nutrient and light relationships in small tundra lakes caused by localized permafrost thaw. *Arctic*, 367-376.

Thormann, M. N., & Bayley, S. E. (1997). Decomposition along a moderate-rich fen-marsh peatland gradient in boreal Alberta, Canada. *Wetlands*, *17*(1), 123-137.

Uhlířová, E., Šantrůčková, H., & Davidov, S. P. (2007). Quality and potential biodegradability of soil organic matter preserved in permafrost of Siberian tussock tundra. *Soil Biology and Biochemistry*, *39*(8), 1978-1989.

Uhlířová, E., Šantrůčková, H., & Davidov, S. P. (2007). Quality and potential biodegradability of soil organic matter preserved in permafrost of Siberian tussock tundra. *Soil Biology and Biochemistry*, *39*(8), 1978-1989.

Van Breemen, N., & Finzi, A. C. (1998). Plant-soil interactions: ecological aspects and evolutionary implications. *Biogeochemistry*, *42*(1-2), 1-19.

Van der Werff, A. (1955). A new method of concentrating and cleaning diatoms and other organisms. *Verhandlungen des Internationalen Verein Limnologie 13*, 276-277.

Vandenberghe, J., French, H. M., Gorbunov, A., Marchenko, S., Velichko, A. A., Jin, H., ... & Wan, X. (2014). The Last Permafrost Maximum (LPM) map of the Northern Hemisphere: permafrost extent and mean annual air temperatures, 25–17 ka BP. *Boreas*, *43*(3), 652-666.

Venterink, H. O., Davidsson, T. E., Kiehl, K., & Leonardson, L. (2002). Impact of drying and re-wetting on N, P and K dynamics in a wetland soil. *Plant and Soil*, *243*(1), 119-130.

Verhoeven, J. T. A., Koerselman, W., & Meuleman, A. F. M. (1996). Nitrogen-or phosphorus-limited growth in herbaceous, wet vegetation: relations with atmospheric inputs and management regimes. *Trends in Ecology & Evolution*, *11*(12), 494-497.

Viner, A. B. (1984). Laboratory experiments on the effects of light and temperature on the uptake of nutrients by Lake Rotongaio phytoplankton. *New Zealand Journal of Marine and Freshwater Research*, *18*(3), 323-340.

Vitousek, P. M., & Howarth, R. W. (1991). Nitrogen limitation on land and in the sea: how can it occur?. *Biogeochemistry*, *13*(2), 87-115.

Vitousek, P. M., Aber, J. D., Howarth, R. W., Likens, G. E., Matson, P. A., Schindler, D. W., ... & Tilman, D. G. (1997). Human alteration of the global nitrogen cycle: sources and consequences. *Ecological Applications*, *7*(3), 737-750.

Vitousek, P. M., Porder, S., Houlton, B. Z., & Chadwick, O. A. (2010). Terrestrial phosphorus limitation: mechanisms, implications, and nitrogen–phosphorus interactions. *Ecological Applications*, *20*(1), 5-15.

Vitt, D. H., Halsey, L. A., & Zoltai, S. C. (1994). The bog landforms of continental western Canada in relation to climate and permafrost patterns. *Arctic and Alpine Research*, 1-13.

Vonk, J. E., Tank, S. E., Bowden, W. B., Laurion, I., Vincent, W. F., Alekseychik, P., ... & Deshpande, B. N. (2015). Reviews and syntheses: Effects of permafrost thaw on Arctic aquatic ecosystems. *Biogeosciences*, *12*(23), 7129-7167.

Vreča, P., & Muri, G. (2010). Sediment organic matter in mountain lakes of north-western Slovenia and its stable isotopic signatures: records of natural and anthropogenic impacts. *Hydrobiologia*, *648*(1), 35-49.

Wallenstein, M. D., McMahon, S. K., & Schimel, J. P. (2009). Seasonal variation in enzyme activities and temperature sensitivities in Arctic tundra soils. *Global Change Biology*, *15*(7), 1631-1639.

Walter, K. M., Edwards, M. E., Grosse, G., Zimov, S. A., & Chapin, F. S. (2007). Thermokarst lakes as a source of atmospheric CH_4 during the last deglaciation. *Science*, *318*(5850), 633-636.

Walvoord, M. A., & Kurylyk, B. L. (2016). Hydrologic impacts of thawing permafrost—A review. *Vadose Zone Journal*, *15*(6).

Walvoord, M. A., & Striegl, R. G. (2007). Increased groundwater to stream discharge from permafrost thawing in the Yukon River basin: Potential impacts on lateral export of carbon and nitrogen. *Geophysical Research Letters*, *34*(12).

Wang, M., & Moore, T. R. (2014). Carbon, nitrogen, phosphorus, and potassium stoichiometry in an ombrotrophic peatland reflects plant functional type. *Ecosystems*, *17*(4), 673-684.

Wang, M., Moore, T. R., Talbot, J., & Riley, J. L. (2015). The stoichiometry of carbon and nutrients in peat formation. *Global Biogeochemical Cycles*, *29*(2), 113-121.

Weedon, T. J., A Kowalchuk, G., Aerts, R., Van Hal, J., Van Logtestijn, R., Taş, N., ... & M van Bodegom, P. (2012). Summer warming accelerates sub-arctic peatland nitrogen cycling without changing enzyme pools or microbial community structure. *Global Change Biology*, *18*(1), 138-150.

Weintraub, M. N., & Schimel, J. P. (2005). Nitrogen cycling and the spread of shrubs control changes in the carbon balance of arctic tundra ecosystems. *AIBS Bulletin*, *55*(5), 408-415.

Weintraub, M. N., & Schimel, J. P. (2005). Nitrogen cycling and the spread of shrubs control changes in the carbon balance of arctic tundra ecosystems. *AIBS Bulletin*, *55*(5), 408-415.

Wetzel, R. G. (2001). *Limnology: lake and river ecosystems.* Gulf Professional Publishing, United States.

Whalen, J. K., Chang, C., & Olson, B. M. (2001). Nitrogen and phosphorus mineralization potentials of soils receiving repeated annual cattle manure applications. *Biology and Fertility of Soils*, *34*(5), 334-341.

White, J., Hall, R. I., Wolfe, B. B., Light, E. M., Macrae, M. L., & Fishback, L. (2014). Hydrological connectivity and basin morphometry influence seasonal water-chemistry variations in tundra ponds of the northwestern Hudson Bay Lowlands. *Arctic, Antarctic, and Alpine research*, *46*(1), 218-235.

Wickland, K. P., Aiken, G. R., Butler, K., Dornblaser, M. M., Spencer, R. G. M., & Striegl, R. G. (2012). Biodegradability of dissolved organic carbon in the Yukon River and its tributaries: Seasonality and importance of inorganic nitrogen. *Global Biogeochemical Cycles, 26*(4).

Wiklund, J. A., Hall, R. I., & Wolfe, B. B. (2012). Timescales of hydrolimnological change in floodplain lakes of the Peace-Athabasca Delta, northern Alberta, Canada. *Ecohydrology*, *5*(3), 351-367.

Williams, B. L., & Wheatley, R. E. (1988). Nitrogen mineralization and water-table height in oligotrophic deep peat. *Biology and Fertility of Soils, 6*(2), 141-147.

Wolf, D., Klemann, V., Wünsch, J., & Zhang, F. P. (2006). A reanalysis and reinterpretation of geodetic and geological evidence of glacial-isostatic adjustment in the Churchill region, Hudson Bay. *Surveys in Geophysics*, *27*(1), 19-61.

Wolfe, B. B., Light, E. M., Macrae, M. L., Hall, R. I., Eichel, K., Jasechko, S., ... & Edwards, T. W. (2011). Divergent hydrological responses to 20th century climate change in shallow tundra ponds, western Hudson Bay Lowlands. *Geophysical Research Letters*, *38*(23).

Woo, M. K. (2012). *Permafrost hydrology*. Springer Science & Business Media.

Woo, M. K., & Guan, X. J. (2006). Hydrological connectivity and seasonal storage change of tundra ponds in a polar oasis environment, Canadian High Arctic. *Permafrost and Periglacial Processes*, *17*(4), 309-323.

Woo, M. K., & Mielko, C. (2007). An integrated framework of lake-stream connectivity for a semi-arid, subarctic environment. *Hydrological Processes, 21*(19), 2668-2674.

Woo, M. K., & Young, K. L. (2003). Hydrogeomorphology of patchy wetlands in the High Arctic, polar desert environment. *Wetlands*, *23*(2), 291-309.

Woo, M. K., & Young, K. L. (2006). High Arctic wetlands: their occurrence, hydrological characteristics and sustainability. *Journal of Hydrology*, *320*(3-4), 432-450.

Wood, M. E., Macrae, M. L., Strack, M., Price, J. S., Osko, T. J., & Petrone, R. M. (2016). Spatial variation in nutrient dynamics among five different peatland types in the Alberta oil sands region. *Ecohydrology, 9*(4), 688-699.

Wright, N., Hayashi, M., & Quinton, W. L. (2009). Spatial and temporal variations in active layer thawing and their implication on runoff generation in peat-covered permafrost terrain. *Water Resources Research*, *45*(5).

Yoshikawa, K., & Hinzman, L. D. (2003). Shrinking thermokarst ponds and groundwater dynamics in discontinuous permafrost near Council, Alaska. *Permafrost and Periglacial Processes*, *14*(2), 151-160.

Zamin, T. J., & Grogan, P. (2012). Birch shrub growth in the low Arctic: the relative importance of experimental warming, enhanced nutrient availability, snow depth and caribou exclusion. *Environmental Research Letters, 7*(3), 034027.

Appendix A:

Table A.1 Ranges of values for extractible nutrient pools and net mineralization rates presented in comparable study regions (both peatland and subarctic sites)

Study Reference	Nutrient Stoichiometry ($g\ g^{-1}$)			Extractable Nutrient Pool ($\mu g\ g^{-1}$ dry soil)				Net Mineralization ($\mu g\ g^{-1}$ dry soil d^{-1})				Field based or laboratory (oxic incubation) based	Study Site
	C:N	N:P	C:P	TIN	NH_4^+	NO_3^-	PO_4^-	TIN	NH_4^+	NO_3^-	PO_4^-		
Andersen et al. (2013)	58 - 134				2.7 - 80.6	0.5 - 13.4	<0.02		-2.0 - 12.0	-0.2 - 1.0	$< 1 \times 10^{-3}$	Field	Restored harvested bog in Quebec, Canada
Bayley et al. (2005)	29 - 79				26 - 318				-0.6 - 19.8			Field	Four natural bog and fen sites, central Alberta, Canada
Bridgham et al. (1998)	16 - 38	24 - 32	526 - 913	12 - 62			1 - 21	2.2 - 4.5			~ 0.02 - 0.3	Field	Three natural bog and fen sites, Minnesota, United States
Fellman & D'Amore (2007)	27 - 44	10 - 25	331 - 847					0.4 - 1.7			.002 - .027	Field	Three natural wetland sites, Alaska, United States
Fellman & D'Amore (2007)								1.1 - 4.9			.004 - .048	Laboratory	
Hartsock et al. (2016)	20 - 67				21.4 - 181.4	1 - 87.9		-12.9 - 26.6				Field	Constructed fen and benchmark natural fens, Alberta, Canada
Kelley et al. (2012)	~ 10 - 40							-2 - 0.5		-0.1 - 0.1		Laboratory	Eight patterned ground features on latitudal gradient from Low Arctic tundra, northern Alaska, USA to High Arctic polar desert, Canada
Macrae et al. (2013)	16 - 53	23 - 57	907 - 1424		7 - 99	2 - 16	0.8 - 2.4	-2.0 - 1.9		-0.5 - 0.5	-0.05 - 0.05	Field	Paired drained and natural open bog and poor fen in Quebec, Canada
Nadelhoffer et al. (1991)	9 - 27	9 - 40	235 - 614		0.7 - 19.8	0.2 - 8.2	0.1 - 5.5	0.1 - 6.0			~ 0.0 - 1.9	Laboratory	Six sedge tundra and heath systems in Alaska , United States
Verhoeven *et al*. (1990)	19 - 59	18 - 37	337 - 2197	25 - 90			~ 1- 35	~ 0.1 - 6.5			~ -0.1 to 2.5	Field	Ten natural and harvested fen and bog sites, Netherlands
Wood *et al*. (2016)	32 - 78			8 .0 – 102.6	7.0 – 94.6	0.3 – 31.4	0 – 93.4	-3.6 – 20.9	-3.6 – 15.9	-0.7 - 0.6	-3.4 – 6.0	Field	Set of five natural and industry-disturbed peatlands, Alberta, Canada
This Study	**12 - 44**	**24 - 85**	**511 - 2255**	**0.7 - 101.1**	**0.7 - 101.1**	**0.0 - 5.0**	**0.0 - 25.5**	**-1.7 - 6.7**	**-2.5 - 3.5**	**-0.1 - 4.6**	**-0.7 - 0.6**	**Laboratory**	**Four sites in permafrost thermokarst bog, Manitoba, Canada**

Appendix B:

Table B.1 Reported sampling designs for studies focused on, or including small (< 1 km^2) lakes and ponds. When categorizing analytes of interest for each study, “nutrients” refers to the measurement of any dissolved or particulate nitrogen or phosphorus speciation, “carbon” refers to any measurements of dissolved or particulate organic or inorganic carbon, “major ions” refers to the measurement of dissolved sodium, magnesium, calcium, potassium, chloride, sulphate, and carbonate, and “metals” refers to the measurement of dissolved or suspended trace metal elements.

Study	Analytes of interest	Region	Study year(s)	Number of ponds/lakes studied	Number of samples per year
Archer et al., 2016	Nutrients, Metals	Ross Sea, Antarctica	2009-2013	41	1
Balasubramaniam et al., 2015	Nutrients, Carbon, Major Ions	Old Crow Flats, Yukon	2007	56	3
Bos and Pellatt., 2012	Nutrients, Carbon, Metals	Hudson Bay Lowlands, Manitoba	2004	32	1
Breton et al., 2009	Nutrients, Carbon	Northern Quebec and Baffin Island	2004-2005	46	1
Hinkel et al., 2016	Nutrients, Carbon, Major Ions	North Slope of Alaska	2012-2013	28	1
Houben et al., 2016	Nutrients, Carbon, Major Ions, Metals	Northwest Territories	2009-2012	38	1
Jacques et al., 2016	Nutrients, Carbon, Major Ions	Hudson Bay Lowlands, Manitoba	2010-2012	33	1
Kokelj et al., 2009	Carbon, Major Ions	Mackenzie River Delta, Canada	2005-2006	73	1
Larsen et al., 2017	Nutrients, Carbon, Major Ions	Environmental Gradient within Alaska	2006-2013	617	1

Lim et al., 2001	Nutrients, Carbon	Bathurst Island, Arctic Canada	1994	38	1
Lyons et al., 2012	Major Ions	Taylor Valley, Antarctica	2000-2010	7	1
MacDonald et al., 2014	Nutrients, Carbon	Hudson Bay Lowlands, Manitoba	2010 - 2012	16	3
MacLeod et al., 2016	Nutrients, Carbon, Major Ions, Metals	Hudson Bay Lowlands, Ontario	2011 - 2012	98	1
Mallory et al., 2006	Nutrients, Carbon, Major Ions, Metals	Southampton Island, Nunavut	2001-2002	32	1
Manasypov et al., 2014	Carbon, Major Ions, Metals	Western Siberia	2010-2011	58	1
Michelutti et al., 2002	Nutrients, Carbon, Major Ions, Metals	Wynniatt Bay, Victoria Island, Arctic Canada	1997	34	1
Niu et al., 2011	Major Ions	Kunlun Mountain pass, Tibet	2007	10	1
Paterson et al., 2014	Nutrients, Carbon, Major Ions, Metals	Hudson Bay Lowlands, Ontario	2009-2011	17	1
Pienitz et al., 1997	Nutrients, Carbon, Major Ions, Metals	Yukon and NWT, Canada	1990	59	1
Pokrovsky et al., 2011	Carbon, Major Ions, Metals	Northwestern Siberia	2008-2010	20	1
White et al., 2014	Nutrients, Major Ions	Hudson Bay Lowlands, Manitoba	2010	20	3

Table B.2 All concentration data of all chemical species over the 2015 study period in each study pond, including an intensive sampling campaign in Frisbee and Strange Ponds coincident with a storm event, DOY 185 to 188.

Location	Date and Time	DON	Cl^-	SO_4^{2-}	Na^+	K^+	Mg^{2+}	Ca^{2+}	NH_4^+	NO_3^-
Erin	2015-05-25 12:00 PM	0.50	12.11	2.47	7.25	0.78	4.99	7.26	0.11	0.01
	2015-06-04 12:00 PM	0.39	10.41	2.16	6.26	0.62	4.45	13.00	0.03	0.01
	2015-06-17 12:00 PM	0.36	10.29	2.11	6.44	0.57	4.70	8.79	0.05	0.01
	2015-07-01 4:05 PM	0.60	12.53	2.43	7.95	0.78	6.11	10.27	0.08	0.01
	2015-07-06 4:30 PM	0.55	10.22	1.95	6.64	0.57	5.10	12.06	0.11	0.01
	2015-07-22 10:39 AM	0.65	12.10	2.27	7.88	0.78	6.42	12.28	0.07	0.01
	2015-08-05 10:16 AM	0.68	12.26	2.38	7.86	0.75	6.59	7.90	0.04	0.00
	2015-08-19 3:03 PM	0.72	13.39	2.38	8.46	0.82	7.15	7.97	0.04	0.01
	2015-09-02 3:23 PM	0.90	14.18	2.41	8.91	0.84	7.72	7.23	0.05	0.01
	2015-09-17 8:39 AM	0.76	14.62	2.60	9.38	0.89	8.46	5.95	0.06	0.01
	2015-10-03 3:37 PM	0.90	15.03	2.99	9.91	0.87	8.94	8.24	0.08	0.01
	2015-10-14 10:00 AM	0.53	12.14	2.78	7.51	0.70	8.00	6.30	0.16	0.01
Frisbee	2015-05-25 12:00 PM	0.41	35.67	7.49	19.44	1.15	6.61	18.81	0.07	0.01
	2015-06-04 12:00 PM	0.40	20.00	7.34	12.32	0.59	5.56	18.02	0.02	0.01
	2015-06-17 12:00 PM	0.72	19.39	9.17	11.65	0.45	7.30	22.04	0.07	0.01
	2015-07-01 3:52 PM	2.25	56.62	18.89	26.60	1.54	15.47	32.34	0.10	0.00
	2015-07-04 7:45 AM	1.66	31.09	10.92	14.69	0.82	10.25	24.91	0.09	0.01
	2015-07-04 2:30 PM	0.88	29.54	10.32	14.60	0.73	10.19	19.73	0.13	0.00
	2015-07-04 8:30 PM	1.02	26.75	12.03	13.61	0.70	10.16	25.50	0.06	0.02
	2015-07-05 7:45 AM	0.61	14.07	7.17	8.70	0.42	6.99	20.90	0.04	0.01
	2015-07-05 3:00 PM	0.60	13.88	6.78	8.89	0.34	6.55	19.01	0.04	0.01
	2015-07-06 7:30 AM	0.64	14.57	8.75	9.70	0.30	7.27	23.42	0.04	0.00
	2015-07-06 4:30 PM	0.89	15.97	9.83	10.08	0.32	7.18	24.40	0.04	0.00
	2015-07-22 10:25 AM	1.33	40.53	17.56	20.66	0.95	15.32	23.01	0.05	0.00
	2015-08-05 10:32 AM	1.17	36.50	14.84	18.81	0.87	15.69	17.05	0.06	0.01
	2015-08-19 3:21 PM	1.67	52.49	18.44	26.61	1.20	19.10	25.29	0.08	0.01
	2015-09-02 3:37 PM	2.36	67.82	19.31	31.20	1.49	24.55	21.60	0.05	0.00
	2015-09-17 8:57 AM	1.86	72.63	17.96	32.99	1.74	27.50	28.84	0.04	0.01
	2015-10-03 3:55 PM	1.25	46.06	23.22	25.03	0.93	24.28	15.00	0.06	0.01
	2015-10-14 9:46 AM	0.46	25.27	22.57	13.80	0.59	15.86	14.87	0.20	0.01
Larch	2015-05-25 12:00 PM	0.15	12.13	2.18	5.88	0.58	4.31	9.18	0.04	0.01
	2015-06-04 12:00 PM	0.32	15.32	5.86	10.33	0.78	8.50	11.59	0.03	0.01
	2015-06-17 12:00 PM	0.33	15.25	3.31	11.39	0.80	9.26	8.46	0.03	0.01
	2015-07-01 3:47 PM	0.43	19.44	7.18	13.40	0.85	10.90	12.24	0.05	0.01

	2015-07-06 4:30 PM	0.51	13.30	1.08	8.96	0.53	7.10	12.22	0.06	0.01
	2015-07-22 10:20 AM	0.47	15.45	2.86	11.19	0.65	9.83	8.93	0.09	0.00
	2015-08-05 10:26 AM	0.58	16.32	2.90	12.03	0.73	11.19	8.99	0.06	0.01
	2015-08-19 3:15 PM	0.58	17.80	3.00	14.80	0.94	13.58	7.98	0.04	0.01
	2015-09-02 3:30 PM	0.65	19.25	3.27	13.42	0.91	12.68	7.56	0.04	0.01
	2015-09-17 8:46 AM	0.59	20.25	3.12	14.47	1.02	14.15	7.81	0.14	0.01
	2015-10-03 3:48 PM	0.57	19.38	2.81	13.66	0.99	13.31	6.99	0.07	0.00
	2015-10-14 9:42 AM	0.55	17.70	2.09	12.15	0.91	11.58	8.81	0.19	0.01
Left	2015-05-25 12:00 PM	0.35	14.73	2.68	9.31	1.09	6.37	8.51	0.06	0.01
	2015-06-04 12:00 PM	0.45	14.47	1.36	12.77	0.98	9.34	10.70	0.07	0.01
	2015-06-17 12:00 PM	0.39	23.38	6.40	14.87	1.00	11.14	10.67	0.03	0.01
	2015-07-01 4:00 PM	1.07	38.83	9.58	22.44	1.52	14.52	13.21	0.10	0.01
	2015-07-06 4:30 PM	0.75	23.17	5.10	13.99	0.82	10.33	17.34	0.00	0.00
	2015-07-22 10:48 AM	0.90	32.89	7.14	18.70	1.18	13.25	14.78	0.08	0.01
	2015-08-05 10:48 AM	0.89	36.20	6.97	20.41	1.21	14.88	12.98	0.03	0.00
	2015-08-19 2:53 PM	1.10	48.32	11.11	26.63	1.33	16.68	10.70	0.07	0.01
	2015-09-02 3:57 PM	1.12	57.11	13.73	31.64	1.28	20.64	12.02	0.05	0.01
	2015-09-17 9:07 AM	1.03	73.92	19.65	40.34	1.42	28.88	13.89	0.16	0.01
	2015-10-03 4:16 PM	0.72	57.13	17.92	32.88	1.43	24.25	10.29	0.03	0.01
	2015-10-14 10:14 AM	0.54	45.56	14.68	25.39	1.82	18.04	9.63	0.04	0.01
Sandwich	2015-05-25 12:00 PM	0.26	8.70	0.65	5.82	0.55	4.21	8.87	0.16	0.01
	2015-06-04 12:00 PM	0.35	14.36	1.31	9.45	0.69	7.25	8.16	0.05	0.01
	2015-06-17 12:00 PM	0.55	15.32	3.55	9.44	0.67	7.54	10.42	0.25	0.01
	2015-07-01 3:43 PM	0.60	17.43	1.06	11.38	0.90	8.56	10.19	0.13	0.01
	2015-07-06 4:30 PM	0.53	13.04	0.95	8.73	0.50	7.15	15.01	0.04	0.01
	2015-07-22 10:17 AM	0.57	14.08	1.04	9.86	0.55	8.34	8.02	0.16	0.01
	2015-08-05 10:24 AM	0.73	15.14	1.04	10.69	0.60	9.34	8.13	0.05	0.01
	2015-08-19 3:11 PM	0.76	17.10	0.87	12.12	0.69	9.86	7.34	0.03	0.00
	2015-09-02 3:27 PM	0.77	18.82	0.88	13.28	0.74	11.27	13.65	0.04	0.01
	2015-09-17 8:45 AM	0.72	20.04	0.83	14.50	0.76	12.77	9.59	0.06	0.01
	2015-10-03 3:45 PM	0.75	20.11	0.90	13.80	0.77	11.77	6.65	0.04	0.01
	2015-10-14 9:39 AM	0.48	19.14	0.81	12.49	0.70	10.98	5.97	0.05	0.01
Strange	2015-05-25 12:00 PM	0.41	12.47	4.11	8.56	1.29	5.68	8.33	0.03	0.01
	2015-06-04 12:00 PM	0.26	13.53	4.42	9.89	1.40	7.35	14.76	0.07	0.01
	2015-06-17 12:00 PM	0.32	13.74	4.93	10.36	1.38	7.90	13.95	0.06	0.01
	2015-07-01 3:56 PM	0.74	17.42	7.13	12.51	1.71	9.50	12.51	0.04	0.01
	2015-07-03 2:30 PM	0.83	17.77	6.76	12.58	1.74	9.68	15.16	0.03	0.01
	2015-07-04 7:45 AM	0.67	15.52	5.79	11.43	1.53	9.32	15.40	0.03	0.01
	2015-07-04 2:30 PM	0.85	15.95	5.96	11.57	1.53	9.36	10.97	0.04	0.01
	2015-07-04 8:30 PM	0.71	15.48	5.93	11.43	1.51	9.37	10.51	0.05	0.01

2015-07-05 7:45 AM	0.55		13.85	5.30	10.38	1.29	8.93	19.89	0.04	0.01
2015-07-05 3:00 PM	0.57		12.99	4.63	10.02	1.17	8.48	18.69	0.06	0.01
2015-07-06 7:30 AM	0.49		11.83	4.32	9.71	1.08	8.42	15.23	0.06	0.01
2015-07-06 4:30 PM	0.50		12.10	5.14	9.79	1.15	8.52	17.65	0.04	0.01
2015-07-22 10:33 AM	0.49		14.87	6.42	12.31	1.37	10.85	12.06	0.03	0.01
2015-08-05 10:37 AM	0.66		15.95	6.49	13.22	1.43	12.01	8.53	0.04	0.01
2015-08-19 3:26 PM	0.72		19.57	8.16	15.84	1.45	13.17	8.42	0.10	0.01
2015-09-02 3:42 PM	0.77		25.40	10.77	18.96	1.57	15.77	8.16	0.08	0.01
2015-09-17 8:55 AM	0.65		49.87	18.58	28.18	2.13	24.31	10.89	0.05	0.01
2015-10-03 4:02 PM	0.51		32.37	14.39	22.93	1.82	19.33	7.53	0.03	0.01
2015-10-14 9:52 AM	0.25		24.95	12.30	18.92	1.84	16.96	6.65	0.05	0.01